

Alma Mater Studiorum – Università di Bologna

**DOTTORATO DI RICERCA IN**

**SCIENZE BIOMEDICHE**

Ciclo XXVII

Settore Concorsuale di afferenza: 05/H1

Settore Scientifico disciplinare: BIO/16

**STUDY OF PI3K/AKT SIGNALING PATHWAY AS POTENTIAL  
MOLECULAR TARGET FOR T-CELL ACUTE LYMPHOBLASTIC  
LEUKEMIA (T-ALL) TREATMENT: PAN-INHIBITION OF PI3K  
CATALITIC ISOFORMS AS BETTER THERAPEUTIC APPROACH**

Presentata da: **Dott.ssa Annalisa Lonetti**

Coordinatore Dottorato

Relatore

**Chiar.mo Prof Lucio Cocco**

**Chiar.mo Prof. Alberto M. Martelli**

Esame finale anno 2015

# TABLE OF CONTENTS

1.	BACKGROUND	5
1.1.	The phosphatidylinositol 3-kinases (PI3Ks) family	6
1.1.1.	PI3Ks classification	6
1.1.2.	PI3Ks substrates	11
1.1.3.	Class I PI3K signaling activation	11
1.1.4.	The main components of class I PI3K signaling network	14
1.2.	Class I PI3K functions	21
1.3.	Roles of class I PI3K signaling in T-lymphocytes	27
1.4.	T-cell acute lymphoblastic leukemia (T-ALL)	29
1.4.1.	Common T-ALL cytogenetic alteration	29
1.4.2.	Aberrant signaling in T-ALL	32
1.4.3.	Novel molecular alterations identified in T-ALL	33
1.5.	Activation of class I PI3K signaling in T-ALL	38
1.6.	Therapeutic strategies to target PI3K/Akt/mTOR pathway	39
2.	AIMS	46
3.	MATERIAL AND METHODS	49
3.1.	Compound and reagents	50
3.2.	Cell lines and primary samples	50
3.3.	Cell viability analysis and cell count	51
3.4.	Flow cytometry analyses	52
3.5.	Western blot analysis	53
3.6.	T-ALL cell co-culture with MS-5 mouse stromal cells	54
3.7.	Flow cytometric detection of T-ALL side population (SP)	54

3.8.	<i>In vivo</i> subcutaneous human T-ALL mouse models	55
3.9.	Gene expression analysis	56
3.10.	Statistical analysis	57
PART I: ACTIVITY OF THE PAN-CLASS I PHOSPHOINOSITIDE 3-KINASE INHIBITOR NVP-BKM120 IN T-CELL ACUTE LYMPHOBLASTIC LEUKEMIA		58
4.	RESULTS	59
4.1.	BKM120 decreases the viability of T-ALL cell lines <i>in vitro</i> by promoting apoptosis	60
4.2.	BKM120 blocks T-ALL cell cycle progression at the G <sub>2</sub> /M phase	61
4.3.	BKM120 affects the PI3K pathway in T-ALL cell lines	61
4.4.	BKM120 retains most of its pro-apoptotic activity also in the presence of bone marrow stromal cells	62
4.5.	BKM120 is cytotoxic to and inhibits the PI3K pathway in primary T-ALL blasts	62
4.6.	BKM120 is synergistic with chemotherapeutics agents in primary T-ALL samples	63
4.7.	BKM120 targets the T-ALL SP	64
4.8.	BKM120 delays T-ALL tumor growth <i>in vivo</i>	64
4.9.	Figures	66
5.	DISCUSSION	72
PART II: PAN-PI3K INHIBITION IMPAIRS MORE EFFICIENTLY PROLIFERATION AND SURVIVAL OF T-CELL ACUTE LYMPHOBLASTIC LEUKEMIA CELL LINES WHEN COMPARED TO ISOFORM-SELECTIVE PI3K INHIBITORS		76

6.	RESULTS	77
6.1.	<i>In vitro</i> assessment of PI3K inhibitors effects on cell viability	78
6.2.	Pan PI3K inhibition affected proliferation in a PTEN-independent fashion	79
6.3.	Antiproliferative effects are independent on total PtdIns(3,4,5)P <sub>3</sub> level reduction	80
6.4.	Pan inhibition of PI3K and PtdIns(3,4,5)P <sub>3</sub> decrease impair Akt-mediated signaling	81
6.5.	Antiproliferative activity of pan PI3K inhibition acts through cell cycle arrest and caspase-independent cell death	82
6.6.	Autophagy is a protective mechanism against pan PI3K inhibition	83
6.7.	Tables	86
6.8.	Figures	87
7.	DISCUSSION	92
	REFERENCES	97

# 1. BACKGROUND

## **1.1. The phosphatidylinositol 3-kinases (PI3Ks) family**

The phosphatidylinositol 3-kinases (PI3Ks) are members of a unique and conserved family of intracellular lipid kinases. Since its discovery in the 1980s, this family of lipid kinases has been found to have key regulatory roles in many cellular processes, including cell survival, proliferation and differentiation. PI3Ks phosphorylate the 3'-hydroxyl group of phosphatidylinositol and phosphoinositides and this reaction leads to the activation of many intracellular signaling pathways that regulate functions as diverse as cell metabolism, survival, polarity, and vesicle trafficking. A host of intracellular signaling proteins have evolved the ability to bind to the lipid products of PI3Ks and therefore become activated by PI3K signaling.

PI3K first became a focus in the cancer-research field when it became apparent that PI3K activity was physically and functionally associated with the transforming activity of viral oncogenes, such as the SRC tyrosine kinase and polyomavirus middle T antigen<sup>1</sup>. Over the past decade, it has become evident that the PI3K signaling pathway is one of the most highly mutated systems in human cancers, underscoring its central role in human carcinogenesis. Indeed, different human cancer genomic studies have revealed that many components of the PI3K pathway as well as proteins involved in the negative regulation of the pathway are frequently targeted by mutations or functional inactivation in a broad range of human cancers. These findings, and the fact that PI3K and other kinases in the PI3K pathway are amenable to pharmacological intervention, make this pathway one of the most attractive targets for therapeutic intervention in cancer<sup>2</sup>.

### **1.1.1. PI3Ks classification**

PI3Ks are grouped into three classes (I–III) according to their structural characteristics and substrate specificity (Figure 1). In mammals, numerous genes encode different isoforms of PI3Ks. All PI3K isoforms are widely expressed, with the exception of the class IA p55 $\gamma$

subunit, which is enriched in the brain and the testes, and the p110 $\delta$  subunit, which is predominantly expressed in lymphocytes. p110 $\gamma$  is mainly expressed in lymphocytes but is also found in the heart, pancreas, liver and skeletal muscle<sup>3-4</sup>.

**Class I PI3Ks.** Class I PI3Ks are divided into two subfamilies, depending on the receptors to which they couple.

Class IA PI3K is a heterodimer that consists of a p85 regulatory subunit and a p110 catalytic subunit. In mammals, there are numerous isoforms of each subunit. Three genes, *PIK3R1*, *PIK3R2* and *PIK3R3* (PI3K regulatory subunit 1, -2 and -3), encode the p85 $\alpha$ , p85 $\beta$  and p55 $\gamma$  isoforms of the p85 regulatory subunit, respectively. The *PIK3R1* gene also gives rise to two shorter isoforms, p55 $\alpha$  and p50 $\alpha$ , through alternative transcription-initiation sites. All these splice variants make functional complexes with p110 subunits. p110 $\alpha$  and p110 $\beta$  are widely distributed in mammalian tissues, in contrast to p110 $\delta$ , which shows a more restricted distribution and is mainly found in leukocytes<sup>5</sup>. The class IA p85 regulatory isoforms have a common core structure consisting of a p110-binding domain (also called the inter-SH2 domain) flanked by two Src-homology 2 (SH2) domains. The two longer isoforms, p85 $\alpha$  and p85 $\beta$ , also have an extended N-terminal region containing an Src-homology 3 (SH3) domain and a BCR homology (BH) domain flanked by two proline-rich (P) regions<sup>6</sup>. The p85 regulatory subunit mediate the activation of class IA PI3K by receptor tyrosine kinases (RTKs). The SH2 domains of p85 bind to phospho-tyrosine residues in the sequence context phospho-YXXM on activated RTKs or adaptor molecules (such as IRS1). This binding both relieves the basal inhibition of p110 by p85 and recruits the p85–p110 heterodimer to its substrate (PtdIns(4,5)P<sub>2</sub>) at the plasma membrane<sup>3</sup>. The p110 catalytic subunit isoforms, p110 $\alpha$ , p110 $\beta$  and p110 $\delta$ , are encoded by three different genes *PIK3CA*, *PIK3CB* and *PIK3CD*, respectively. They possess an N-terminal p85-binding domain that interacts with the p85 regulatory subunit, a Ras-binding domain (RBD)

that mediates activation by the small GTPase Ras, a C2 domain, a phosphatidylinositol kinase homology (PIK) domain and a C-terminal catalytic domain. The PIK and catalytic domains of p110 are homologous to domains found in a family of protein kinases that includes mTOR (mammalian target of rapamycin), ATM (ataxia telangiectasia mutated), ATR (ataxia telangiectasia Rad3 related) and DNA-PK (DNA-dependent serine/threonine protein kinase), indicating that these proteins share an ancient evolutionary origin<sup>3</sup>.

Class IB PI3Ks are heterodimers consisting of a p101 regulatory subunit and a p110 $\gamma$  catalytic subunit. Although p110 $\gamma$  shares extensive homology with the class IA p110 proteins, p101 is distinct from p85 proteins. Two other regulatory subunits of class IB PI3Ks, p84 and p87 PI3K adaptor proteins, have also been described<sup>7-8</sup>.

*In vivo*, class I PI3Ks primarily generate PtdIns(3,4,5)P<sub>3</sub> from PtdIns(4,5)P<sub>2</sub><sup>3</sup> (Figure 2 A and B).

**Class II PI3Ks.** Members of this class consist of a single p110-like catalytic subunit. There are three class II PI3K catalytic isoforms, the ubiquitously expressed PI3KC2 $\alpha$  and PI3KC2 $\beta$  and liver-specific PI3KC2 $\gamma$ . These catalytic isoforms are encoded by distinct genes. All three isoforms share significant sequence homology with the class I p110 subunits. In addition, class II PI3Ks have an extended divergent N terminus, and additional PX and C2 domains at the C terminus. However, the specific cellular functions of this family is still unclear<sup>3-4</sup>.

Class II PI3Ks preferentially use PtdIns or PtdIns(4)P as substrates to generate PtdIns(3)P and PtdIns(3,4)P<sub>2</sub> *in vitro*, and might generate PtdIns(3)P, PtdIns(3,4)P<sub>2</sub> and possibly PtdIns(3,4,5)P<sub>3</sub> *in vivo*<sup>3-4</sup> (Figure 2 A).

**Class III PI3Ks.** Class III PI3Ks consist of a single member and are the homolog of the yeast vesicular-protein-sorting protein Vps34p. The catalytic member Vps34p binds Vps15

(also known as PIK3R4 in mammals). Vps15 consists of a catalytic domain (which is thought to be inactive), HEAT domains (which probably mediate protein–protein interactions) and WD repeats, which have structural and functional characteristics similar to a G $\beta$  subunit. The WD repeats are essential for interaction with RAB5–GTP141 and the yeast guanine nucleotide-binding protein 1a (Gpa1; the homologue of the mammalian G $\alpha$  of heterotrimeric G proteins) and autophagy-related protein 14 (Atg14; a potential G $\gamma$  protein)<sup>9</sup>. *In vitro*, these PI3Ks can use only PtdIns as a substrate, and *in vivo* they only produce PtdIns(3)P from PtdIns which is an important regulator of membrane trafficking<sup>3</sup> (Figure 2 A). Class III PI3Ks are likely to be responsible for the generation of most of the PtdIns(3)P in cells. Vps34 has been shown to function as a nutrient-regulated lipid kinase that mediates signaling through mammalian target of rapamycin (mTOR), indicating a potential role in regulating cell growth. Interestingly, it has also been implicated as an important regulator of autophagy, a cellular response to nutrient starvation<sup>10</sup>.

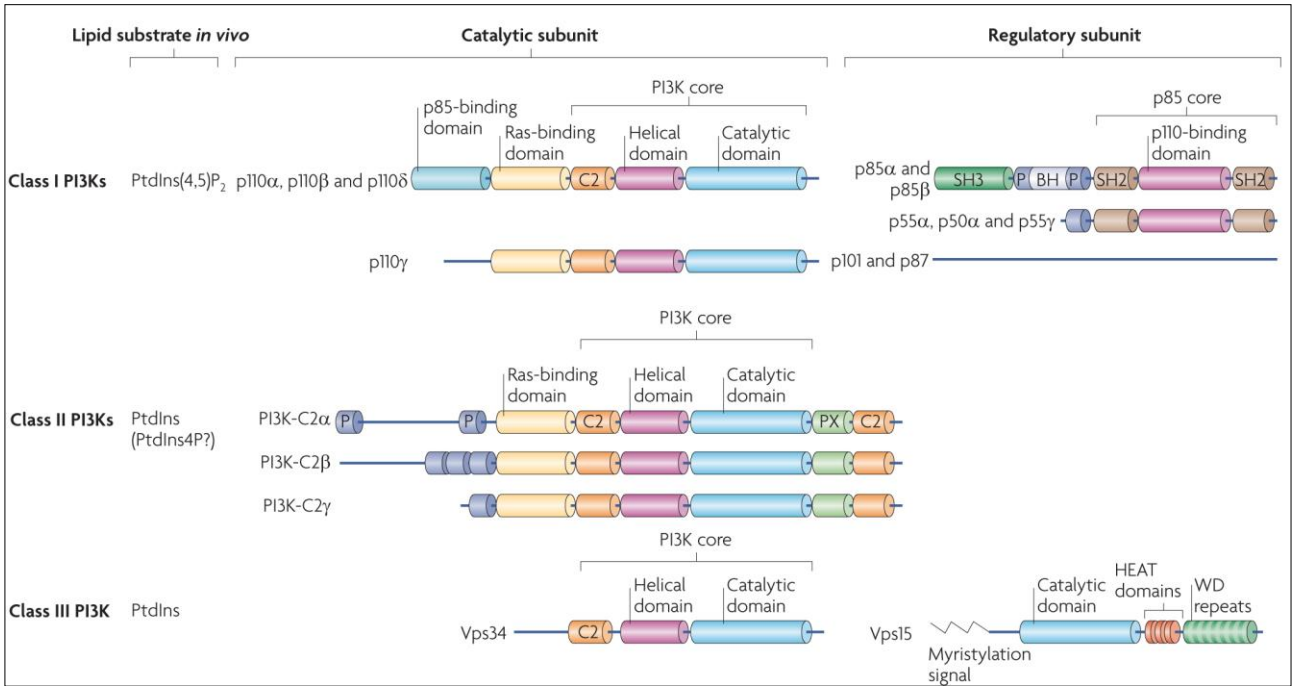


Figure 1: Classification and domain structure of mammalian PI3Ks<sup>9</sup>.

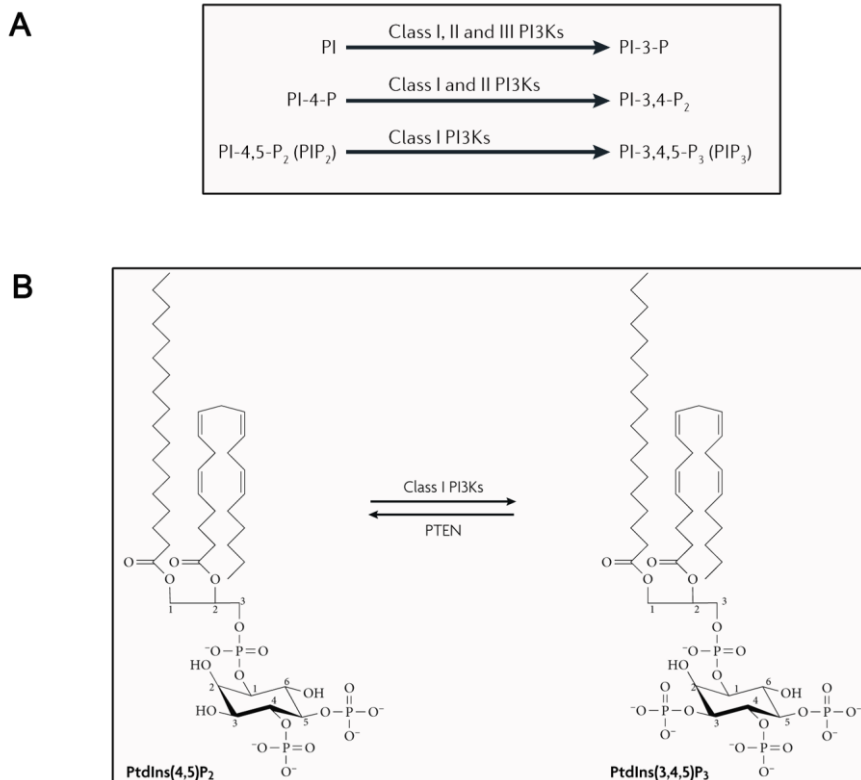


Figure 2: (A) Schematic representation of the substrate preferences of class I, II and III PI3Ks<sup>3</sup>. (B) Class I PI3K phosphorylates PtdIns(4,5)P<sub>2</sub> producing PtdIns(3,4,5)P<sub>3</sub>, whereas: the phosphatase PTEN antagonize PI3K signaling<sup>4</sup>.

### 1.1.2. PI3Ks substrates

Phosphatidylinositol (PtdIns), the basic building block for the intracellular inositol lipids in eukaryotic cells, consists of D-myo-inositol-1-phosphate linked via its phosphate group to diacylglycerol. The inositol head group of PtdIns has five free hydroxyl groups, three of which have been found to be phosphorylated in cells, in different combinations. PtdInsPs all reside in membranes and are substrates for kinases, phosphatases and lipases resident in or recruited to these membranes. The PI3Ks use PtdIns and its phosphorylated forms as substrates<sup>5</sup>. Inositol lipids and inositol phosphates levels in mammalian cells have been determined. PtdIns is the most abundant inositol lipid under basal conditions, present at levels 10–20 times higher than those of PtdIns(4)P and PtdIns(4,5)P<sub>2</sub>, which are present in roughly equal amounts. Of the total singly phosphorylated PtdIns in cells, 90–96% is PtdIns(4)P, whereas PtdIns(3)P and PtdIns(5)P each make up about 2–5%. PtdIns(4,5)P<sub>2</sub> is the most abundant of the doubly phosphorylated PtdIns (>99%); PtdIns(3,4)P<sub>2</sub> and PtdIns(3,5)P<sub>2</sub> each make up about 0.2% of the PtdInsP<sub>2</sub>. The levels of PtdIns(3,4,5)P<sub>3</sub> vary enormously but can be comparable to those of PtdIns(3,4)P<sub>2</sub> and PtdIns(3,5)P<sub>2</sub><sup>5</sup>. All of these lipid products are membrane-limited, and thus compartmentalized allowing a selective action. PtdIns(3,4,5)P<sub>3</sub>, which activates multiple downstream signaling pathways, is mainly produced through class I PI3Ks. PtdIns(3,4,5)P<sub>3</sub> is a lipid with key signaling functions and a major role in the control of cell survival, growth and proliferation.

### 1.1.3. Class I PI3K signaling activation

PI3K signaling can be activated by multiple stimuli: activated tyrosine kinase growth factor receptors; cell adhesion molecules, such as integrins and G-protein-coupled receptors (GPCR); and oncogenes, such as Ras. As mentioned above, class IA and IB isoforms

differ in the receptors they couple: the first are activated by tyrosine kinase receptors or Ras; the latter are activated by heterotrimeric G proteins or Ras<sup>3</sup>.

In class IA PI3Ks, p85 subunits provide at least three functions to p110 proteins: stabilization, inactivation of their kinase activity in the basal state and recruitment to phospho-Tyr residues in receptors and adaptor molecules. Inactive p85–p110 complexes are present in the cytoplasm of resting cells, poised for activation in response to appropriate cues. Class IA PI3K can become activated by at least three independent pathways, all of which start with binding of ligand to RTKs or to adaptor proteins associated with the receptors [for example, insulin receptor substrate 1 (IRS1)]<sup>11-12</sup>. RTKs dimerize and undergo autophosphorylation at tyrosine residues, which allows them to interact with SH2-domain-containing molecules. Therefore, the p85–p110 complex is recruited to the receptor by interaction of the SH2 domain of p85 with consensus phosphotyrosine residues on the RTK or with the IRS1/IRS2 signaling intermediate, in some cases. Engagement of the p85 SH2 domains by phosphorylation relieves the p85-mediated inhibition of p110 isoforms and also brings them in contact with their lipid substrates in the membrane. In one activation pathway, the 85 kDa regulatory subunit of PI3K (p85) binds directly to phospho-YXXM motifs (in which X indicates any amino-acid) within the RTK, triggering activation of PI3K's 110 kDa catalytic subunit (p110)<sup>13</sup>. Indeed, the binding relieves the intermolecular inhibition of the p110 catalytic subunit by p85 and localizes PI3K to the plasma membrane where its substrate resides<sup>12</sup>. Other PI3K signaling pathways depend on the adaptor protein GRB2 (growth factor receptor-bound protein 2) which binds preferentially to phospho-YXN motifs of the RTK. GRB2 binds to the scaffolding protein GAB (GRB2-associated binding protein), which in turn can bind to p85. PI3K can also be stimulated by activated Ras, which directly binds p110<sup>14</sup>. Each of the class I PI3K catalytic isoforms has a segment known as the RAS-binding domain (RBD), which can induce inputs through Ras or other small GTPases. Ras has a documented role

in the activation of p110 $\alpha$  and p110 $\gamma$ , whereas a role for Ras in p110 $\beta$  activation is less clear, with indirect evidence in favor and against<sup>9</sup>. Several studies indicate that p110 $\alpha$ -RBD interacts directly with oncogenic RAS, whereas p110 $\beta$  interacts with GTP-bound RAC and cell division cycle 42 (CDC42)<sup>15</sup>. There is also evidence for a role of the Ras family member TC21 (also known as RRAS2) upstream of p110 $\delta$ . TC21 recruits p110 $\delta$  to antigen receptors in lymphocytes and, consistent with this, TC21-null and p110 $\delta$ -null mice have striking similarities in their immunological-phenotypes<sup>9</sup>. GRB2 activates Ras (through the activation of SOS), and Ras activates p110 independently of p85. GRB2 can also exist in a large complex that contains both SOS, Ras, and GAB or other scaffolding proteins, bringing these activators into close proximity with p110 PI3K<sup>13</sup>. It is not clear precisely which of these pathways predominates in different physiological situations. Additionally, the p110 $\beta$  isoform of class IA PI3K is regulated not only by the p85 regulatory subunit but also by binding to G $\beta\gamma$  subunits of heterotrimeric G proteins<sup>16</sup>. Therefore, the class IA p110 $\beta$  isoform might integrate signals from GPCRs as well as RTKs. In addition to their SH2 domains, which engage class I PI3Ks with Tyr kinase signaling pathways, all p85 isoforms have a Pro-rich region amino-terminal to the N-SH2 domain. The p85 N-termini are distinct for each p85 isoform and might allow additional signaling input and output, the roles of which are not well investigated<sup>9</sup>. For example, p85 $\alpha$  (PIK3R1) and p85 $\beta$  (PIK3R2) also contain an SH3 domain, a second Pro-rich region and a BCR homology (BH) domain, which might have intrinsic GTPase-activating protein (GAP) activity for Rab family members<sup>9</sup>. Related to this, there is some evidence to suggest that p85 isoforms can interact with small GTPases (such as Rac, Rho and Cdc42), but this has only been investigated for isolated p85, not when p85 is in complex with p110<sup>9</sup>.

Class IB PI3K do not comprise p85 family regulatory subunits and therefore are not regulated by RTKs. G protein-coupled receptors (GPCRs) directly stimulate p110 $\gamma$  through interacting directly with the  $\beta\gamma$  subunits of heterotrimeric G proteins. The p101 regulatory

subunit facilitates the activation of the p101–p110 $\gamma$  heterodimer by G $\beta$  $\gamma$ <sup>4</sup>. Moreover, also p110 $\gamma$  subunit possess the RAS-binding domain and tyrosine kinases can activate p110 $\gamma$  in some cell types via RAS. The Ras family member TC21 (also known as RRAS2) may have a role in the activation of p110 $\delta$ <sup>9</sup> and the RBD domain of p110 $\gamma$  is required for PI3K signaling in neutrophils<sup>15</sup>.

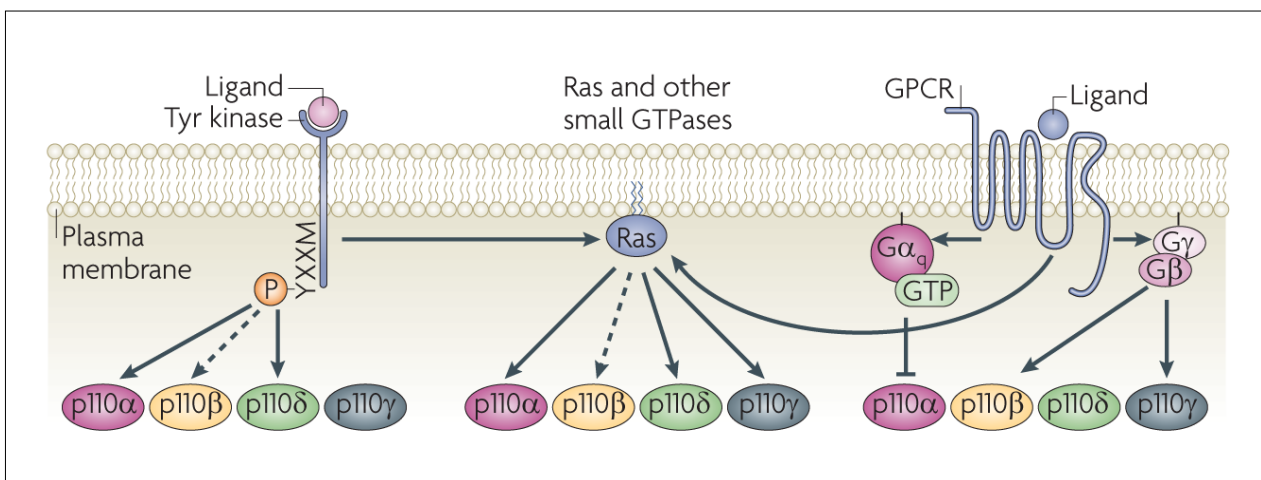


Figure 3: Upstream signals feeding into class I PI3Ks<sup>9</sup>.

#### 1.1.4. The main components of class I PI3K signaling network

**PDK1.** PDK1 belongs to the family of AGC kinases (serine and threonine kinases) that show a sequence homology in their catalytic domain to cAMP-dependent protein kinase 1, cyclic guanosine monophosphate-dependent protein kinase, and protein kinase C (PKC).

PDK1 was originally discovered in 1997 as the kinase responsible for the phosphorylation of the Akt activation loop, at residue Thr308, which is essential for enzyme activation, thus linking PDK1 to the upstream activation of PI3K<sup>17</sup>. PDK1 kinase is a protein of 556 amino acids that possesses an N-terminal catalytic domain, a C-terminal PH domain, and a nuclear export sequence. The nuclear export sequence is a short sequence of four amino

acids that are essential for exporting PDK1 from the cell nucleus to the cytoplasm through the nuclear pore complex using nuclear transport<sup>18</sup>. The amino-terminal small lobe and the carboxy-terminal large lobe comprise one adenosine triphosphate molecule essential for the subsequent substrate phosphorylation. As many AGC kinases, PDK1 possesses two phosphorylation sites that regulate its activation: one in the activation loop, which is located within the kinase domain; and another in the hydrophobic motif, which is located in a region adjacent to the catalytic domain<sup>18</sup>. The PDK1 phosphorylation site within the activation loop (Ser241) is phosphorylated in resting cells and is not affected by growth factor stimulation. The phosphorylation of PDK1 in Ser241 is catalyzed by an autophosphorylation reaction in *trans*<sup>19</sup>. PDK1 kinase activity is therefore constitutively active, and the regulation of PDK1-activated signaling involves different mechanisms. The phosphorylation of the other sites increases kinase activity and leads to enzymatic full activation<sup>18</sup>. PDK1 localized at the plasma membrane due to the interaction of its PH domain with PtdIns(3,4,5)P<sub>3</sub>, PtdIns(3,4)P<sub>2</sub>, and PtdIns(4,5)P<sub>2</sub> and PDK1 membrane localization is essential for Akt phosphorylation in Thr308. PDK1 phosphorylates many other kinases, such the serum glucocorticoid-dependent kinase (SGK), ribosomal protein S6 kinases 1 (S6K1), p90 ribosomal protein S6 kinase (RSK), and atypical PKC isoforms, but the mechanism of activation of these kinases differs from the Akt activation mechanism<sup>18</sup>.

**Akt.** Akt is a 57 kD Ser/Thr kinase and the cellular homologue of the viral oncoprotein v-Akt, which is known to be responsible for a type of leukemia in mice<sup>20</sup>. This protein kinase is expressed as three isoforms, Akt1, Akt2 and Akt3, which are encoded by the genes *PKB $\alpha$*  (14q32), *PKB $\beta$*  (19q13.1–13.2) and *PKB $\gamma$*  (1q44), respectively<sup>21</sup>. Akt2 and Akt3 have 81 and 83% homology in amino acid sequence with Akt1, respectively<sup>22</sup>. The three isoforms share a similar structure consisting in a PH domain in the N-terminus, a central

serine–threonine catalytic domain and a C-terminal regulatory domain. The PH domain in the N-terminal region of Akt interacts with 3'-phosphoinositides, contributing to recruitment of Akt to the plasma membrane. Akt preferentially binds PtdIns(3,4,5)P<sub>3</sub> over other PtdIns. All three mammalian Akt genes are widely expressed in various tissues, but Akt1 is most abundant in brain, heart, and lung, whereas Akt2 is predominantly expressed in skeletal muscle and embryonic brown fat, and Akt3 is predominantly expressed in brain, kidney, and embryonic heart<sup>22</sup>. Once PDK1 is activated by PtdIns(3,4,5)P<sub>3</sub>, it propagates the signal to the Ser/Thr kinase Akt by phosphorylating its catalytic domain. Akt activation is initiated by translocation to the plasma membrane, which is mediated by docking of the PH domain in the N-terminal region of Akt to PtdIns(3,4,5)P<sub>3</sub> on the membrane. Thus, PtdIns(3,4,5)P<sub>3</sub> brings PDK1 and Akt into close proximity. Recruitment to the membrane results in a conformational change of Akt that exposes two main phosphorylation sites, Thr308 in the kinase domain and Ser473 in the C-terminal regulatory domain. PDK1 phosphorylates Akt in its activation loop on Thr308, an event that alone stabilizes the active conformation of Akt and stimulates partial activation<sup>21</sup>. Phosphorylation of Thr308 is a requirement for the activation of Akt, but phosphorylation of the residue located in the regulatory domain at C-terminus is required for full activation of the kinase. The mammalian target of rapamycin complex 2 (mTORC2) phosphorylates Akt at Ser473<sup>23</sup>. Although if mTORC2 is the primary source for complete Akt activation, several other kinases are capable of phosphorylating Akt at Ser473, including PDK1, integrin-linked kinase (ILK), an ILK-associated kinase, Akt itself and DNA-dependent protein kinase (DNA-PK)<sup>21</sup>. Phosphorylation of the three Akt isoforms occurs by the same mechanisms. The corresponding phosphorylation sites of Akt2 are Thr309 and Ser474, whereas those of Akt3 are Thr305 and Ser472. Several evidences have highlighted that Ser473 phosphorylation precedes Thr308 phosphorylation and actually enhances it<sup>24</sup>. Furthermore, it has been shown that additional phosphorylative steps may increase Akt

activation, including phosphorylation of multiple tyrosine residues and phosphorylation on Ser129 through casein kinase 2 (CK2), but relevance of these phosphorylative events awaits full elucidation<sup>24</sup>. Akt activity is tightly regulated by several proteins which act by phosphorylating other sites. Among these, there is S6K1, a downstream substrate of mTOR which plays an important role in negative feedback regulation of Akt by catalyzing an inhibitory phosphorylation on IRS proteins, abolishing their association and activation of PI3K<sup>21</sup>. Akt activity is also modulated by a complex network of regulatory proteins that interact with the PH domain, or the kinase domain or the C-terminal of Akt. One of these proteins is heat-shock protein-90 (HSP-90), a molecular chaperone that forms a complex with the co-chaperone Cdc37. This complex binds a variety of proteins, including tyrosine and serine/threonine protein kinases. The HSP-90/Cdc37 complex interacts with the Akt kinase domain<sup>24</sup>.

Once Akt has been phosphorylated and activated, it phosphorylates many other proteins regulating a wide range of cellular processes involved in protein synthesis, cell survival, proliferation and metabolism.

**mTOR.** mTOR is an atypical serine/threonine protein kinase that belongs to a group of serine–threonine protein kinases of the PI3K superfamily, referred to as class IV PI3Ks, including ATM, ataxia telangiectasia and RAD3-related protein (ATR), DNA-PK and SmG1 (SmG1 homologue, phosphatidylinositol 3-kinase-related kinase)<sup>4</sup>. mTOR exists in 2 multiprotein complexes: mTOR complex 1 and 2 (mTORC1 and mTORC2). mTORC1 is composed of the mTOR catalytic subunit, mammalian LST8, proline-rich Akt1 substrate 40 (PRAS40), and the regulatory associated protein of mTOR, raptor, whereas mTORC2 consists of a complex of mTOR, mLST8, mammalian stress-activated protein kinase interacting protein (mSIN1), protor, and rictor<sup>21</sup>.

Akt activates mTORC1 through at least 2 mechanisms: either directly by phosphorylating mTORC1 at Ser244850<sup>25</sup> or indirectly through TSC2<sup>26</sup>. Indeed, one of the key control nodes for mTORC1 activity is the TSC complex containing TSC1, TSC2 and TBC1 domain family member 7 (TBC1D7) proteins. By phosphorylating TSC2, Akt suppresses the inhibitory effect of the TSC complex on mTORC1. A GTPase-activating domain of TSC2 catalyzes the conversion of the Ras-like protein, Ras homolog enriched in brain (Rheb)-GTP to Rheb-GDP leading to inactivation of mTOR function. Thus, Akt by decreasing TSC2 activity, increases levels of Rheb-GTP, which then leads to activation of mTORC1<sup>21</sup>. TSC2 inactivation results in upregulation of mTORC1 activity through a cascade of signaling molecules. mTORC1 is a central regulator of cellular metabolism and biosynthesis, and is subject to complex regulation by growth factors, nutrients and cellular stress. Growth factors, energy sensors and cellular stress converge at the level of the TSC complex. Amino acids regulate mTORC1 through the Ragulator and GATOR (GAP activity toward RAGs) complexes. mTORC1 promotes anabolic programmes through many substrates, including S6K1, eIF4E binding proteins (4E-BPs) and autophagy regulators such as UNC51 like kinase 1 (ULK1). When conditions are favorable for cell growth, mTORC1 phosphorylates several substrates to promote anabolic processes (such as ribosome biogenesis, translation and the synthesis of lipids and nucleotides) and suppress catabolic processes (such as autophagy)<sup>27</sup>. mTORC1 plays a pivotal role in protein translation through its substrate: eukaryotic initiation factor 4E-binding protein 1 (4E-BP1) and S6K1. Hyperphosphorylation of 4E-BP1 by mTORC1, inhibits its binding to eukaryotic initiation factor 4E (eIF4E), thereby activating cap-dependent translation. In addition to protein translation, mTORC1 regulates cell proliferation, survival, and angiogenesis by regulating eIF4E-mediated translation of Bcl-2, Bcl-xL, and vascular endothelial growth factor (VEGF). mTORC1 also phosphorylates S6K1, which in turn leads to phosphorylation of S6 ribosomal protein, and other targets, including insulin receptor substrate 1 (IRS1),

eukaryotic initiation factor 4B (eIF4B), programmed cell death 4 (PDCD4), eukaryotic elongation factor-2 kinase (eEF2K), mTOR, and glycogen synthase kinase-3, which are implicated in cellular transformation. In addition, mTORC1 regulates the transition from G<sub>1</sub> to S phase through downregulation of cyclin D1 and c-Myc, which are required for progression through this phase of the cell cycle<sup>21</sup>. mTORC1 activity exerts feedback control on growth factor signaling. One canonical feedback pathway is initiated by S6K1, that phosphorylates adaptor proteins of the IRS1 family to attenuate growth factor receptor signaling to PI3K and RAS. Phosphorylation of IRS1 by S6K1 inhibits IRS1 and thereby PI3K activation, forming a negative feedback loop which has an important role in the regulation of mTORC1<sup>28</sup>.

In comparison with mTORC1, less is known about mTORC2 complex. mTORC2 seems to have basal activity and is stimulated by association with ribosomes and by growth factors. mTORC2 responds to growth factors, such as insulin, through a poorly defined mechanism that requires PI3K and ribosomes, as ribosomes are needed for mTORC2 activation and mTORC2 binds them in a PI3K-dependent fashion. mTORC2 controls several members of the AGC subfamily of kinases, promoting their stability and activity, including Akt, serum-induced and glucocorticoid-induced protein kinase 1 (SGK1), and protein kinase C alpha (PKC $\alpha$ )<sup>21</sup>. Akt is phosphorylated by mTORC2 at its hydrophobic motif (Ser473), a site required for its maximal activation. Indeed, mTORC2 deletion, associated with defective Akt-Ser473 phosphorylation, impairs the phosphorylation of some Akt targets. mTORC2 also directly activates SGK1, a kinase controlling ion transport and growth and mTORC2 deletion results in complete loss of SGK-1 activity. PKC $\alpha$  is another AGC kinase regulated by mTORC2. Along with other effectors, mTORC2 plays a role in cell migration by regulating phosphorylation of PKC $\alpha$  and control of the actin cytoskeleton in cell-type-specific fashion<sup>21</sup>.

**PTEN.** The PI3K signaling is negative regulated by several phosphatases. The Phosphatase and Tensin homolog deleted on chromosome TEN (PTEN) was originally identified as a tumor suppressor gene mutated and lost in various cancers and was mapped on chromosome 10q23<sup>29</sup>. Several lines of evidence soon highlighted PTEN as a lipid phosphatase-hydrolysing phosphates in position 3' from phosphoinositides. The major function of PTEN is the buffering of PI3K signaling<sup>30</sup>. PTEN is a dual-specificity phosphatase that dephosphorylates both protein and lipid substrates. PTEN preferentially removes the 3-phosphate mainly from PtdIns(3,4,5)P<sub>3</sub> but is also active on PtdIns(3,4,)P<sub>2</sub><sup>24</sup>. PtdIns(3,4,5)P<sub>3</sub> PTEN dephosphorylation forms the inactive PtdIns(4,5)P<sub>2</sub>. Thus, PTEN antagonizes PI3K function and negatively regulates Akt activities. The discovery that the tumor suppressor PTEN works by antagonizing PI3K established the first direct link between PI3K activation and human cancer. PTEN functions as a tumor suppressor by controlling cellular differentiation, inhibiting cell growth and enhancing cellular sensitivity to apoptosis<sup>13</sup>. Loss of PTEN function and its activity in cancer occurs through multiple mechanisms, which include mutations, loss of heterozygosity, methylation, aberrant expression of regulatory microRNA, protein instability, and protein phosphorylation. PTEN is the second most frequently mutated tumor suppressor gene and, as shown in multiple studies, it is mutated or deleted in many human cancer types, including bladder, breast, prostate, glioblastoma, melanoma and endometrial cancers<sup>21</sup>. PTEN loss-of-function results in Akt upregulation. Therefore, PTEN acts as a negative regulator of PI3K/Akt signaling and loss of PTEN activity leads to permanent PI3K/Akt pathway activation<sup>24</sup>. PTEN also acts in the nucleus in a phosphatase-independent manner to further impact cell cycle, apoptosis and chromosomal integrity<sup>31</sup>.

Other mechanisms exist to downregulate PI3K/Akt pathway. The Src-homology 2 (SH2)-containing phosphatases (SHIP1 and SHIP2) abrogate signaling through PI3K by

removing the 5-phosphate and converting PtdIns(3,4,5)P<sub>3</sub> to PtdIns(3,4)P<sub>2</sub>. SHIP1 is predominantly expressed in hematopoietic cells whereas SHIP2 is more ubiquitous. However, their role on Akt function is not well understood, and in some cases they could not reverse Akt activation, something PTEN can do<sup>32</sup>. Protein phosphatase 2A (PP2A), is capable of directly dephosphorylating and downregulating Akt, whereas several work indicates that Ser473 phospho-Akt is dephosphorylated by a PP2C family phosphatase, referred to as PHLPP<sup>24</sup>. Furthermore, extensive crosstalk exists with other cellular signaling networks to downregulate PI3K signaling pathway, in addition to the control exerted by mTOR through IRS1 downregulation. For example, activation of the tumor suppressor p53 causes both increased PTEN and decreased p110 expression. Further, p53 degradation is reduced indirectly by PTEN via its antagonism of PI3K. These actions safeguard the cell in times of genotoxic strain against ongoing DNA replication, though the interplay between p53 and PTEN requires further elucidation<sup>33</sup>.

## **1.2. Class I PI3K functions**

The most ancient role for PI3K family of enzymes is probably to mark specific cellular membranes for trafficking events, and this seems to be the primary function of the single form of PI3K that is found in yeast: Vps34. However, in multicellular eukaryotes, the additional isoforms of PI3K have evolved for the dedicated purpose of signal transduction<sup>3</sup> (Figure 4).

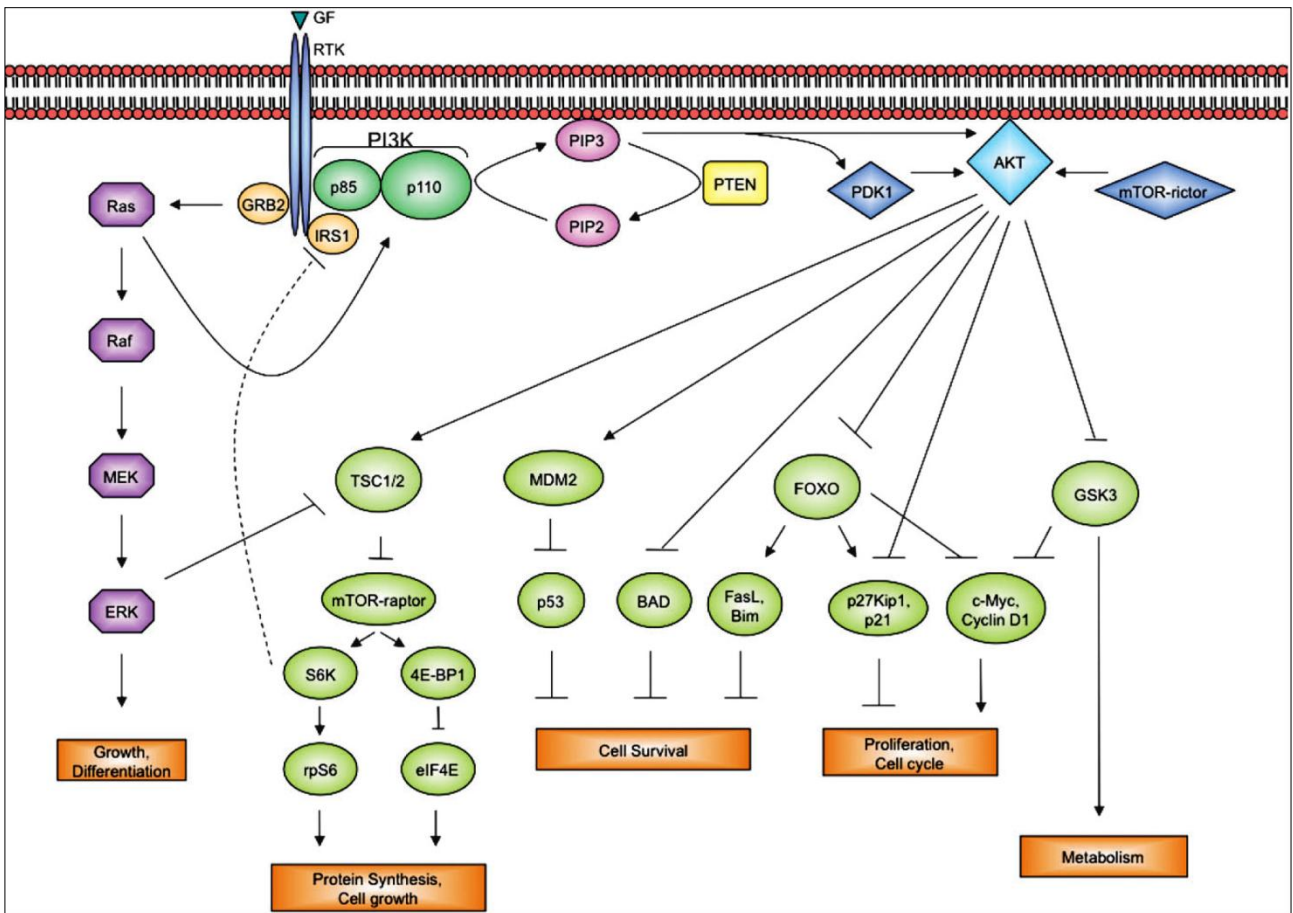


Figure 4: Signaling through class I PI3Ks<sup>33</sup>.

**Cell survival and apoptosis inhibition.** Akt could promote growth factor-mediated cell survival both directly and indirectly. Akt phosphorylates Bad, a proapoptotic member of the Bcl-2 family, at Ser136. This phosphorylation event promotes Bad sequestration by 14-3-3 proteins in the cytosol, thereby preventing Bad from interacting with either Bcl-2 or Bcl-XL at the mitochondrial membrane. The final effect is inhibition of apoptosis<sup>34</sup>. A similar negative regulation has been demonstrated for Yes-associated protein, whose phosphorylation by Akt leads to repression of p53-related transcription factor p73 and reduced expression of the proapoptotic protein Bax<sup>35</sup>. Akt may interfere with JNK (Stress-activated protein kinase/c-Jun N-terminal kinase) signaling. JNK is a MAP kinase activated by various cell stimuli, that targets specific transcription factors, thus mediating immediate-

early gene expression in response to cell stimuli. JNK has been found required for tumor-necrosis factor alpha (TNF $\alpha$ ) induced apoptosis<sup>36</sup>. Akt phosphorylate and thereby inactivate ASK1, a protein kinase which transduces signals to JNK. Akt also promotes phosphorylation and nuclear translocation of Mdm2, an E3 ubiquitin ligase which mediates ubiquitinylation and proteasome-dependent degradation of the p53 tumor suppressor protein, downregulating p53 and antagonizing p53-mediated cell cycle checkpoint<sup>37</sup>. Mdm2 phosphorylation contributes to centrosome hyperamplification and chromosome instability in cancer<sup>38</sup>. Akt also indirectly promote cell survival activating transcription factors that upregulate antiapoptotic genes or negatively affecting factors that promote death gene expression. For example, Akt phosphorylation of many effectors regulates their localization by generating binding sites for 14-3-3 proteins, which are important in regulating cellular location and degradation of various molecule. The FoxO family of transcription factors functions as a trigger for apoptosis through expression of genes necessary for cell death. FoxO proteins are predominantly localized in the nucleus where they are able to promote transcription of proapoptotic target genes such as Fas ligand (Fas-L) and Bim. Akt phosphorylate FoxO proteins leading to their nuclear export, as phospho-FoxO factors specifically interact with 14-3-3 proteins, which serve as chaperone molecules to escort them out of the nucleus. Once in the cytoplasm, they are degraded via the ubiquitin-proteasome pathway<sup>39</sup>. FoxO factor phosphorylation requires intranuclear localization of active Akt. In addition, Akt is capable of upregulating nuclear factor-kappa B (NF- $\kappa$ B), a transcription factor which is deeply involved in the regulation of cell proliferation, apoptosis and survival. NF- $\kappa$ B induces expression of antiapoptotic proteins including cIAP-1 and -2, XIAP, c-FLIP, Bcl-XL, caspase inhibitors and c-Myb. Under non-stimulated conditions, NF- $\kappa$ B is retained in the cytoplasm trough its association with I- $\kappa$ B. Phosphorylation of I- $\kappa$ B by upstream kinases, IKKs, promotes its degradation via the ubiquitin-proteasome pathway. This, in turn, allows NF- $\kappa$ B nuclear translocation and upregulation of target genes. Akt

phosphorylates directly and activates IKK $\alpha$  and, more importantly, it is believed to be essential for IKK-mediated destruction of I- $\kappa$ B<sup>24</sup>. In addition, Akt phosphorylates and activates the cyclic AMP-response element-binding protein, which increases the transcription of anti-apoptotic genes, such as those for Bcl-2, Mcl-1, and Akt itself<sup>22</sup>.

**Cell cycle regulation.** PI3K pathway activation is required for G<sub>1</sub>/S progression and PI3K inhibition leads to G<sub>1</sub> arrest in many cell types. Moreover, PI3K pathway may also regulate the efficiency of G<sub>2</sub>/M phase progression. Cyclin D1 and c-Myc play distinct roles in cell cycle progression through G<sub>1</sub> phase and their expression is induced early in G<sub>1</sub> upon growth factor stimulation<sup>40</sup>. Cyclin D1 and c-Myc are short-lived proteins whose levels are regulated by phosphorylation-dependent proteolytic degradation. Proteolysis of both c-Myc and cyclin D1 is regulated by the PI3K pathway. In fact, glycogen synthase kinase 3 beta (GSK3 $\beta$ ) phosphorylates cyclin D1 at Thr286. This phosphorylation promoted association of cyclin D1 with its nuclear exporter CRM1 and triggered nuclear-cytoplasmic translocation leading to ubiquitin-mediated proteolytic degradation of cyclin D1 in the cytoplasm<sup>41</sup>. The activity of GSK3 $\beta$  is inhibited by Akt-dependent phosphorylation, and thus Akt-mediated GSK3 $\beta$  inhibition stabilized cyclin D1. The stability of c-Myc is controlled by phosphorylation at Ser62 and Thr58, as the first stabilizes c-Myc and the latter creates a priming site that is necessary for subsequent phosphorylation by GSK3 $\beta$  at Thr58, which appear to activate the ubiquitin dependent degradation of c-Myc. Thus, also in this case, Akt stabilizes c-Myc through inhibition of GSK3 $\beta$ <sup>42</sup>. Akt also promotes transcriptional activation of cyclin D1 and c-Myc genes, as well as translation of cyclin D1 mRNA through eIF4E<sup>42</sup>. p27<sup>Kip1</sup> is a direct inhibitor of cyclin-dependent kinase (cdk) 2, one of the cdk2s responsible for the activation of E2F1 transcription factors that promote DNA replication<sup>43</sup>. High levels of p27<sup>Kip1</sup> are required to maintain many cell types in quiescence and, therefore, its downregulation is critical for cell cycle progression<sup>42</sup>. Akt can inactivate

p27<sup>Kip1</sup> by phosphorylating on Thr157 and inducing its localization in the cytoplasm where it cannot exert its inhibitory effect, so that cell proliferation is enhanced<sup>44</sup>. Moreover, Akt can directly phosphorylate another cyclin-dependent kinase inhibitor, p21<sup>cip1/Waf1</sup>, causing its cytoplasmic accumulation and preventing its access to nuclear cyclin-Cdk targets<sup>42</sup>. Akt can also regulate G<sub>1</sub>/S cell cycle progression through inhibition of FoxO transcriptional factors. In fact, FoxO factors once in the nucleus, upregulate expression of three target genes which lead to G<sub>1</sub>/S arrest, p27<sup>Kip1</sup>, p21<sup>Waf/Cip1</sup> and the retinoblastoma family member p130<sup>24</sup>. Akt-dependent phosphorylation of these transcription factors leads to their nuclear exclusion and thus inhibition of FoxO factor-mediated gene expression. Moreover, FoxO factors can also promote cell cycle arrest by repressing the expression of cyclin D1 and D2, two positive cell cycle regulators<sup>45</sup>. It has also been reported that Akt plays a role in G<sub>2</sub>/M phase transition and its constitutive activation may lead to a defect in DNA damage checkpoint control. Gadd45a gene (Growth arrest and DNA damage 45a) is transactivated by FoxO3a. Thus, Akt would lead to FoxO3a phosphorylation and sequestration in the cytoplasm, thereby reducing Gadd45a expression<sup>46</sup>. Chk1 is also one of the candidates regulated by Akt pathway and involved in regulation of G<sub>2</sub>/M transition. Akt can phosphorylate Chk1 at Ser280 causing its inactivation that impair Chk1 mediated Cdc25C phosphorylation. Cdc25C is a phosphatase that positively regulates Cdc2, the cyclin-dependent kinase 1 which is essential for G<sub>1</sub>/S and G<sub>2</sub>/M phase transitions of eukaryotic cell cycle. Following DNA damage, Chk1 phosphorylates Cdc25C leading to inhibition of Cdc2. Thus, Akt-mediated Chk1 inhibition could lead to resistance to DNA damage mediated G<sub>2</sub>/M arrest<sup>42</sup>.

**Cell metabolism regulation.** Activated Akt protein modulates the function of numerous substrates related to the regulation of cell proliferation, such as GSK3 $\beta$ , membrane translocation of the glucose transporter (GLUT4), mTOR and TSC2. Akt-mediated

activation of mTOR is important in stimulating cell proliferation, as mTOR acts as a checkpoint sensor indicating to cells that there are sufficient nutrients available to proceed through the cell cycle. mTOR regulates translation by phosphorylating components of the protein synthesis machinery, including S6K1 (which can also be directly activated by PDK1) and 4E-BP1: the first phosphorylates the 40s ribosomal protein, S6, leading to active translation of mRNAs, the latter induces release of the translation initiation factor eIF4E, allowing eIF4E to participate in assembly of a translational initiation complex<sup>24</sup>. mTOR favors the production of key molecules such as c-Myc, cyclin D1 and ribosomal proteins. By controlling protein synthesis, S6K1 and 4E-BP1 also regulate cell growth and hypertrophy. The TSC1/TSC2 complex opposes these effects by inhibiting S6K1 and activating 4E-BP1 to sequester eIF4E<sup>47</sup>. Akt inhibits TSC2 function through direct phosphorylation. TSC2 is a GTPase-activating protein (GAP) that functions to inactivate the small G protein Rheb (Ras homolog enriched in brain). TSC2 phosphorylation by Akt represses GAP activity of the TSC1/TSC2 complex, allowing Rheb to accumulate in a GTP-bound state<sup>24</sup>. Rheb-GTP then activates the protein kinase activity of mTOR when associated in the mTORC1 complex, and so this pathway is controlled by complicated interactions and feedback loops. For example, the TSC/Rheb/mTOR/S6K1 cascade regulates IRS1/2, which comprises an important feedback loop. In addition, the PI3K/Akt pathway interacts with molecular mechanisms controlling cellular energy control and glucose metabolism. LKB1-mediated activation of AMP-activated protein kinase (AMPK), an evolutionarily conserved sensor of the cellular ATP/ADP ratio, leads to inhibition of mTOR through TSC2 in response to energy depletion, thereby allowing energy conservation<sup>48</sup>. Another Akt substrate important for metabolic function is GSK3 $\beta$ , which phosphorylates and inactivates glycogen synthase in response to insulin stimulation. When phosphorylated by Akt on Ser9, GSK3 $\beta$  is downregulated<sup>49</sup>. Interestingly, GSK3 $\beta$  has been implicated in the signaling pathway elicited by Wnt, a ligand for transmembrane

receptor frizzled. The  $\beta$ -catenin protein is at the core of the canonical Wnt signaling pathway. Wnt stimulation leads to  $\beta$ -catenin accumulation, nuclear translocation and interaction with transcription factors to regulate genes important for development and proliferation, including FGF20, c-Myc, cyclin D1, DKK1, WISP1 and Glucagon (GCG)<sup>50-51</sup>. Phosphorylation of  $\beta$ -catenin by GSK3 $\beta$  on key N-terminal residues targets it for ubiquitination and breakdown in the proteasome. Therefore, Akt inhibition of GSK3 $\beta$  stimulates the transcription of such target genes. PI3K signaling also controls angiogenesis, growth, proliferation, senescence and other processes through mechanisms including vascular endothelial growth factor (VEGF) transcriptional activation and induced hypoxia inducible factor-1 $\alpha$  (HIF1 $\alpha$ ) expression. The von Hippel Lindau (vHL) tumour-suppressor protein, through its oxygen-dependent polyubiquitylation of HIF1 $\alpha$  leading to HIF1 $\alpha$  degradation, has a central role in the mammalian oxygen-sensing pathway by opposing the effects of the PI3K pathway<sup>52</sup>.

### **1.3. Roles of class I PI3K signaling in T-lymphocytes**

Acquisition of a complete peripheral T cell repertoire requires that T cell progenitors undergo a series of tightly regulated developmental events that depend on integration of signaling cascades downstream of the pre-T cell receptor (TCR) and then the mature TCR. The first step in T cell development is the emigration of early thymic progenitors (ETPs) from the bone marrow to the thymus. ETPs then transit through four stages as CD4/CD8 double negative (DN) cells (DN1–4) before upregulating CD8 and CD4 to become double positive (DP) thymocytes. Emergence of mature T cells requires that developing thymocytes pass through several pre-TCR/TCR-dependent selection events: the first at the DN3 stage and then two others at the DP stage. DN3 thymocytes test the newly created pre-TCR $\beta$  chain for its ability to be functionally expressed during a process

known as  $\beta$ -selection, while DP cells test the reactivity of the mature TCR for selfpeptide/MHC during positive and negative selection<sup>53</sup>.

The PI3K signaling regulates many steps in the development, activation and differentiation of T-cells. p110 $\delta$  and p110 $\gamma$  are widely involved in thymocyte development, and differentiation, especially during  $\beta$ -selection and transition between immature DP and mature SP thymocytes<sup>54-55</sup> and several genetic approaches have been taken to investigate the functional role of PI3K signaling during T-cell development, maturation and function. Indeed, the catalytic and regulatory subunits of class I PI3K exhibit complex patterns of redundant expression and it has been difficult to use genetically altered mice with single PI3K mutations to unravel the complete role for this signaling pathway in early thymocyte development or subsequent mature T cell function.

PI3K activation, which occurs within seconds of T-cell activation, is essential during the early phases for T-cell proliferation. DN3 cell survival requires that signals delivered by multiple receptors, including Notch, the receptor for interleukin-7 (IL-7), and the pre-TCR, be appropriately integrated, and one pathway common to all three receptors is the PI3K signal transduction cascade. With regard to the PI3K regulatory subunits, it has been observed a redundancy in their function, as lack of p85 $\alpha$  and/or p85 $\beta$  subunits exerted limited effects<sup>53</sup>. Although loss of function of the catalytic subunit p110 $\delta$  had no measurable effect on T cell development, absence of p110 $\gamma$  resulted in decreased numbers of DP cells and a corresponding decrease in thymic cellularity. However, p110 $\alpha$  and p110 $\beta$  seem to compensate the absence of p110 $\delta$  expression<sup>56</sup>. Moreover, mice deficient in both catalytic subunits, p110 $\delta$  and p110 $\gamma$ , have small thymi due to a combination of increased apoptosis and decreased proliferation at the  $\beta$ -selection checkpoint and DP stages<sup>53</sup>. Further studies demonstrated the predominant role, during the  $\beta$ -selection checkpoint, of PDK1 to sustain proliferation and of Akt to maintain survival and cellular metabolism for this continued division<sup>53</sup>. Finally, genetic and pharmacological

experiments have shown that PI3K activation also regulates many steps in the activation and differentiation of T-cells<sup>55</sup>.

#### **1.4. T-cell acute lymphoblastic leukemia (T-ALL)**

T-cell acute lymphoblastic leukemia is a malignant disorder of T-cell lymphoid progenitor cells that affects 15% of children and 25% of adults ALL<sup>57</sup>, and is characterized by cytogenetic and molecular alterations that contribute to the acquisition of the transformed leukemic phenotype (Figure 5). Clinically, T-ALL patients show diffuse infiltration of the bone marrow by immature T cell lymphoblasts, high white blood cell counts, mediastinal masses with pleural effusions, and frequent infiltration of the central nervous system at diagnosis<sup>58</sup>. In T-ALL, recurrent chromosomal rearrangements together with novel identified genetic alterations led to the aberrant expression of T-cell oncogenes that define different leukemogenic pathways associated with outcome. Furthermore, recent genomic profile and high-throughput sequencing studies have identified mutations affecting novel recurring targets.

##### **1.4.1. Common T-ALL cytogenetic alteration**

Structural chromosomal aberrations are identified in approximately 50% of T-ALL<sup>59</sup> and frequently involve the juxtaposition of strong promoter and enhancer elements from T-cell receptor (TCR) genes (both *TCRαδ* at 14q11 and *TCRβ* at 7q34)<sup>60</sup> with transcription factors genes as consequence of an illegitimate event during V(D)J recombination in normal T-cell development. This lead to the aberrant expression of these fusion partners resulting in thymocyte differentiation block at various stages of maturation.

The basic helix-loop-helix (bHLH) family of transcription factors is characterized by a basic domain that mediates DNA binding, and a HLH motif that mediates homo and heterodimeric complex formation. *TAL1* (1p32), *LYL1* (19p13), *TAL2* (9q32) and *BHLH1*

(21q22) are members of class II bHLH not expressed in normal thymus. *TAL1* results ectopically expressed in T-ALL as consequence of t(1;14)(p32;q11)<sup>61</sup> (3% in childhood T-ALL) and more frequently as a consequence of the intrachromosomal deletion resulting in *SIL-TAL1* fusion gene, while *LYL1*, *TAL2* and *BHLH1* are upregulated in the rare translocations t(7;19)(q34;p13)<sup>62</sup>, t(7;9)(q34;q32)<sup>63</sup> and t(14;21)(q11;q22)<sup>64</sup>, respectively. Their aberrant expression may contribute to leukemia through the formation of heterodimers with class I bHLH members that regulate T-cell specific genes, with consequent differentiation and proliferation impairment. LIM domain only genes, *LMO1* (11p15) and *LMO2* (11p13), are involved in t(11;14)(p15;q11)<sup>65</sup> and t(11;14)(p13;q11)<sup>66</sup> with *TCRαδ* loci and in translocations with *TCRβ*<sup>60</sup>. LMO proteins function during the early stages of hematopoiesis by associating with other proteins, including *TAL1* and other bHLH components<sup>67</sup>, and their abnormal expression associate with deregulation of *LYL1* and *TAL1*, even in absence of specific translocations<sup>68</sup>. The homeobox (HOX) genes are a highly conserved family of transcription factors that play an important role in morphogenesis during embryonic development and in normal hemopoiesis<sup>69</sup>. The inv(7)(p15q34) and t(7;7)(p15;q34) bring the *TCRB* regulatory elements in the vicinity of the *HOXA* genes cluster disrupting the normal regulatory elements of the cluster with subsequent upregulation, especially of *HOXA9*, *HOXA10* and *HOXA11*<sup>70-71</sup>. *TLX1* (*HOX11*) is expressed at high level in more than 30% of adult T-ALL as consequence of t(10;14)(q24;q11) and t(7;10)(q34;q24)<sup>72</sup>, while *TLX3* (*HOX11L2*) is involved in t(5;14)(q35;q32) with the fusion partner *BCL11B* in about 20% children and 4% adults<sup>73</sup>. Additional genes rarely involved in *TCR* loci rearrangements are *LCK*<sup>74</sup>, *CCND2*<sup>75</sup> and *IRS4*<sup>76</sup>.

Furthermore, gene expression profiling studies have identified overexpression of these genes with a higher frequency compared with chromosomal rearrangements. Resulting signatures enable to classify T-ALL into major subgroups that are indicative of leukemic

arrest at specific stages of normal thymocyte development (*HOX11*<sup>+</sup> early cortical thymocytes; *LYL1*<sup>+</sup> early pro-T thymocytes; *TAL1*<sup>+</sup> late cortical thymocytes) and have clinical relevance, because are associated with a favorable or worse prognosis<sup>68</sup>. Moreover these results suggest that additional genetic lesions are involved in aberrant expression of these transcription factors.

Additional genetic abnormalities in T-ALL include translocations that generate fusion transcripts encoding new chimeric proteins with oncogenic properties. The *MLL* gene (11q23) rearranges with multiple partners in both myeloid and lymphoid malignancies and is generally associated with a worse prognosis. In T-ALL overall *MLL* fusions represent about 8% and preferential partners are *AF4* t(4;11)(q21;q23) and *ENL* t(11;19)(q23;p13.3), with the last one linked with a favorable outcome<sup>77</sup>. The t(10;11)(p13;q14) encoding *CALM-AF10* fusion oncogene is found in about 10% of T-ALL, both in children and adults, despite it is often cryptic and requires molecular characterization<sup>78</sup>. Content in AF10 and prognostic significance appear to depend on stage of maturation arrest. The cryptic deletion del (9)(q34.11q34.13) results in the *SET-NUP214* fusion product, which transcriptionally activate specific members of the *HOXA* cluster maybe contributing to T-ALL pathogenesis by the inhibition of T-cell maturation<sup>79</sup>. The *ABL1* cytoplasmic tyrosine kinase plays a role in T-cell signaling, leading to the induction of IL-2 production and proliferation following TCR activation<sup>80</sup>. *ABL1* fusion genes can be identified in about 8% of T-ALL. *EML1-ABL1* fusion due to a cryptic t(9;14)(q34;q32), *BCR-ABL1* t(9;22)(q34;q11), and *ETV6-ABL1* t(9;12)(q34;p13) are seldom reported chimeric genes in T-ALL, although they are frequent in other hematologic malignancies. In contrast, the most frequent and strictly associated with T-ALL is the *NUP214-ABL1* fusion identified in 6% of cases, in both children and adults. However, its prognostic relevance is unclear<sup>81</sup>. The Janus kinase-signal transducer (JAK) family are protein kinases that play an important role in promoting cell proliferation, differentiation, and survival in hematopoietic precursors. JAK2 is

constitutively activated in the rare t(9;12)(p24;p13) encoding the *ETV6-JAK2* fusion oncoprotein, while JAK1 is widely mutated in adult T-ALL (18%) and less in children (3%), and associates with a poor response to therapy<sup>82</sup>. Finally, a recent study identified a novel fusion partner of *ETV6* in one T-ALL patient, harboring *ETV6-ARNT* t(1;12)(q21;p13)<sup>83</sup>.

#### 1.4.2. Aberrant signaling in T-ALL

*NOCTH1* role in leukemogenesis was initially identified in the rare chromosomal translocation t(7;9)(q34;q34.3), that fuses the intracellular form of NOTCH1 to the TCR $\beta$  and leads to the expression of TAN1, a truncated and constitutively activated form of NOTCH1<sup>84</sup>. Subsequently, activating or loss of function mutations has been identified in more than 50% of T-ALL cases, representing the most common alteration in T-ALL<sup>85</sup>. After a protease cleavage mediated by  $\gamma$ -secretase, intracellular and active part of NOTCH1 (ICN) translocates to the nucleus where it regulates many downstream targets including *HES1*, *DTX1*, *PTCRA*, *NOTCH3*, *PTEN* and *MYC*<sup>86</sup>. NOTCH1 activating mutations seem to correlate with a good prognosis in pediatric T-ALL<sup>87</sup>. Other components of this pathway are mutated in T-ALL, as *FBXW7*<sup>88</sup>, a NOTCH1 proteasome-degradation mediator whose mutations lead to ICN activation, or *PTEN*<sup>89</sup>, a NOTCH1 target and negative regulator of PI3K/Akt signaling pathway whose mutations lead to uncontrolled proliferation of T-cells. Other mutated genes in T-ALL are *NRAS*<sup>90</sup>, the negative regulator of the RAS pathway *NF1* that is inactivated because of deletions or mutations<sup>91</sup>, and rarely *FLT3*<sup>92-93</sup> and *PTPN2*<sup>94</sup>, that are affected by activating mutations and focal deletions, respectively. All these genes play crucial roles as regulators and alterations in their function may affect critically different signal transduction pathways.

Another important pathway frequently deregulated in T-ALL is PI3K/Akt, as discussed below.

### 1.4.3. Novel molecular alterations identified in T-ALL

The introduction of high resolution microarray technologies has improved the identification of novel aberrations that can contribute to the onset or development of leukemia. The recurrent genetic alteration, predominantly a heterozygous frameshift mutation, in the tumor suppressors *WT1* has been identified in more than 10% of both pediatric and adult T-ALL and is associated with aberrant rearrangements of the oncogenic *TLX1*, *TLX3*, and *HOXA* transcription factor oncogenes<sup>95</sup>. *LEF1*, a member of the *LEF/TCF* family of DNA-binding transcription factors, which interacts with nuclear  $\beta$ -catenin in the *WNT* signaling pathway, is inactivated in 15% of childhood T-ALL and correlates with increased expression of *MYC* and *MYC* targets<sup>96</sup>. Deletion of 9p21.2 is a frequent event in T-ALL, being present in more than 70% of patients<sup>97</sup>. Recent genomic profiling studies confirmed this observation, indicating that loss of the tumor suppressor genes *CDKN2A/B* and *CDKN1B* is a common and early event in leukemogenesis<sup>98-100</sup>. Other lesions identified in T-ALL are copy number alterations that affected the early lymphoid regulators *IKZF1*, *IKZF2*, and *LEF1*<sup>100</sup>.  $TGF\beta$  is involved in proliferation of T-cell and its tumor suppressor pathway resulted inhibited in children T-ALL, through the loss of the intermediate *Smad3*. In recent years application of the novel whole genome scale technologies increased the knowledge about the genomic abnormalities which might sustain the onset/development of T-ALL, or which might contribute to the aggressiveness of the disease<sup>101</sup>. Despite that, T-ALL pathogenesis is still unclear and no effective targeted therapies exist. Because T-ALL is an extremely heterogeneous disease, application of next generation sequencing (NGS) is further improving its characterization with novel notions translatable to clinical practice. Through the X-chromosome DNA capture followed by NGS, Ferrando et al<sup>102</sup>. identified a new X-linked tumor suppressor gene, *PHF6* (PHD finger protein 6 on Xq26.3) with a proposed role in controlling gene expression, which inactivation is already associated with Borjeson-Forssman-Lehmann syndrome (BFLS, MIM301900). In T-ALL, mutational loss of

*PHF6* is a somatically acquired leukemia-associated genetic events, mainly due to widespread nonsense and frameshift mutations, and to a lower extent to missense mutations, which impair gene expression or protein function. *PHF6* mutations seem to be restricted to T-lineage ALL, are more frequent in males than females<sup>103</sup> and prevail in adults compared to pediatric patients. Moreover, *PHF6* mutations resulted associated with the aberrant expression of *TLX1* and *TLX3*<sup>68</sup> and with mutations of *NOTCH1*, *JAK1* and rearrangement of *SET-NUP214*<sup>104</sup>. However, the knowledge on *PHF6* role in leukemogenesis is extremely limited and its clinical significance is still unclear<sup>102</sup>. The recently identified early T cell precursor leukemia (ETP ALL) is a novel subtype of T-ALL which comprises up to 15% of T-ALL and confers a poor prognosis<sup>105</sup>. ETP ALL is characterized by a peculiar immunophenotype pattern (absence of CD1a and CD8 expression, weak CD5 expression, and expression of one or more myeloid- or stem cell-associated markers such as CD13, CD33, CD34 and CD117). This pattern is similar to that of murine early T-cell precursor<sup>106</sup> the thymic progenitors that have lost B-cell potential but still retain myeloid potential<sup>107</sup>. An extensive study of pediatric ETP ALL based on whole genome sequencing (WGS), transcriptome sequencing (mRNA-seq) and whole-exome sequencing (WES), has been conducted to define common genetic abnormalities<sup>108</sup>. Although ETP ALL appeared as a uniform immunophenotypic entity, no common alteration has been found. Overall, WGS analysis of 12 ETP ALL followed by a validation analysis in a recurrence cohort of 52 ETP ALL and 42 non-ETP ALL, confirmed a high degree of genetic instability<sup>105</sup> which induces both structural rearrangements and sequence mutations. Interestingly, among the genes involved in translocations, the authors identified *ETV6*, a transcription factor frequently altered in leukemia which is deleted or mutated in a large proportion of ETP ALL compared to non-ETP ALL (33% vs 10%)<sup>108</sup>. In addition to genes commonly mutated in T-ALL, pediatric ETP ALL sequence mutations/indels prevalently targeted cytokine receptor and RAS signaling pathway (e.g.

*BRAF*, *FLT3*, *IGFR1*, *JAK1*, *JAK3*, *KRAS*, *NRAS* ad *IL7R*); genes involved in hematopoietic development (e.g *RUNX1*, *IKZF1*, *ETV6*, *GATA3* and *EP300*); components of the polycomb repressor complex 2 (PRC2) which contributes to histone modifications (e.g *EED*, *EZH2* and *SUZ12*)<sup>108</sup>. In all the cases the percentage of mutated ETP ALL were extremely higher compared to non-ETP ALL. Novel recurrent somatic mutations have been found in *DNM2*, *ECT2L* and *RELN*, with unknown functions in normal lymphoid or leukemic development<sup>108</sup>. In adult ETP ALL<sup>109</sup>, WES analysis confirmed the presence of mutations in several genes, including the novel *DNM2*, and revealed the involvement of epigenetic regulators, in particular *MLL2*, *DNMT3A*, and with a lower rate *PRC2*. Of note, *DNMT3A* mutations are highly recurrent in patients with *de novo* acute myeloid leukemia (AML)<sup>110</sup>, highlighting the early maturational stage of ETP ALL, and encouraging the application of therapies used for AML treatment. *RUNX1* and *DNMT3A* mutations have also been identified in adult T-ALL, were resulted associated with shorter overall survival<sup>111</sup>. The mutational spectrum of typical T-ALL has been recently analyzed with WES in a large cohort of more than 60 adult and pediatric samples<sup>112</sup>. Through an accurate filtering approach, novel mutations have been detected in a set of candidate driver genes, including *CNOT3*, proposed to act as a tumor suppressor, and *RPL5* and *RPL10*, two genes encoding ribosomal proteins. Moreover, this study pointed out the clear correlation between the increase in patients age and mutation number, and the differences in mutation distribution between adult and pediatric T-ALL, with *CNOT3* mutations mainly present in adults, whereas *RPL10* mutations almost exclusively found in children. Nowadays, only one study has been conducted to compare matched diagnosis, remission and relapse samples, by means of WES<sup>113</sup>. The most remarkable finding of this study was the identification of relapse-associated mutations in *NT5C2* (5'-nucleotidase, cytosolic II), involved in cellular purine metabolism. *NT5C2* mutations prevail in relapsed T-ALL compared to relapsed B-ALL (19% vs 3%, respectively). These mutations affect the

nucleotidase activity of NT5C2 compared to wild-type, and confer resistance to the nucleoside analogs 6-mercaptopurine (6-MP) and 6-thioguanine (6-TG) commonly used in ALL treatment, as assessed in *in vitro* cellular model.

The sensitivity and accuracy of the high-throughput sequencing (HTS) have been translated into clinical practice through a targeted sequencing of TCR gene loci (TCRB and TCRG) by Wu et al., who identified in pre-treatment samples the recombined TCR gene sequences representing the patient's clonal neoplastic T lymphoblasts, and evaluated minimal residual disease (MRD) in paired post-treatment T-ALL patients<sup>114</sup>. The importance to assess MRD in order to predict clinical outcomes of patients is broadly recognized<sup>115</sup>. Compared to conventional multiparametric flow cytometry (mpFC) approach, there were no cases in which MRD was detected by mpFC but not by HTS. Moreover, HST enabled detection of the clonal TCR rearrangement in post-treatment samples where mpFC failed to do it, highlighting the potential of this technology to improve clinical diagnosis, patients' stratification and subsequent MRD monitoring with lower detection thresholds.

NGS approach has also been successfully used in T-ALL murine<sup>116</sup> and cellular model<sup>117</sup>. Exon capture sequencing in a murine model for heritable T-ALL, called Spontaneous dominant leukemia (Sdl), detected a spontaneously acquired dominant mutation in *Mcm4* ( $Mcm4^{D573H}$ ), which encodes for a protein essential for the initiation of eukaryotic genome replication.  $Mcm4^{D573H}$  is likely the causative tumor genetic lesion in Sdl, although if the role of MCM proteins is still unclear in human cancers<sup>116</sup>. Whole transcriptome deep sequencing of Jurkat cell line identified T-ALL-R-LncR1 as a novel long non-coding RNAs associated to T-ALL<sup>117</sup>. LncRNAs are transcribed RNA molecules but do not encode proteins and have an emerging role in cancer progression<sup>118</sup>. T-ALL-R-LncR1 were not detected in normal tissue specimens, while its expression was confirmed in tumor tissues and T-ALL patients samples. Moreover, knockdown of T-ALL-R-LncR1 predisposed T-ALL

Jurkat cells to undergo Par-4 (the proapoptotic factor prostate apoptosis response protein-4)-induced apoptosis. Although if these results obtained in murine or cellular models require further investigations in human T-ALL, they provided novel findings suitable to identify innovative targeted therapies.

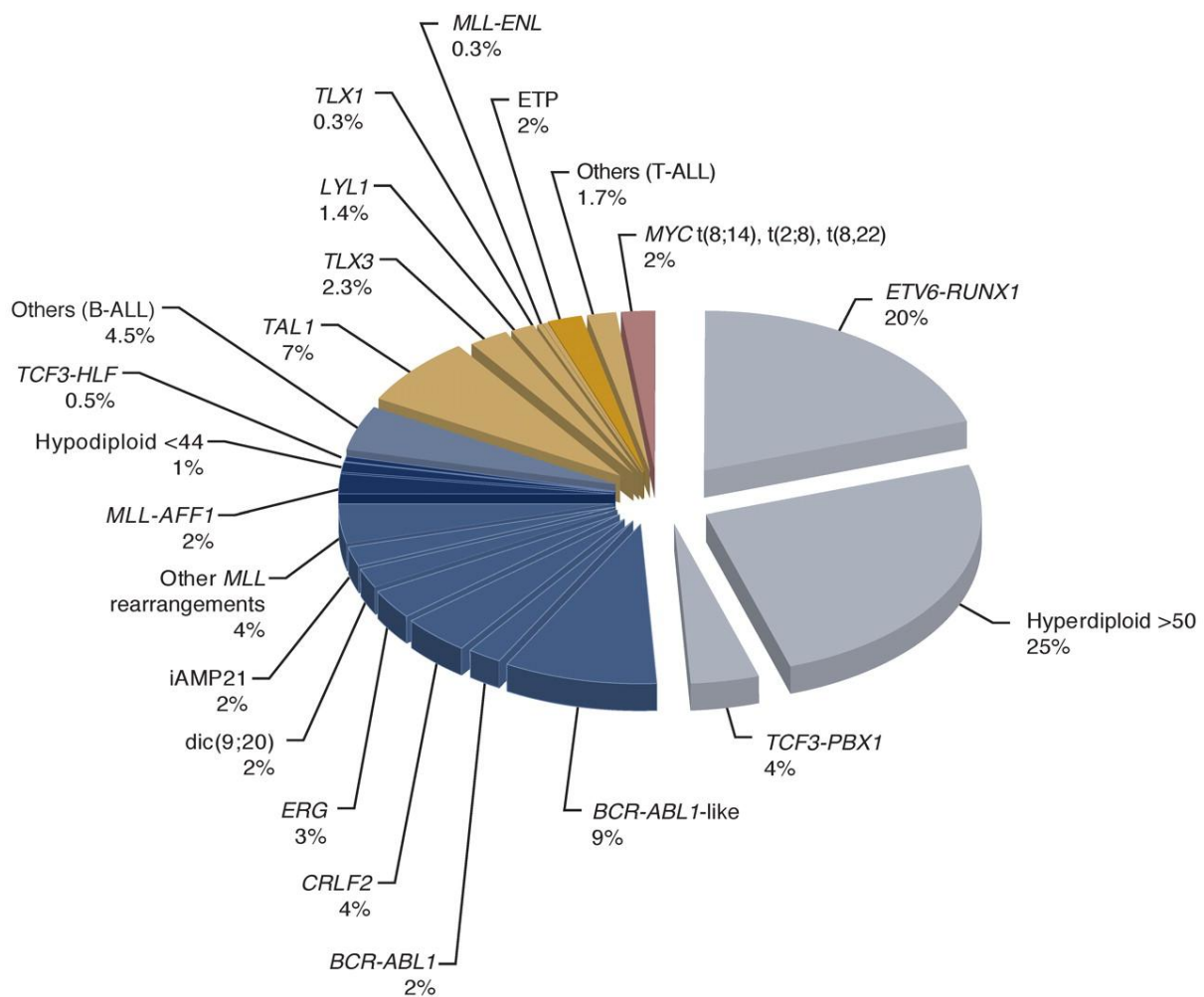


Figure 5: Estimated frequency of specific genotypes in childhood ALL. The pie chart includes comprises both B-lineage and T-lineage ALLs, to illustrate the relative frequency of each. The genetic lesions that are commonly associated with T-ALL are indicated in gold and those commonly associated with B-ALL in blue. The darker gold or blue color indicates those subtypes generally associated with poor prognosis<sup>119</sup>.

### 1.5. Activation of class I PI3K signaling in T-ALL

PI3K/Akt pathway is constitutively activated in more than 80% of T-ALL cases<sup>120</sup>. One mechanism responsible for PI3K activation is the presence of growth factors in the leukemia milieu that signal through cytokine receptors. Moreover, T-ALL cell lines present constitutively phosphorylated forms of Akt independently of external growth factors. In addition, NF- $\kappa$ B, a downstream target of PI3K/Akt, is constitutively activated in some primary T-ALL samples<sup>121</sup>. Nevertheless, conversely to solid tumors<sup>122</sup>, no activating mutations of PI3K and/or Akt have been described in T-ALL. It has been suggested that PI3K/Akt pathway over-activation results as a consequence of *PTEN* gene mutations<sup>89</sup>. However, whereas lack of PTEN protein is frequent in T-ALL cell lines, *PTEN* deletions as well as *PTEN* inactivating mutations predicted to cause protein truncation are low frequency events in T-ALL samples. Moreover, *PTEN* mutations resulting in protein truncation have been identified more frequently in T-ALL cell lines established from relapsed patients than in diagnostic clinical specimens, which suggests that *PTEN* deletion is a late event in human T-ALL<sup>123</sup>. In contrast, studies using mouse models have shown that PTEN deregulation is important at early stages of leukemogenesis. In these models, PTEN expression was shown to be essential to maintain the hematopoietic stem cell pool and to prevent leukemia development<sup>124-125</sup>. According to these observations, several studies have demonstrated that non-deletional inactivation of PTEN is a major contributor to hyperactivation of PI3K/Akt in primary T-ALL samples. PTEN posttranslational inactivation includes CK2-mediated phosphorylation and ROS-dependent oxidation of PTEN<sup>120</sup>. CK2 and PTEN can physically interact, and CK2-mediated phosphorylation of PTEN affects its activity and stabilizes the protein by preventing proteasome-mediated degradation. CK2 is overexpressed and hyperactivated in primary T-ALL cells and CK2-mediated phosphorylation of PTEN at Ser380 stabilizes PTEN expression and inhibits its activity, ultimately leading to PI3K/Akt pathway constitutive activation<sup>120</sup>. Moreover, high

ROS levels determine constitutive oxidation and inactivation of PTEN in T-ALL cells<sup>120</sup>. Further studies demonstrated a crosstalk between PI3K/Akt signaling pathway and ROS that is essential for IL-7-mediated T-ALL cell survival, as IL-7-mediated activation of PI3K pathway upregulates ROS through the upregulation of the glucose transporter Glut1 in T-ALL cells<sup>126</sup>. As mentioned above, gain-of-function mutations in *NOTCH1* are common in T-ALL. It exists a complex interplay between PI3K-Akt upregulation, loss of PTEN function and *NOTCH1* mutations that might be crucial for risk assessment, prediction of response and identification of effective targeted therapies in T-ALL patients<sup>127</sup>. Indeed, NOTCH1 regulates the expression of PTEN and the activity of the PI3K/Akt signaling pathway in normal and leukemic T cells. NOTCH1 mediates the transcriptional downregulation of *PTEN* through HES1, a transcription factor directly controlled by NOTCH1<sup>89</sup>. Therefore, activation of NOTCH1 in T-ALL also mediate the upregulation of the PI3K/Akt. This finding provide the basis for the design of therapeutic approach for T-ALL based on combined inhibition of both NOTCH1 and PI3K.

### **1.6. Therapeutic strategies to target PI3K/Akt/mTOR pathway**

Class I PI3K signaling is activated in different human cancers via several different mechanisms. In solid tumors, increased PI3K signaling is often due to direct mutational activation or amplification of genes encoding key components of the PI3K pathway such as *PIK3CA*, *PIK3CB*, *PIK3R1*, *AKT1* and *PDK1*<sup>4</sup>. *PTEN* is frequently mutated or deleted in solid tumors, as gastric, prostate or endometrial cancers, whereas it is frequently deregulated by posttranslational inactivation in T-ALL. PI3K also can be activated by genetic mutations and/or amplification of upstream RTKs, and possibly by mutationally activated Ras<sup>16</sup>. Moreover, in class I PI3Ks, the different isoforms of p110 and p85 preferentially mediate specific signaling processes, as suggested by biochemical and gene knockout studies with, however, a degree of redundancy. Therefore, it might be necessary

to develop isoform-specific inhibitors to decrease toxicity or pan inhibitors to increase efficacy. The mechanism of PI3K activation in an individual cancer may suggest the most effective type of therapeutic to inhibit the pathway (Table 1 and Figure 6).

**Dual PI3K/mTOR Inhibitors.** The catalytic domains of the p110 subunits and mTOR are structurally similar, because they all belong to the phosphatidylinositol kinase-related kinase family of kinases. Many chemical inhibitors under development inhibit both mTOR and the p110 catalytic subunits. These are termed dual PI3K/mTOR inhibitors. When compared with the other types of PI3K pathway inhibitors, dual PI3K/mTOR inhibitors have the possible advantage of inhibiting all PI3K catalytic isoforms, mTORC1 and mTORC2. Thus, they should effectively turn off this pathway completely and overcome feedback inhibition normally observed with mTORC1 inhibitors (e.g. rapamycin) that may limit their efficacy. However, it remains unknown if dual PI3K/mTOR inhibitors will be tolerable at doses that effectively inhibit all p110 isoforms and mTOR, or if their use will necessitate sacrificing complete inhibition of one or more of the potential targets. The pioneer PI3K/mTOR inhibitor is LY294002, which has been extensively used to explore the therapeutic potential of PI3K/mTOR inhibition in different cancer models, although it is unsuitable for patient use. Subsequently, other PI3K/mTOR inhibitors have entered clinical trials. Dual inhibitors being investigated in the clinical setting include BEZ235, SF1126, XL765 (SAR245409), PF-04691502, PF-05212384, GDC-0980, GSK2126458, and DS-7423<sup>128</sup>. With the potential to block compensatory signaling or feedback loops, dual PI3K/mTOR inhibitors represent an interesting drug class. Preliminary data show that simultaneous inhibition of all PI3K isoforms, mTORC1, and mTORC2 is feasible in the clinical setting, although several adverse events have been reported<sup>128</sup>. Robust clinical trials are needed to determine whether dual PI3K/mTOR inhibitors have a significant therapeutic advantage.

**Pan PI3K Inhibitors.** The PI3K inhibitors can be divided into isoform-specific inhibitors or pan-PI3K inhibitors. Pan PI3K inhibitors target all class IA PI3K isoforms ( $\alpha$ ,  $\beta$ ,  $\gamma$ ,  $\delta$ ). It has been hypothesized that inhibiting all 4 isoforms of class I PI3K may be advantageous over inhibiting specific isoforms. Some pre-clinical studies suggest that functional redundancy may lead to compensatory signaling after genetic or pharmacological inactivation of specific isoforms<sup>128</sup>. Pan PI3K inhibitors include wortmannin derivatives such as PX-886 or wortmannin prodrugs such as the self-activating viridians modified by dextran linker moieties<sup>16</sup>. Recently, novel pan PI3K inhibitors have been tested in both preclinical and clinical models. Pan PI3K inhibitors such as BKM120, XL147 (SAR245408), BAY 80-6946, PX-866, and GDC-0941 have demonstrated potent anticancer activity. BKM120 is a dimorpholinopyrimidine derivative that blocks Akt phosphorylation and inhibits tumor growth. The pan inhibitor BKM120 has been evaluated in both preclinical leukemic models<sup>129</sup> and phase I clinical trials for patients with solid tumors<sup>130-132</sup>, demonstrating its efficacy as a single agent or in combination with other therapies. BKM120 is at present extensively studied in phases I-III clinical trials which prevalently involve patients with advanced solid tumors. Moreover, BK120 efficacy is being evaluated in hematologic malignancies. A phase I study enrolling adults with advanced leukemias (NCT01396499); two studies enrolling Refractory Non-Hodgkin Lymphoma (NCT01719250, NCT01693614); a phase I study enrolling relapsed or refractory indolent B-Cell Lymphoma patients (NCT02049541). ZSTK-474 is another pan PI3K inhibitor which has been tested in preclinical settings<sup>133-135</sup> and is currently in clinical development. Overall, pan PI3K inhibitors have shown encouraging anticancer activity as single agents or in combination with other agents, and results from ongoing trials are eagerly awaited. Further investigation is needed to determine whether complete inhibition of all isoforms is necessary or the reliance of different tumors on PI3K isoforms will only require selective

isoform inhibitors, and whether the doses required for total target inhibition will be tolerable in patients.

***Isoform-specific PI3K inhibitors.*** Selective PI3K inhibitors may have benefit in tumors in which a particular isoform is predominantly expressed or more critical for survival. For example, PI3K $\alpha$  is expressed and frequently mutated in many tumor types; p110 $\beta$  has been suggested to control basal PtdIns(3,4,5)P<sub>3</sub> production and drive prostate tumour formation when PTEN is inactivated<sup>136</sup>; p110 $\delta$  and p110 $\gamma$  are mainly expressed in hematopoietic cells. Blocking the activity of specific isoforms that are crucial for survival could theoretically provide complete target inhibition at tolerable doses and maximize the toxic effects of this drug class. PI3K $\alpha$ -specific inhibitors are expected to be highly effective in tumors harboring *PIK3CA* activating mutations and several drugs, as BYL719, INK1117, and GDC-0032 are being evaluated in patients with solid tumors. KIN-193 and GSK2636771 specifically target the p110 $\beta$  isoform, and the latter entered clinical trials for PTEN-deficient solid tumors<sup>128</sup>. Because of the important role of p110 $\delta$  and p110 $\gamma$  isoforms in hematopoietic cells, dual PI3K inhibitors represent a possible strategy to treat blood malignancies. Accordingly, efficacy of IPI-145, that selectively inhibits p110 $\delta$  and p110 $\gamma$ , is being evaluated in several clinical trials enrolling ALL, CLL (Chronic Lymphocytic Leukemia) and Lymphoma patients<sup>128</sup>. Among the isoform specific PI3K inhibitors in development, idelalisib (CAL-101) which selectively inhibit p110 $\delta$ , is the most studied in hematologic malignancies and is being evaluated in several phase III studies. Because of the important role of p110 $\delta$  in B-cell, CAL-101 resulted high effective in CLL treatment<sup>137</sup>.

***Other strategies to inhibit PI3K signaling.*** As mentioned above, PI3K signaling pathway might be activated due to mutations that affect different components of the pathway as

well as alterations in upstream molecules. Therefore, beyond PI3K inhibition, other therapeutic strategies have been developed, including Akt and mTOR inhibition. Cancers with Akt1 mutations and Akt1 and Akt2 amplifications may be expected to be among the more sensitive to Akt inhibitors. However, this class of inhibitors will not block the non-Akt effectors of PI3K signaling and, paradoxically, could actually increase PI3K-dependent activation of those effectors via loss of negative feedbacks. This is especially important in light of the findings that the PDK1 substrate SGK3, and not Akt, may play a more prominent role in promoting PI3K-dependent viability in some cancers harboring PIK3CA mutations<sup>16</sup>. Whereas rapamycin specifically inhibits mTOR only in mTORC1, ATP-competitive mTOR inhibitors target the kinase domain of mTOR to impede the activity of both mTORC1 and mTORC2. Inhibiting mTORC2 would provide the theoretical advantage of blocking Akt activation<sup>16</sup>.

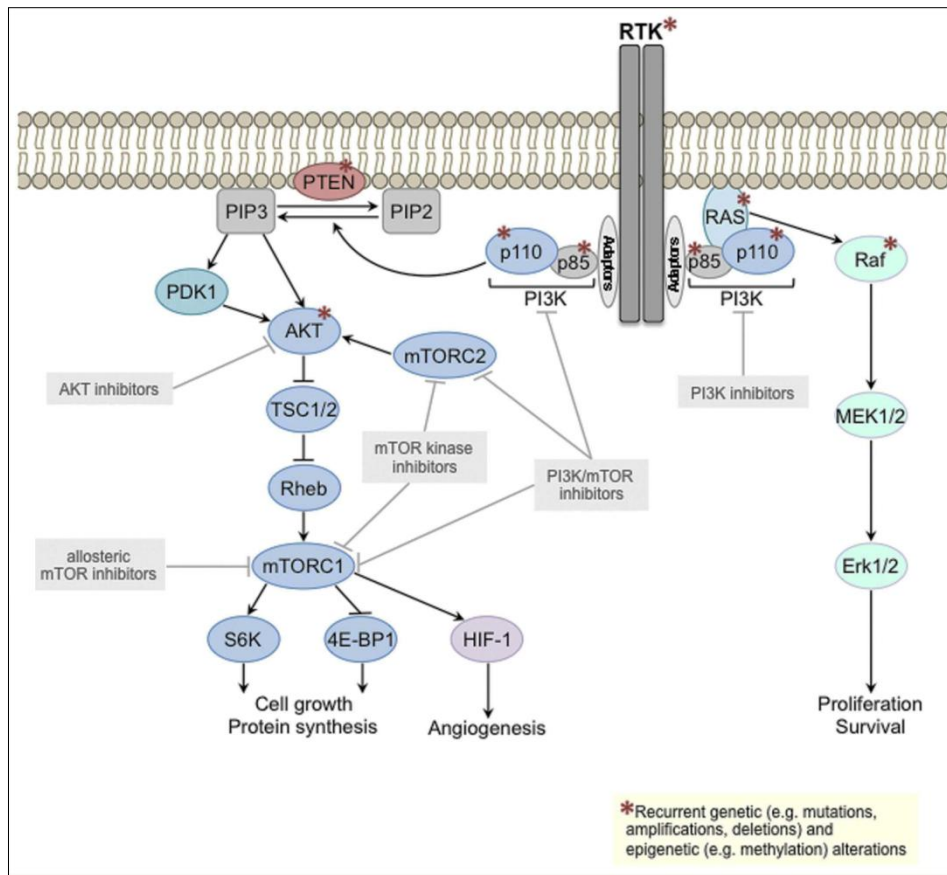


Figure 6: Schematic representation of class I PI3K signal transduction pathway. Points of therapeutic inhibition are highlighted<sup>138</sup>.

**Table 1: Several PI3K pathway inhibitors which are tested in clinical trials. Adapted from Weigelt and Downward<sup>138</sup>.**

Inhibitor name	Target	Clinical trial phase	Cancer type
<b>PAN-CLASS I PI3K INHIBITORS</b>			
BAY80-6946	Class I PI3K	I	Solid cancers
ZSTK474	Class I PI3K	I	Solid cancers
GSK1059615	Class I PI3K	I	Solid cancers
BKM120	Class I PI3K	I/II	Solid cancers, hematological malignancies (leukemia)
GDC-0941	Class I PI3K	I/II	Solid cancers, hematological malignancies (lymphoma)
<b>ISOFORM SPECIFIC PI3K INHIBITORS</b>			
BYL719	p110 $\alpha$	I	Solid cancers
GDC-0032	p110 $\alpha$	I	Solid cancers
INK-1117	p110 $\alpha$	I	Solid cancers
GSK2636771	p110 $\beta$	I/IIa	Solid cancers
IPI-145	p110 $\gamma/\delta$	I	Hematological malignancies
AMG319	p110 $\delta$	I	Hematological malignancies
CAL-101	p110 $\delta$	I/II/III	Hematological malignancies
<b>DUAL PI3K/mTOR INHIBITORS</b>			
GDC-0980	PI3K/mTOR	I	Solid cancers, hematological malignancies (lymphoma)
GSK2126458	PI3K/mTOR	I	Solid cancers
BEZ235	PI3K/mTOR	I/II	Solid cancers
BGT226	PI3K/mTOR	I/II	Solid cancers
PF-05212384	PI3K/mTOR	I/II	Solid cancers
XL765	PI3K/mTOR	I/II	Solid cancers
<b>mTOR INHIBITORS</b>			
INK-128	mTOR (kinase)	I	Solid cancers, hematological malignancies (myeloma)
OSI-027	mTOR (kinase)	I	Solid cancers, hematological malignancies (lymphoma)
CC-223	mTOR (kinase)	I/II	Solid cancers, hematological malignancies
Everolimus	mTOR (allosteric)	I/II/III	Solid cancers, hematological malignancies
Temsirolimus	mTOR (allosteric)	I/II	Solid cancers, hematological malignancies
<b>AKT INHIBITORS</b>			
GDC-0068	Akt	I/II	Solid cancers
GSK2110183	Akt	I/II	Solid cancers, hematological malignancies

## **2. AIMS**

Despite improvements in cure rates due to the introduction of intensified chemotherapy in modern protocols, the outcome of T-ALL patients with chemoresistant or relapsed leukemia is still poor<sup>58</sup>. T-ALL requires aggressive chemotherapy with well-known long-term side effects. To minimize and ultimately overcome the detrimental effects of current therapeutic regimens, it is essential to identify novel molecular targets in T-ALL in order to develop and test selective inhibitors of such targets<sup>58</sup>. In T-ALL, PI3K/Akt pathway activation is a common event that results from alterations such as phosphorylation, oxidation, and gene deletion/mutation, which directly affect PTEN function<sup>89,120,126</sup> or affect upstream regulators of the pathway<sup>139</sup>. Therefore, PI3K is an attractive target to efficiently treat T-ALL<sup>140-141</sup>.

The overall aim of this research has been to investigate the therapeutic potential of PI3K signaling inhibition in T-ALL. Studies were conducted in order to:

- I. Investigate the efficacy of the pan inhibitor BKM120 both *in vitro* and *in vivo* in T-ALL models-
- II. Define the better therapeutic approach to treat T-ALL, by comparing pan and isoform-specific PI3K inhibition.

BKM120 is a potent and highly selective pan-class I PI3K inhibitor which belongs to the 2,6-dimorpholino pyrimidine derivatives. It inhibits wild type and mutant PI3K p110 $\alpha$ ,  $\beta$ ,  $\delta$ , and  $\gamma$  isoforms but is inactive against class III PI3K and other kinases<sup>142</sup>. BKM120 has also been shown to exert a strong antiproliferative effect and to induce apoptosis in several cancer cell lines and mouse models of solid cancers by specifically inhibiting the biologic function of the PI3K downstream target Akt<sup>143-145</sup>. During this research period, BKM120 efficacy has been assessed for the first time in T-ALL demonstrating the potential of BKM120 in T-ALL treatment.

However, which class of agents among isoform-specific or pan inhibitors can achieve the greater efficacy is still an open question, as recent studies reported opposite results about the usefulness of dual p110 $\gamma$  and p110 $\delta$ <sup>146</sup> or the importance to blockade all class I PI3K isoforms to efficiently inhibit cell proliferation in T-ALL<sup>147</sup>. However, both these studies considered only PTEN-null T-ALL, whereas deletion of PTEN are rare events in T-ALL. Therefore, further analyses have been conducted to investigate the effects of PI3K inhibition in both a PTEN deleted and non-deleted cellular context, in order to elucidate the mechanisms responsible for the proliferative impairment of T-ALL.

### **3. MATHIERIAL AND METHODS**

### 3.1. Compound and reagents

PI3K inhibitors BKM-120, PIK-90, ZSTK-474, A-66, TGX-221, AS-605240, CAL-101 and IPI-145, the caspase inhibitor z-VAD and the autophagy inhibitors 3-methyladenine (3-MA), Bafilomycin A1 (Baf A1) and E64D were from Selleck Chemicals (Houston TX, USA). The chemotherapeutic drugs doxorubicin and vincristine were from Sigma-Aldrich (St. Louis, MO, USA). Drugs were dissolved in DMSO at a final concentration of 10 mM for *in vitro* studies or as described below for *in vivo* administration, and stored at -80°C until use. The insulin-transferrin-sodium selenite (ITS) supplement was purchased from Sigma-Aldrich. For western blotting analysis, the PI3K p110 $\delta$  and  $\beta$ -Actin antibodies were from Santa Cruz Biotechnology (Heidelberg, Germany). All other primary and secondary antibodies were bought from Cell Signaling Technology (Danvers, MA, USA). RPMI 1640 and MEM Alpha media, Hanks' balanced salt solution (HBSS) and fetal bovine serum (FBS) were from Life Technologies Italia (Monza, Italy).

### 3.2. Cell lines and primary samples

Human T-ALL cell lines Jurkat, Loucy, RPMI-8402, BE-13, HPB-ALL, PF-382, P12-ICHIKAWA, DND-41, MOLT-4, ALL-SIL, CCRF-CEM (CEM-S) and its resistant variant CEM-R (CEM-VBL100, drug-resistant cells overexpressing the ABCB1 drug transporter<sup>148</sup>) were grown in RPMI 1640 medium supplemented with 10-20% FBS, 100 U/ml penicillin and 100  $\mu$ g/ml streptomycin (Sigma-Aldrich) at 37°C in a humidified atmosphere of 5% CO<sub>2</sub>. DND-41 and MOLT-4 cells stably expressing luciferase and eGFP (DND-41.Luc.GFP and MOLT-4.Luc.GFP cells) were generated as described elsewhere<sup>149</sup>, grown in the same conditions and used for *in vivo* studies. MS-5 mouse stromal cells were grown in MEM Alpha medium supplemented with 10% FBS. Samples from T-ALL patients (n=6) were obtained with informed consent according to institutional guidelines, isolated using

Ficoll-Paque (GE Healthcare Bio-Sciences AB, Uppsala, Sweden) and grown in RPMI 1640 medium supplemented with 20% FBS and ITS.

### **3.3. Cell viability analysis and cell count**

To test the effects of PI3K inhibitors, T-ALL cell lines were cultured for 24 or 48 h in the presence of the vehicle (DMSO 0.1%) or increasing drug concentrations, and cell viability was determined using the MTT [3-(4,5-Dimethylthiazol-2-yl)-2,5-diphenyltetrazolium bromide] cell proliferation kit (Roche Diagnostic, Basel, Switzerland), according to manufacturer's instructions. Briefly, cells were plated in a 96-well plate (2.5 to 5x10<sup>4</sup> cells per well, 100 µl cell suspension per well) and cultured overnight in 10-20% serum to allow for exponential growth of cells. Cells were then treated with increasing concentrations of the drugs for the indicated times. At the end of the treatment, 10 µl 1X MTT labeling reagent was added to each well and incubated for another 4 h. The samples were solubilized with 100 µl of solubilization solution overnight at 37 °C. The optical density absorbance value of each well was read on a microplate reader (Bio-Rad) at 570 nm with a the reference wavelength at 690 nm. Every sample was performed in triplicate and in three independent experiments. The fraction of viable cells was calculated as follows: mean optical density value treated cells/mean optical density value control cells.

For drug-combination experiments, a combination index (CI) number was calculated using the CalcuSyn software (Cambridge, UK) based on the Chou and Talalay method<sup>150</sup>. CIs are calculated with the formula  $C_a/C_{xa} \times C_b/C_{xb}$ , where  $C_{xa}$  and  $C_{xb}$  are the concentrations of compound a and b alone, respectively, needed to achieve a given effect (x%) and  $C_a$  and  $C_b$  are the concentrations of compound a and b needed for the same effect (x%) when the drugs are combined. CI values between 0.1-0.9 define different grades of synergism, values between 0.9-1.1 are additive, whereas values >1.1 are antagonistic. Growth curves were generated by counting viable and non-viable cell

numbers by the Trypan blue dye exclusion method. Cells were seeded in 6-well plates, treated with the inhibitors at indicated concentrations or the vehicle alone (DMSO 0.1%) and counted at regular intervals up to 72 h. Doubling time was calculated with Roth V. 2006 (<http://www.doubling-time.com/compute.php>).

### 3.4. Flow cytometry analyses

**Apoptosis detection.** Apoptosis was determined by the binding of Annexin V-FITC to phosphatidylserine exposed to the cell membrane using the Annexin V-FITC Apoptosis Detection Kit (eBiosciences) and according to the manufacturer's instructions. A propidium iodide (PI) staining was also performed to simultaneously detect different populations of living, apoptotic and necrotic cells. Briefly,  $1 \times 10^6$  cells per sample were collected by centrifugation, washed in phosphate buffered saline (PBS, pH 7.4), and incubated with Annexin V-FITC in binding buffer for 15 min. After that, cells were washed, resuspended in binding buffer, stained with PI and analyzed.

**Cell cycle analysis.** Cell cycle analysis was performed using a PI/RNase A staining according to standard procedures. Cells were collected, washed with cold PBS and fixed/permeabilized with 70% ethanol at  $-20^{\circ}\text{C}$  overnight. Subsequently, cells were washed in cold PBS, stained with PI (40  $\mu\text{g/ml}$ ) in the presence of RNase, and analyzed. At least 10,000 events/sample were recorded.

**Flow cytometric detection of p-Akt(Ser473) and p-S6RP(Ser235/236).** Cells were collected by centrifugation, washed in PBS, fixed at  $37^{\circ}\text{C}$  for 10 min in PBS with 2% formaldehyde and left overnight at  $-20^{\circ}\text{C}$  in methanol 90% for permeabilization. Cells were then washed in PBS supplemented with 4% FBS and incubated overnight with the primary antibody (Cell Signaling Technology) at  $4^{\circ}\text{C}$ . Finally, after washing, cells were incubated 1 hour with the appropriate secondary FITC-conjugated antibody and analyzed.

**Flow Cytometry analysis of Ki-67 and PtdIns(3,4,5)P<sub>3</sub>.** In order to evaluate effects on proliferation, Ki-67 antigen expression during the different phases of cell cycle was evaluated. After 72 h treatment, cells were permeabilized with methanol/acetic acid (3:1) and incubated with the Ki-67 primary antibody (Cell Signaling Technology). Afterwards, samples were stained for 1 h with a FITC-conjugated secondary antibody (Beckman Coulter, Miami, FL, USA) followed by further 20 min incubation with PI. To detect PtdIns(3,4,5)P<sub>3</sub> levels, control (DMSO 0.1%) and treated (6 h) cells were fixed in 4% paraformaldehyde for 15 min, permeabilized in 0.4% Triton X-100 for 10 min, washed in PSB 1X with 1% BSA and incubated over night at 4°C with the FITC-conjugated Anti-PI(3,4,5)P<sub>3</sub> antibody (Echelon Biosciences Inc., Salt Lake City, UT).

All the analyses were performed on an FC500 flow cytometer (Beckman Coulter, Miami, FL, USA) with the appropriate software (CXP, Beckman Coulter).

### **3.5. Western blot analysis**

Immunoblotting was performed by standard methods. Cells were lysed using the M-PER Mammalian Protein Extraction Reagent supplemented with the Protease and Phosphatase Inhibitor Cocktail (Thermo Fisher Scientific Inc., Rockford, IL, USA). Cells were plated in RPMI 1640 complete medium at an initial concentration of 2.5 to 5x10<sup>5</sup> cells per ml and incubated for 24 h before drug treatment. Cells were collected by centrifugation and washed in cold PBS. Cell pellets were then lysed in 100–200 µl of M-PER Mammalian Protein Extraction Reagent (Thermo Fisher Scientific Inc., Rockford, IL, USA) supplemented with Protease and Phosphatase Inhibitor Cocktail (Thermo Fisher Scientific Inc.) and incubated on ice for 30 min. Cell debris were removed by centrifugation at 13000 r.p.m. for 25 min at 4 °C in a microfuge. Protein supernatants were collected, heated to 95 °C for 5 min, cooled on ice and were used for further analysis or stored at -80 °C. Equal amounts of protein samples (30 µg) were separated on sodium dodecylsulfate-

polyacrylamide gel electrophoresis and electrotransferred onto nitrocellulose membranes. Membranes were briefly washed in PBS-0.1% Tween-20 (PBS-T) and nonspecific binding sites were blocked in 5% non-fat dry milk in PBS-T for 1 h at room temperature with gentle agitation. After PBS-T washes, membranes were incubated overnight at 4 °C with primary antibodies diluted according to the manufacturer's instructions. Membranes were then incubated with horseradish peroxidase-conjugated secondary antibodies diluted 1:2000 in 5% non-fat dry milk in PBS-T for 1 h at room temperature with gentle agitation. Proteins were detected using the Amersham ECL Prime Western Blotting Detection Reagent (GE Healthcare, Little Chalfont, Buckinghamshire, UK), the ChemiDoc-It2 Imaging System and the VisionWorksLS Software for the analysis (UVP, LLC, Upland, CA).

### **3.6. T-ALL cell co-culture with MS-5 mouse stromal cells**

Jurkat cells were seeded at  $2.5 \times 10^5$ /ml and, after an overnight incubation, cell suspension was transferred on the top of MS-5 mouse stromal cells (at ~70% confluence) and treated with BKM120. After 48 h, Jurkat cells were harvested, washed and incubated with a phycoerythrin (PE)-conjugated anti-CD45 antibody (Beckman Coulter, Brea, CA, USA) or with an irrelevant isotypic control antibody. After a 30 min incubation, cells were resuspended in binding buffer containing Annexin V-FITC and analyzed by flow cytometry after electronic gating on CD45<sup>+</sup> leukemic cells.

### **3.7. Flow cytometric detection of T-ALL side population (SP)**

Vybrant® DyeCycle (Life Technologies Corporation, Grand Island, NY, USA), a cell-permeable DNA binding dye suitable for SP analysis on a violet laser flow cytometer, was employed for staining SP cells. Cells were suspended in HBSS containing 2% FBS and 2 mM HEPES buffer and incubated for 90 minutes at 37°C with 10 µM Vybrant® DyeCycle in 5% CO<sub>2</sub> atmosphere. To demonstrate staining specificity, control and treated cells were

pre-incubated with the multidrug transporter inhibitor Verapamil (Sigma-Aldrich) at a final concentration of 50  $\mu$ M before dye addition. SP cells were co-stained with Annexin V-FITC to detect apoptosis. After DyeCycle incubation, cells were washed twice with RPMI 1640, containing FBS 2%, and 10  $\mu$ L of cell pellet were resuspended in 5  $\mu$ L of Annexin V-FITC (Actiplate-FITC kit, Tau Technology, Kattendijke, NL) and 485  $\mu$ L of binding buffer, following the manufacturer's instructions. Cells were then maintained at 4°C for 20 min and analyzed on a Navios flow cytometer, equipped with a violet laser diode 405, and Kaluza software (Beckman Coulter). The flow cytometer filter set consisted of a 405 nm blue band-pass and a 675 nm red band-pass filter, for SP analysis. For Annexin V-FITC analysis, the 488 nm laser excitation was used (basic set).

### **3.8. *In vivo* subcutaneous human T-ALL mouse models**

Mice were housed and bred in a specific pathogen-free animal facility, treated in accordance with the European Union guidelines and approval of the Institutional Ethical Committee of Instituto de Medicina Molecular, Lisbon, Portugal. Eight week old NOD/SCID mice were subcutaneously injected in both flanks with  $10 \times 10^6$  DND-41.Luc.GFP or MOLT-4.Luc.GFP cells resuspended in 100 $\mu$ L of PBS. At day 5, mice were injected with luciferin to assess tumor burden by whole-body bioluminescence imaging and were equally distributed in 2 groups to receive 40mg/Kg BKM120 dissolved in 10% *N*-Methyl-2-pyrrolidone, 90% PEG 300 (po, daily) or vehicle control. Tumor growth was monitored twice weekly by bioluminescence and caliper measurements and mice were weighed frequently to determine treatment-induced toxicity. For bioluminescence imaging, mice were anaesthetized, intraperitoneally (i.p.) injected with 1.5mg luciferin/g, and scanned with an IVIS Lumina bioimaging device (Caliper Life Sciences, Hopkinton, MA, USA), after 15 minutes, as described<sup>149</sup>. Total flux (photons per second) was calculated using Living Image software (Caliper Life Sciences). For caliper measurements tumor volume was

calculated using the formula: volume = length x width<sup>2</sup> / 2, as described<sup>153</sup>. Mice were sacrificed at day 40 (DND-41.Luc.GFP cells) and day 50 (MOLT-4.Luc.GFP cells) after cell transfer.

### 3.9. Gene expression analysis

Total RNA was isolated either from control (DMSO 0.1%) and from 24 h ZSTK-474 treated cells using RNeasy Mini Kit (QIAGEN, Valencia, CA, USA) according to the manufacturer's instructions. RNA concentration was determined by measuring the absorbance at 260 nm; for all samples, the OD 260/OD 280 absorbance ratio was of at least 2.0. 3.5 µg of total RNA were reverse-transcribed into cDNA using the iScript<sup>TM</sup> Advanced cDNA Synthesis Kit (Bio-rad, Hercules, CA, USA). Gene expression of specific autophagy markers was measured using the PrimePCR<sup>TM</sup> Assay for real-time (Bio-rad). For each sample, cDNA was mixed with 2x SsoAdvanced<sup>TM</sup> universal supermix (25 ng cDNA/reaction) containing SYBR Green (Bio-rad) and aliquoted in equal volumes to each well of the real-time PCR arrays. The quantitative PCR reaction was performed using a 7300 Real-Time PCR system (Applied Biosystems, Foster City, CA, USA). The quantitative PCR thermal protocol consisted of 95°C for 2 minutes, followed by 40 cycles of 95° C for 5 seconds and 60° C for 30 seconds. *RLP0* was used as control gene and the relative gene expression among samples was calculated as  $2^{-\Delta Ct154}$ . These data were then subjected to hierarchical clustering using the Spearman's rank correlation metric and the average-linkage method and heatmaps were generated using the data analysis tool TIGR Multiexperiment Viewer (<http://www.tm4.org/>)<sup>155</sup>. To examine the effects of pan PI3K inhibition in the different cell lines, gene expression of the treated cell lines was compared with that of untreated control and fold change due to the treatment was expressed as  $2^{-\Delta\Delta Ct154}$ . A 2.0-fold change in gene expression was used as the cut-off threshold.

### **3.10. Statistical analysis**

Significant effects between treatment and control groups in the *in vitro* studies were analyzed using the Student's unpaired *t* test and the Dunnett's test. *In vivo* differences in tumor development and survival were determined by two-way ANOVA and LogRank test, respectively. Differences were considered significant for  $p < 0.05$ .

**PART I: ACTIVITY OF THE PAN-CLASS I PHOSPHOINOSITIDE  
3-KINASE INHIBITOR NVP-BKM120 IN T-CELL ACUTE  
LYMPHOBLASTIC LEUKEMIA**

## 4. RESULTS

#### **4.1. BKM120 decreases the viability of T-ALL cell lines *in vitro* by promoting apoptosis**

We first evaluated the baseline expression levels of critical components of the PI3K/Akt pathway in T-ALL cell lines by western blotting analysis. Despite some heterogeneity, all the T-ALL cell lines expressed the PI3K isoforms p110 $\alpha$ ,  $\beta$ ,  $\delta$ ,  $\gamma$  (Figure 7 A). Importantly, all cell lines displayed phosphorylated Akt, which is indicative of constitutive activation of PI3K signaling pathway (Figure 7 A). Moreover, as previously reported<sup>89</sup> and according to the presence of cell line gene mutations as reported in the COSMIC database (cancer.sanger.ac.uk)<sup>156</sup>, we confirmed the absence of PTEN protein expression in most T-ALL cell lines analyzed, except for BE-13, DND-41 and HPB-ALL. However, in these three cell lines PTEN was phosphorylated at Ser380, a marker of PTEN posttranslational inactivation and consequent PI3K pathway activation<sup>23</sup>. To assess the cytotoxic effects of BKM120, T-ALL cell lines were incubated with increasing concentrations of the drug for 24 and 48 h. Cell viability decreased in a concentration-dependent fashion and the IC<sub>50</sub> values ranged between 1.4 and 5.3  $\mu$ M at 24 h and 0.9 and 5.5  $\mu$ M at 48 h (Figures 7 B and C). Because in a phase I clinical study the maximum tolerated dose of BKM120 resulted to be 100 mg/d, corresponding to a maximum plasma concentration ( $C_{max}$ ) of about 2  $\mu$ M after the first day treatment and 4  $\mu$ M at the steady-state<sup>132</sup>, for subsequent experiments we have not exceeded these concentrations. Because effects on cell viability may result either from cell death or cell cycle arrest, we then investigated both these aspects.

To evaluate whether the effects of BKM120 on cell viability could be related to apoptosis, flow cytometric analysis was performed. In response to treatment with 2  $\mu$ M BKM120, we detected a statistically significant increase in the percentage of early apoptotic (single-positive for Annexin V) and/or late apoptotic (Annexin V and PI double-positive) cells after either 24 or 48 h of treatment (Figure 7 D). Apoptosis was further investigated by western

blotting, which revealed a time- and concentration-dependent cleavage of caspase-9, -3 and -2 (Figure 7 E).

#### **4.2. BKM120 blocks T-ALL cell cycle progression at the G<sub>2</sub>/M phase**

We next evaluated the effect of BKM120 on cell cycle progression. Analysis of PI-stained T-ALL cells treated with 2  $\mu$ M BKM120 documented the occurrence of a block in the G<sub>2</sub>/M phase of the cell cycle in almost all the tested cell lines at 24 h of treatment (Figure 8 A). Comparison with the untreated cells revealed a dramatic increase from 20% to 50% in G<sub>2</sub>/M cells, with a consequent reduction of G<sub>0</sub>/G<sub>1</sub> and S phase cells. Then, cell cycle arrest was followed by apoptosis, as documented by the increase in the subG<sub>1</sub> cell population at later times of treatment (Figure 8 B, MOLT-4 cells). CEM-R cells were the only exception, immediately showing a significant increase in subG<sub>1</sub> cells, indicating rapid induction of cell death (Figure 8 A). Of note, CEM-S and DND-41 cells remained in the G<sub>2</sub>/M phase of the cell cycle up to 72 h of treatment, without cell death induction, in accordance with the low apoptotic-rate detection by Annexin V/PI staining (Figure 8 B, DND-41 cells).

#### **4.3. BKM120 affects the PI3K pathway in T-ALL cell lines**

To assess the effects of BKM120 on the PI3K pathway, we analyzed the expression and activation of key downstream targets in our panel of leukemic cell lines. We detected a concentration- and time- dependent decrease of Ser473 p-Akt and Ser235/236 p-S6RP (S6 ribosomal protein) in all the cell lines, while total proteins levels were unaffected, confirming the effectiveness of the drug in inhibiting PI3K activity (Figure 9 A). Of note, CEM-S, CEM-R and Jurkat cell lines also displayed reduced levels of Thr37/46 p-4E-BP1 [eukaryotic translation initiation factor (eIF)-4E-binding protein 1] indicating full inhibition of mTORC1 activity which leads to oncogenic protein synthesis impairment (Figure 9 B).

Moreover, BKM120 did not induce the activation of alternative and Akt-related cell proliferation pathways such as Raf/MEK/ERK<sup>158</sup>, as documented by the unchanged levels of phosphorylated, active, Erk1/2 in both Jurkat and DND-41 cells (data not shown).

#### **4.4. BKM120 retains most of its pro-apoptotic activity also in the presence of bone marrow stromal cells**

Mesenchymal stromal cells (MSCs) are important components of the bone marrow (BM) niche which supports and maintains hematopoietic stem cells (HSCs) but also leukemic stem cells (LSCs) through similar interactions<sup>159</sup>. MSCs are intrinsically resistant to most chemotherapeutic agents<sup>160</sup> and therefore may protect LSCs against chemotherapy-induced apoptosis. Hence, we investigated this issue by analyzing by flow cytometry the pro-apoptotic activity of BKM120 in Jurkat cells co-cultured with MS-5 murine stromal cells. As documented in Figure 10 A, BKM120 induced apoptosis in about 70% of Jurkat cells cultured alone. When co-cultured with MS-5 cells, the percentage of apoptotic Jurkat cells was reduced to around 50%, indicating that the drug retained a significant cytotoxicity also under these conditions (Figure 10 B). Of note, the PI3K/Akt pathway was activated in MS-5 cells (data not shown), and BKM120 was able to partially affect MS-5 cell survival, as it induced apoptosis in about 20% of cells (Figure 10 B and C). Thus, also this effect of BKM120 on stromal cells could be important for leukemia cell eradication.

#### **4.5. BKM120 is cytotoxic to and inhibits the PI3K pathway in primary T-ALL blasts**

To better assess the potential therapeutic value of BKM120 in T-ALL, we analyzed six pediatric T-ALL patient samples isolated from either BM or peripheral blood. The sensitivity of blast cells to BKM120 was evaluated using MTT assays and flow cytometry. After 72 h

of treatment with increasing concentrations of BKM120, cell viability was markedly reduced in all patient samples analyzed (n=6), with IC<sub>50</sub> values ranging between 1.04 and 5.25 μM (Figures 11 A and B). Flow cytometric and western blotting analysis revealed high levels of Ser473 p-Akt and Ser235/236 p-S6RP in untreated samples, indicating the constitutive activation of the PI3K pathway in these patients. Treatment with 2-4 μM BKM120 for 24 h induced a considerable decrease in the levels of these phosphorylated proteins and partially reduced p-4EB-P1 levels (Figure 11 C and D), indicating a potent inhibition of PI3K pathway. Finally, Annexin V-FITC/PI staining documented the presence of apoptotic cells following drug administration (Figure 11 E). Overall, these findings demonstrate that BKM120 has potent cytotoxic activity against leukemic cells from T-ALL patients displaying constitutive PI3K activation.

#### **4.6. BKM120 is synergistic with chemotherapeutics agents in primary T-ALL samples**

We further investigated whether BKM120 could synergize with chemotherapeutic agents commonly used in T-ALL therapy regimens. For this purpose, patients lymphoblasts were treated with increasing concentrations of vincristine or doxorubicin, either alone or in combination with BKM120 at fixed ratios (vincristine/BKM120, 1:100 and doxorubicin/BKM120 1:2). The synergistic effect was particularly evident with the BKM120/doxorubicin combination, that displayed CIs < 0.3, indicating a strong synergism (Figure 12 A). In contrast, with the BKM120/vincristine combination, a milder synergism (CIs >0.3) was observed.

#### **4.7. BKM120 targets the T-ALL SP**

LSCs represent a rare population of the leukemic clone which potentially can reconstitute the tumor after a successful therapy due to their self-renewing capacity<sup>161</sup>. LSCs share with the normal HSC counterpart different characteristics, including the expression of ABC transporter protein family members, among which ABC subfamily G member 2 (ABCG2) is one of the most important and well characterized<sup>162</sup>. The high expression of these transporters enables a flow cytometric identification of these cells as SP, which is characterized by a low retention of vital dyes<sup>163</sup>. We identified the SP in primary T-ALL blasts using the Vybrant® DyeCycle. As a control, ABC transporter activity was inhibited using Verapamil hydrochloride (Figure 12 B and C). In untreated samples, about 10% of SP cells were Annexin V-positive. After 24 h of treatment with BKM120, about 50% of SP cells were apoptotic (i.e. Annexin V-positive), thus documenting the ability of BKM120 to target the SP.

#### **4.8. BKM120 delays T-ALL tumor growth *in vivo***

The significant *in vitro* antitumor activity of BKM120 on T-ALL cells led us to investigate its anti-leukemic efficacy in animal models. NOD/SCID mice were injected subcutaneously either with DND-41.Luc.GFP or MOLT-4.Luc.GFP cells. At day 5 after cell transfer, mice were equally distributed according to tumor burden in 2 groups to receive 40mg/Kg of BKM120 or vehicle control. For both cell lines we observed a significant delay in tumor growth in the BKM120-treated group (Figure 13 A), resulting in prolonged survival of treated mice (Figure 13 B). Treatment was well tolerated as indicated by the maintenance of body weight and the lack of other signs of toxicity (data not shown). To confirm the *in vivo* effects of BKM120 on the PI3K pathway, mice were sacrificed 1 hour after BKM120 treatment at day 40 (for DND-41.Luc.GFP cells) or day 50 (for MOLT-4.Luc.GFP cells)

after cell transfer and cell lysates were obtained from the tumor mass. In both cell lines a significant reduction in the phosphorylation levels of Ser473 p-AKT and Ser235/236 p-S6RP was observed (Figure 13 C and D), showing that BKM120 effectively blocks the aberrant activity of the PI3K signaling pathway *in vivo*.

## 4.9. Figures

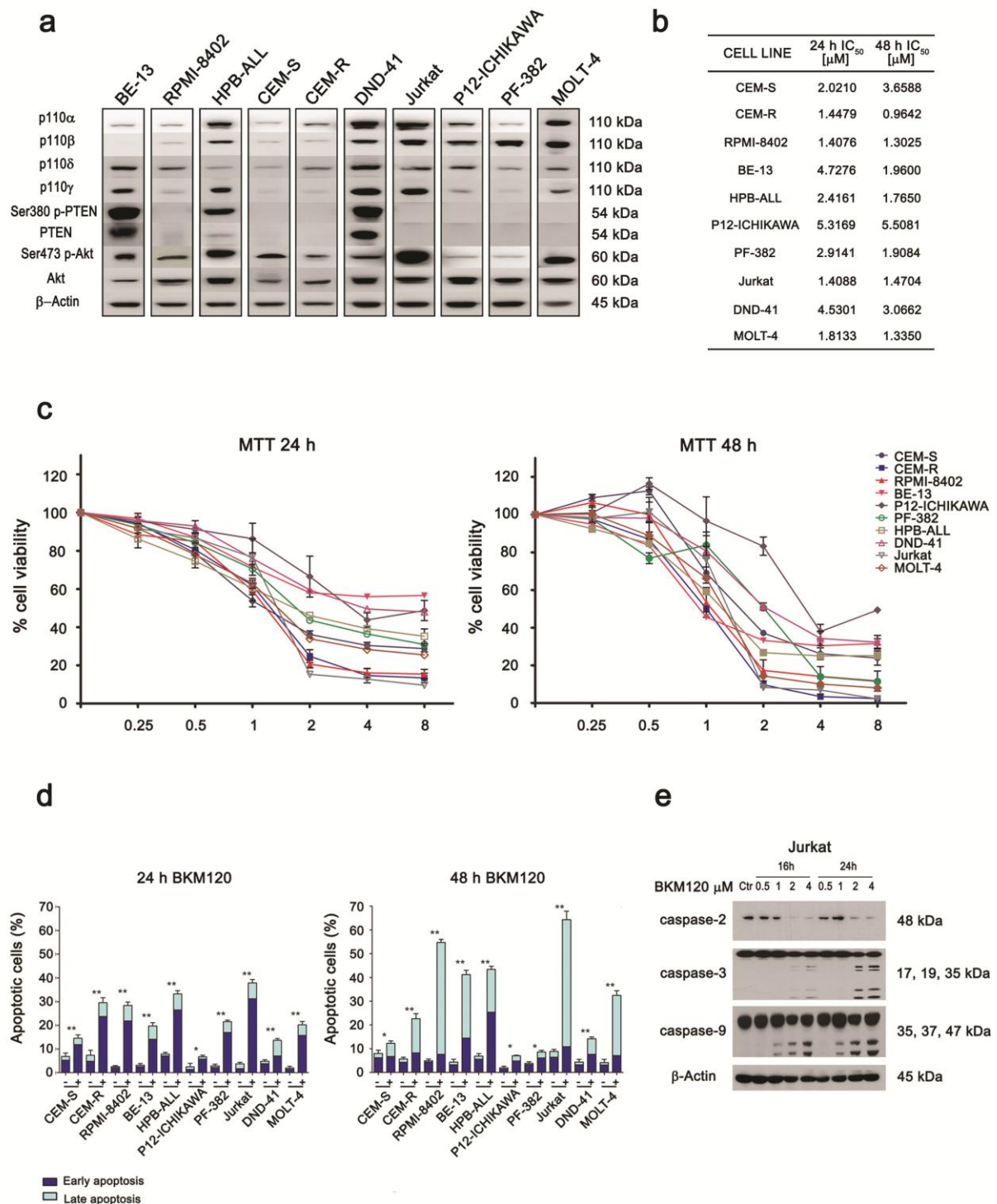


**Figure 7: BKM120 induces apoptosis of T-ALL cell lines with constitutively active PI3K/Akt pathway. (a)** Western blot analysis of T-ALL cell lines to detect the expression levels of the class I PI3Ks isozymes, and the expression/phosphorylation of both the PI3K regulator PTEN and the PI3K downstream target, Akt. **(b)** IC<sub>50</sub> values obtained through MTT assay **(c)** after 24 and 48 h treatment with increasing concentration of BKM120 (bars, SD). **(c)** Flow cytometric analysis of Annexin V-FITC/PI-stained T-ALL cells treated with 2 μM of BKM120 for 24 and 48 h documented a significant increase in apoptotic cells with respect to untreated cells. Asterisks indicate statistically significant differences with respect to untreated cells (\*:  $p < 0.05$ ; \*\*:  $p < 0.005$ ). **(d)** Western blotting demonstrated a concentration- and time-dependent cleavage of caspases-2, -3 and -9, in agreement with the intrinsic apoptotic pathway activation.

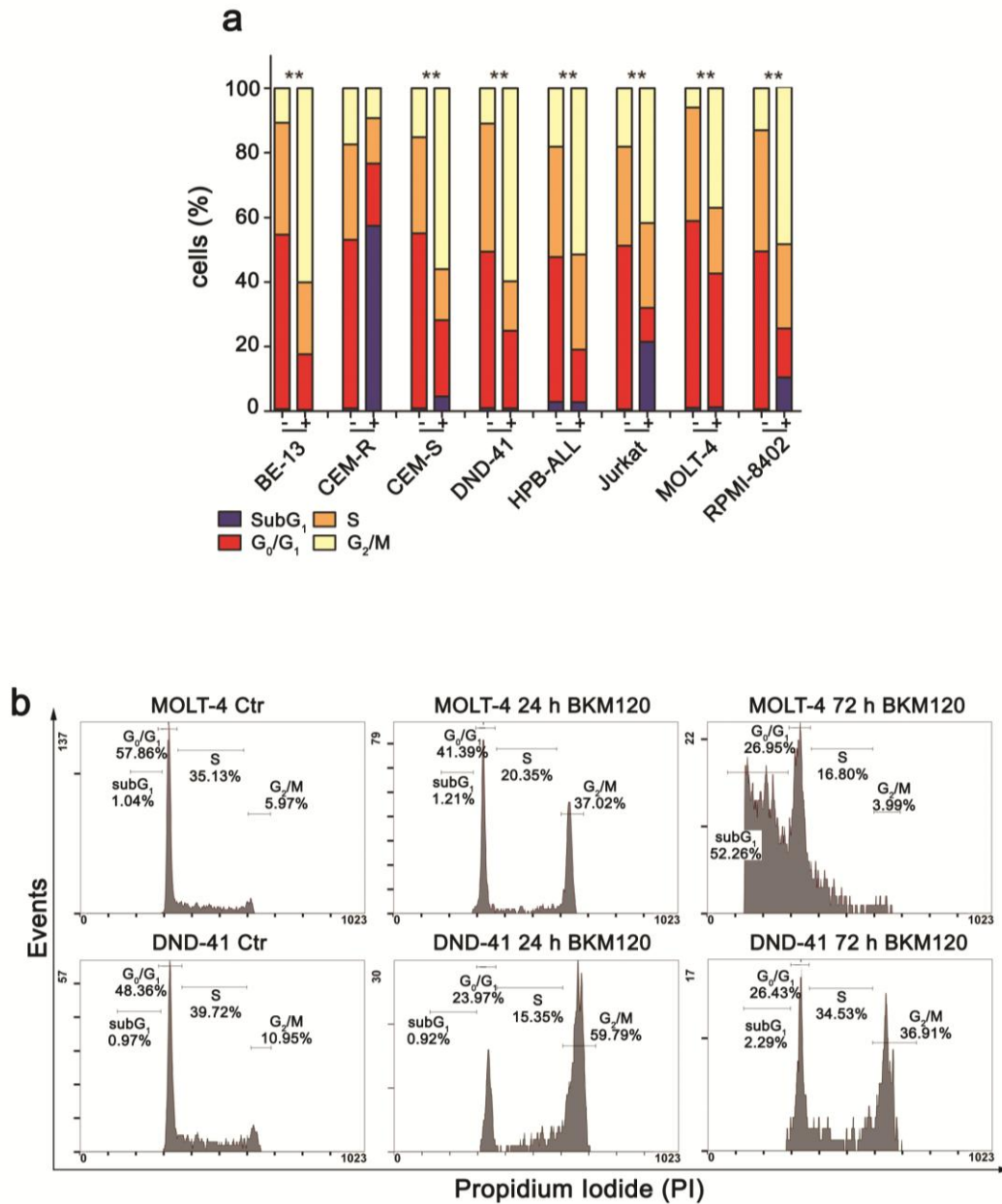


**Figure 8: BKM120 arrests cell cycle at the G<sub>2</sub>/M phase. (a)** Flow cytometric analysis of PI-stained cells revealed an increase in the G<sub>2</sub>/M cell fraction in seven out of eight cell lines induced by treatment with 2  $\mu$ M of BKM120 for 24 h. Results are the mean of three different experiments  $\pm$  SD. Asterisks indicate statistically significant differences with respect to untreated cells (\*\*:  $p < 0.005$ ). **(b)** Cell cycle time-course analysis. Similar results were obtained in CEM-S cells (not shown). Ctr, untreated cells.

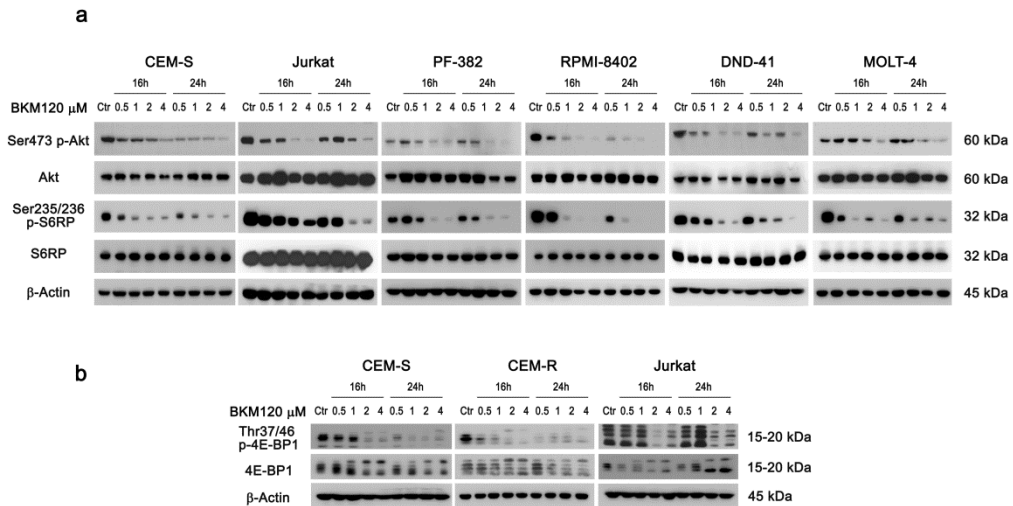


**Figure 9: BKM120 cytotoxicity is related to PI3K pathway inhibition.** Cells were cultured for different times in the presence of increased concentrations of BKM120, as indicated, and western blot analysis was then performed. BKM120 induced a concentration- and time-dependent dephosphorylation of the main PI3K downstream targets Akt, S6RP (a) and 4EB-P1 (b).

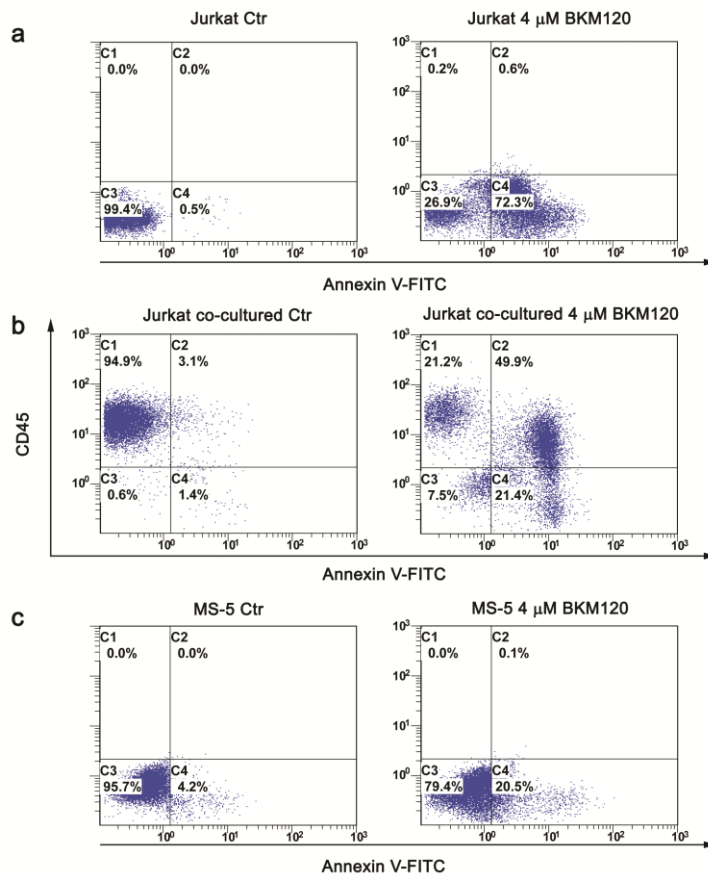


**Figure 10: BKM120 overcomes the protective effects induced in Jurkat cells by co-culturing with MS-5 stromal cells, which mimic the bone marrow microenvironment.** (a) Flow cytometric analysis of Annexin V-FITC in Jurkat cells maintained as suspension cultures and treated for 48 h with 4  $\mu$ M BKM120. (b) Flow cytometric analysis of Annexin V-FITC/CD45-PE staining of Jurkat cells (CD45+) growing in a co-culture system with MS-5 cells (CD45-) and treated with BKM120, evidenced the persistence of apoptosis induction nearly to 50% (C2 quadrant). Cells in C4 quadrant are apoptotic MS-5 cells (CD45-). (c) Flow cytometric analysis of Annexin V-FITC staining of MS-5 cells cultured alone with BKM120. Ctr, untreated cells.

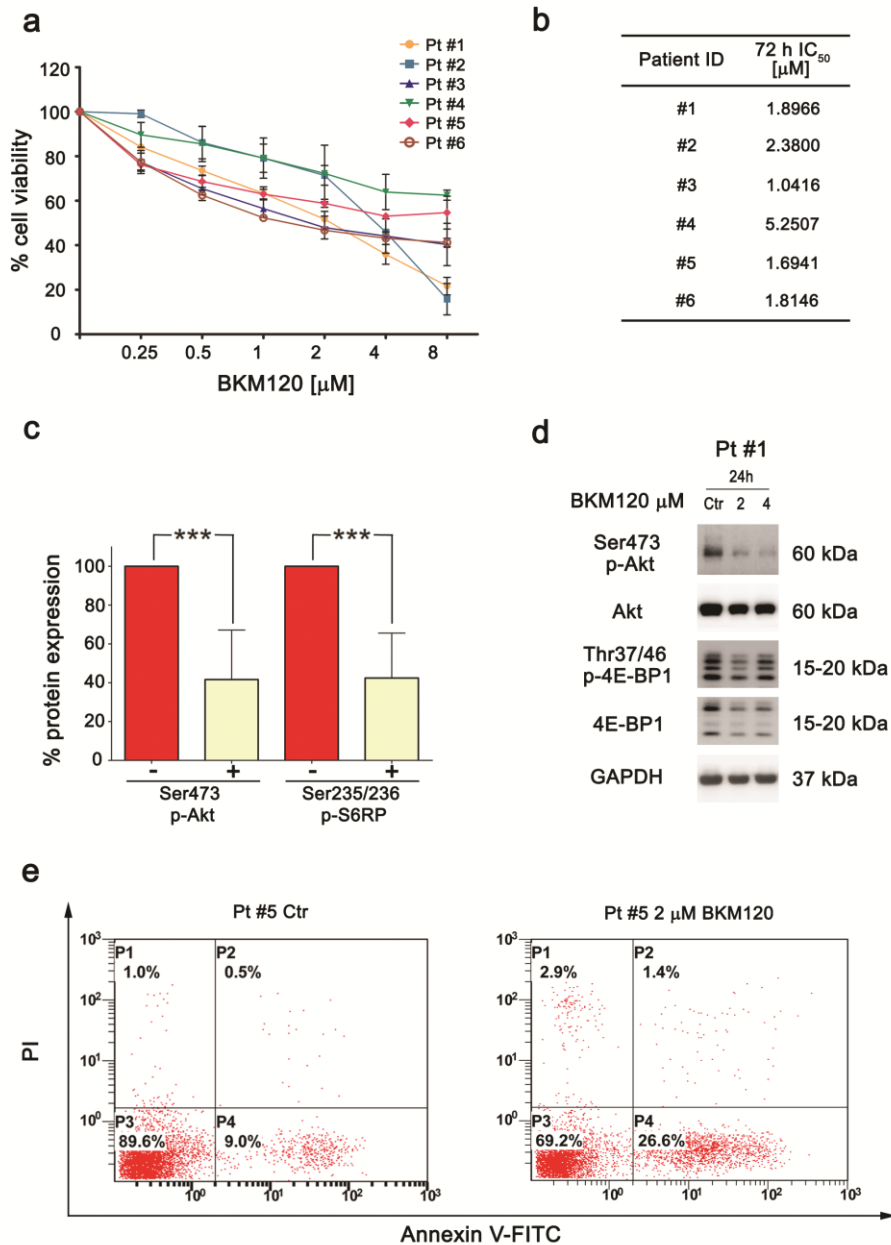
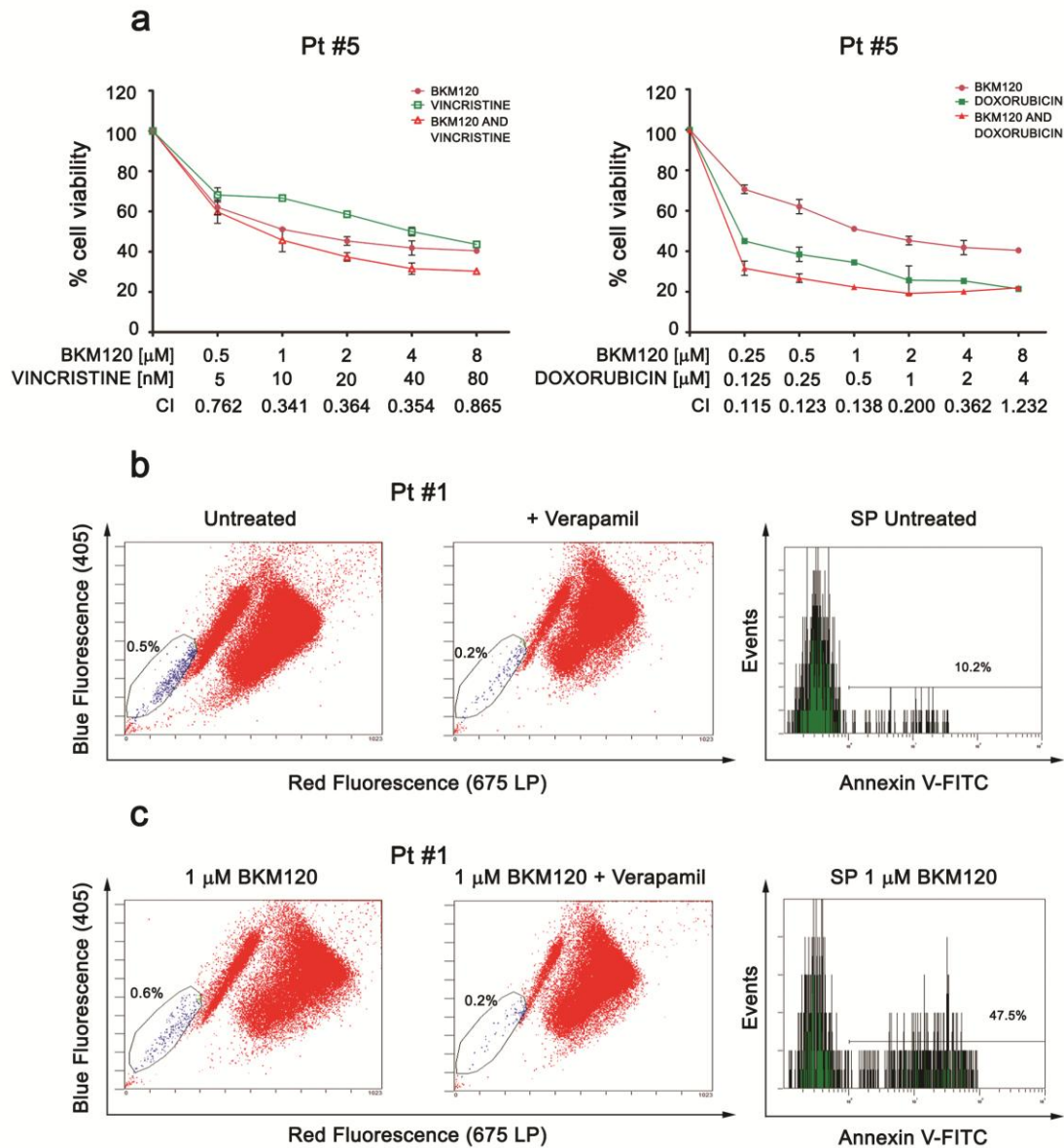
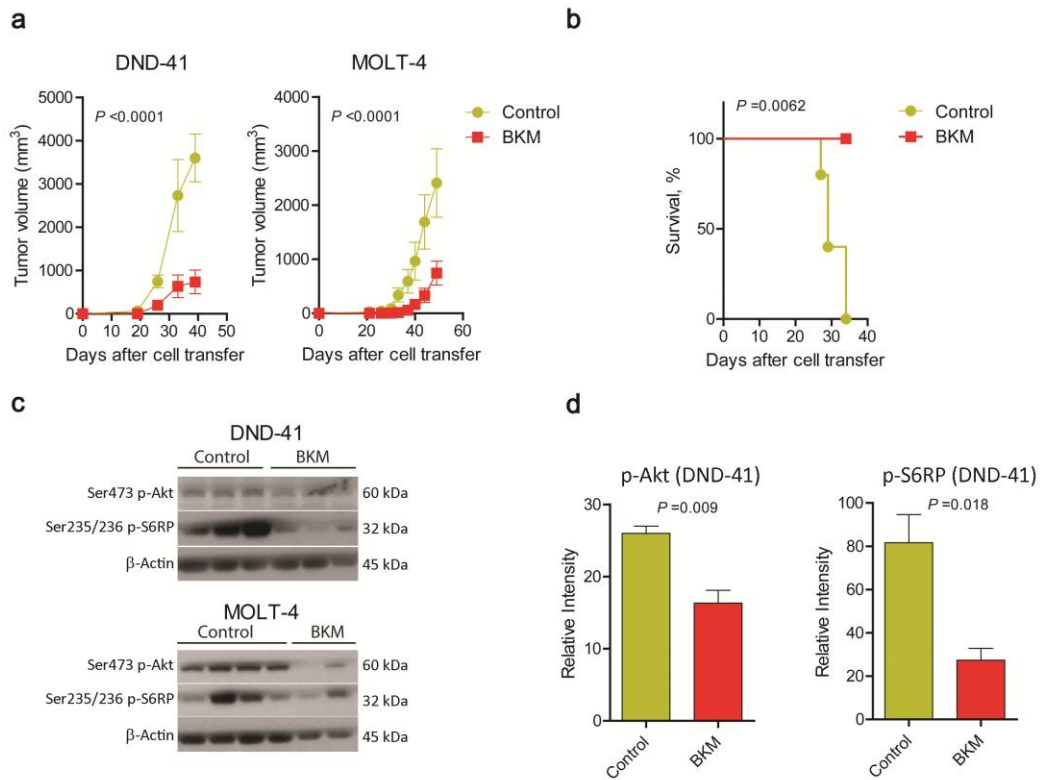


Figure 11: BKM120 is cytotoxic to primary lymphoblasts from T-ALL patients (Pt) with activated PI3K signaling. (a) MTT assays of T-ALL blasts treated with BKM120 for 72 h and (b) IC<sub>50</sub> values. (c) Flow cytometric analysis revealed a mean decrease of p-Akt and p-S6RP staining levels of 41.62% and 42.42%, respectively, in response to 2 μM BKM120 treatment for 24 h ( $p < 0.0005$ ). Ctr, untreated cells. (d) Western blot analysis confirmed a concentration-dependent decrease in p-Akt and p-4E-BP1 levels in primary cells treated with BKM120. (e) Flow cytometric analysis of Annexin V-FITC/PI-stained patients blasts treated for 24 h with BKM120 documented a significant increase in the apoptotic cells. A representative patient is shown. Ctr, untreated cells.



**Figure 12: Synergistic effects of BKM120 with conventional chemotherapeutic agents and efficacy on the SP in primary T-lymphoblasts. (a) MTT assays of patient T-lymphoblasts treated for 72 h with BKM120 alone or in combination with vincristine or doxorubicin at a fixed ratio. The combined treatments resulted in a strong synergism (CIs 0.1-0.3), synergism (CIs 0.3-0.7) or moderate/slight synergism (CIs 0.7-0.9). (b and c) Flow cytometric analysis of SP in primary T-lymphoblasts cultured in the absence (b) or presence (c) of 1  $\mu$ M BKM120 for 24 h. Cells were stained with the Vybrant® DyeCycle in the absence or the presence of Verapamil (50  $\mu$ M). The SP, which disappeared in the presence of Verapamil, was gated and Annexin V-FITC staining evaluated. In BKM120-treated samples (c) about 50% of the SP cells resulted apoptotic, while only about 10% of the SP cells were apoptotic in untreated samples (b), indicating that BKM120 is able to efficiently target the SP.**



**Figure 13: BKM120 delays T-ALL tumor growth and prolongs survival of transplanted mice through inhibition of the PI3K pathway.** NOD/SCID mice were injected subcutaneously with  $10 \times 10^6$  DND-41.Luc.GFP or MOLT-4.Luc.GFP cells in each flank. Five days after cell transfer, mice were equally distributed according to tumor burden in 2 groups ( $n=6$  per group): Control (vehicle control) and BKM (BKM120, 40mg/Kg, po, daily). (a) Tumor volume was assessed at the indicated time points after cell transplantation for mice receiving DND-41.Luc.GFP (left) or Molt-4.Luc.GFP (right) cells. Statistical differences were evaluated using two-way ANOVA. Control and BKM120-treated groups presented a significant difference in tumor development for both cell lines ( $p < 0.0001$ , two-way ANOVA). (b) Survival curves for Control and BKM120-treated mice transplanted with DND-41.Luc.GFP, considering a 2000 mm<sup>3</sup> tumor volume cut-off. Survival time was significantly increased in the BKM120-treated group ( $p = 0.0062$ , LogRank test). (c) Mice transplanted with DND-41.Luc.GFP or MOLT-4.Luc.GFP cells were sacrificed at day 40 or 50, respectively, after cell transplantation, 1 hour after vehicle or BKM120-treatment. Cell lysates were obtained from the tumor mass and immunoblotted with antibodies against Ser473 p-Akt, Ser235/236 p-S6RP or  $\beta$ -Actin as loading control. (d) Corresponding densitometric analysis of p-Akt and p-S6RP, normalized to  $\beta$ -Actin loading control ( $p = 0.009$  for p-Akt and  $p = 0.018$  for p-S6RP, unpaired t test).

## **5. DISCUSSION**

Despite continuous efforts to uncover the molecular complexity of T-ALL, treatments are still based on chemotherapeutic regimens, and prognosis of this disease remains poor, especially in the adult and in chemoresistant/relapsed patients. In view of the critical role of PI3K/Akt signaling in T-ALL cell homeostasis, the activity of the pan-PI3K inhibitor BKM120 was examined in T-ALL cell lines and in primary T-ALL lymphoblasts. Studies were performed both *in vitro* and *in vivo*. BKM120 reduced cell viability in a concentration-dependent manner in all the tested cell lines and primary patient samples. In a phase I clinical study, the maximum plasma concentration ( $C_{max}$ ) of BKM120 obtained after administration of the maximum tolerated dose of the drug was  $4 \mu\text{M}$ <sup>132</sup>. Interestingly, 9 out of 10 of the T-ALL cell lines tested in our study displayed an  $IC_{50}$  below the  $C_{max}$ , and 5 of 6 patient samples displayed a clinically achievable  $IC_{50}$ , encouraging BKM120 application in T-ALL. The BKM120 cytotoxic effects correlated with a significant induction of apoptosis and cleavage of caspases-9, -3 and -2, suggesting the activation of the intrinsic apoptotic pathway. In agreement with previous findings in other cancers<sup>165-166</sup>, treatment with BKM120 induced cell cycle arrest in  $G_2/M$  phase in 7 out of 8 T-ALL cell lines, suggesting an impairment in mechanisms involved in cell cycle progression and mitosis regulation. This condition presumably induces accumulation of DNA damage<sup>167-168</sup>, which finally leads to cell death, as evidenced by the increase in the sub $G_1$  cell fraction which followed cell cycle block. To determine whether the cytotoxic effects observed in our study were related to BKM120-induced PI3K inhibition, we investigated the phosphorylation status of Akt, a direct downstream target of PI3K, as well as that of S6RP in T-ALL cell lines and primary samples. In all cell lines and primary samples, BKM120 inhibited Akt phosphorylation on Ser473 and S6RP phosphorylation on Ser235/236. Although we cannot exclude that the drug concentrations used in our *in vitro* studies may lead to off target effects in T-ALL cells, namely by inhibiting microtubule dynamics by direct binding of BKM120 to tubulin<sup>169</sup>, our data are consistent with a major direct effect on PI3K/Akt signaling pathway. Indeed,

BKM120 was effective also in T-ALL primary cells, that are mostly blocked in the G<sub>0</sub>/G<sub>1</sub> phase of the cell cycle, hence not susceptible to alterations of microtubule dynamics during the G<sub>2</sub>/M phase of the cell cycle. It is also worth emphasizing that BKM120 induced dephosphorylation of 4E-BP1. Phosphorylation of the translation repressor 4E-BP1 is the limiting step for the assembly of the translation initiating complexes which are especially important for oncogenic protein synthesis<sup>157, 170</sup>. Therefore, drugs that target 4E-BP1 are considered more effective in cancer therapy than molecules that do not affect it, such as rapamycin/rapalogs<sup>157</sup>. The difficulty in eradicating acute leukemias might result from the conventional treatments targeting the bulk of the leukemic cells, but not the LSCs, which are postulated to be the cause of relapse<sup>171</sup>. Therefore, strategies that eliminate these cells could have significant clinical implications. Remarkably, we have documented that BKM120 induced apoptosis in the T-ALL patient SP, which is likely enriched in LSCs. This observation might be of relevance, since an efficient targeting of these cells could lead to leukemia eradication. In addition, it has been suggested that stromal cells of the leukemic stem cell niche exert a protective effect on LSCs<sup>171</sup>. Interestingly, BKM120 retained most of its pro-apoptotic activity even when Jurkat cells were co-cultured with MS-5 murine bone marrow stromal cells, which partly mimic the leukemic bone marrow microenvironment. Also of note, we demonstrated that combination of BKM120 with either doxorubicin or vincristine, commonly used drugs in T-ALL treatment<sup>172</sup>, was clearly synergistic. This finding may be of significance in the clinical setting in the future.

Further evaluation of the clinical potential of BKM120 in T-ALL, using xenotransplant mouse models of T-ALL, demonstrated that the PI3K inhibitor can clearly retard tumor development, without obvious side-effects. Moreover, although we cannot rule out off target *in vivo* impacts, the dose we administered is consistent with essentially on-target effects<sup>169</sup> and our molecular analyses confirmed that BKM120 effectively inhibits PI3K-mediated signaling in the tumor mass, as evidenced by decreased p-Akt and p-S6RP

levels. Interestingly, p-S6RP levels have been used previously as a read-out for proving BKM120 efficacy in patients<sup>132</sup>. Whether, in agreement with our observations *in vitro*, BKM120 synergizes *in vivo* with currently used chemotherapeutic drugs warrants further investigation. A recent paper, has highlighted that in PTEN-null models of murine T-ALL, genetic inactivation of both p110 $\gamma$  and p110 $\delta$  PI3Ks suppressed tumor formation. Consistently, a dual p110 $\gamma$ /p110 $\delta$  inhibitor reduced disease burden and prolonged survival in mice. The dual inhibitor was also effective against human T-ALL cell lines and primary samples, although in this case the dependence of the cytotoxic effects on the absence of PTEN was much less evident<sup>146</sup>. However, our preliminary results indicated that, at least in T-ALL cell lines, BKM120 was much more effective in inducing cytotoxicity than a combined inhibition of p110 $\gamma$  and p110 $\delta$  isoforms (data not shown), suggesting that also p110 $\alpha$  and p110 $\beta$  isozymes may play a role in T-ALL cell proliferation and survival, as previously reported<sup>173</sup>. Our observations have been confirmed in a recent paper which documented that only pan inhibition of PI3K was able to suppress Akt phosphorylation and to significantly reduce the proliferation of T-ALL cell lines<sup>174</sup>. Furthermore, even in pre-clinical models of B-CLL, i.e. a disease where the use of p110 $\delta$  PI3K inhibitors has been strongly advocated<sup>175</sup>, the *in vitro* cytotoxicity of BKM120 against malignant B-CLL lymphocytes was much stronger (at 3.6 fold) than that of CAL-101, a selective p110 $\delta$  PI3K inhibitor<sup>144</sup>.

Taken together, our pre-clinical study provided evidence of the effectiveness of BKM120 in T-ALL as a single agent or in combination with doxorubicin and vincristine. The drug showed high antitumor activity against T-ALL cell lines and primary leukemia blasts from T-ALL patients. In conclusion, BKM120 is a promising treatment option for T-ALL and our findings support its clinical evaluation in this malignancy.

**PART II: PAN-PI3K INHIBITION IMPAIRS MORE EFFICIENTLY  
PROLIFERATION AND SURVIVAL OF T-CELL ACUTE  
LYMPHOBLASTIC LEUKEMIA CELL LINES WHEN COMPARED  
TO ISOFORM-SELECTIVE PI3K INHIBITORS**

## 6. RESULTS

### 6.1. *In vitro* assessment of PI3K inhibitors effects on cell viability

In order to establish the role of the different PI3K catalytic subunits in supporting leukemic cells proliferation and survival, we exploited a pharmacological approach by using selective inhibitors together with dual p110 $\gamma/\delta$  and pan inhibitors. The pan inhibitor BKM120 has been evaluated in both preclinical leukemic models<sup>129</sup> and phase I clinical trials for patients with solid tumors<sup>130-132</sup>, whereas ZSTK-474<sup>133-135</sup> and PIK-90<sup>147</sup> efficacy has been assessed only in preclinical models. To specifically inhibit p110 $\alpha$ , p110 $\beta$ , p110 $\delta$  and p110 $\gamma$  we employed A-66, TGX-221, CAL-101 and AS-605240, respectively, whose selectivity has been elsewhere reported<sup>146-147,176</sup>, and that at least in some settings have shown effectiveness in hematological malignancies<sup>137</sup>. Because of the prominent role of p110 $\delta$  and p110 $\gamma$  isoforms in T-lymphocytes<sup>55</sup>, effects of the dual inhibitor IPI-145 as well as the combination of CAL-101 plus AS-405260 were also evaluated. Cells were cultured with increasing concentration of the drugs for 48 h followed by metabolic activity assessment by MTT assay (Figure 14 A and C). In both *PTEN* deleted (Jurkat and Loucy) and *PTEN* non deleted (DND-41 and ALL-SIL) cells, growth rate diminished after treatment with BKM120 and ZSTK-474 with IC<sub>50</sub> values ranging between 1.05-2.34  $\mu$ M for BKM120 and 0.99-3.39  $\mu$ M for ZSTK-474. Conversely, PIK-90 mildly affected these cells, with the exception of Loucy cells (IC<sub>50</sub> 0.096  $\mu$ M). As expected, selective inhibition of p110 $\alpha$ , p110 $\beta$ , p110 $\delta$  and p110 $\gamma$  isoforms resulted ineffective, with IC<sub>50</sub> values not attained at the tested concentrations. We further investigated the effectiveness of combining p110 $\delta$  and p110 $\gamma$  inhibitors, by treating T-ALL cell lines with CAL-101 and AS-405260 at a fixed ratio (1:1). As shown in Fig. 14 (B and D), these two inhibitors resulted in a strong (CI < 0.3) to moderate (CI < 0.9) synergism in ALL-SIL, Loucy and Jurkat at concentrations above 1  $\mu$ M, whereas in DND-41 combination of CAL-101 and AS-605240 did not exert a synergistic but an antagonistic (at 1 and 2  $\mu$ M) or additive (at 4 and 8  $\mu$ M) effect. Nevertheless, IC<sub>50</sub> values achieved by the combination were higher compared to those of

pan inhibitors (Figure 14 C). Interestingly, the dual p110 $\gamma/\delta$  inhibitor IPI-145 had an effect only on Loucy cells. Overall, pan inhibition resulted more efficient to affect T-ALL cell viability with regard to specific as well as dual p110 $\gamma/\delta$  inhibition. Based on these results, we selected ZSTK-474 as pan inhibitor and we used the concentration of 5  $\mu$ M for the following experiments to simplify comparison of the results obtained with the different inhibitors.

## **6.2. Pan PI3K inhibition affected proliferation in a PTEN-independent fashion**

We investigated more in detail the role of PI3K pathway inhibition on cell proliferation observing the long-term cell growth over 3 days post treatment. The pan inhibitor ZSTK-474 significantly impaired cell proliferation in all the cell lines, independently from *PTEN* status, whereas p110 $\alpha$  and p110 $\beta$  inhibition produced negligible effects (Figure 15 A). Specific and dual inhibition of p110 $\gamma$  and p110 $\delta$  isoforms displayed an irregular trend. Jurkat and DND-41 proliferation was unaffected by their inhibition, conversely in Loucy and ALL-SIL p110 $\delta$  or dual p110 $\gamma/\delta$  significantly impaired cell growth (Figure 15 A). Compared to untreated controls, ZSTK-474 strongly slowed down the doubling time in Loucy, DND-41 and ALL-SIL cells, whereas a negative doubling time was estimated in Jurkat cells, suggesting cell death induction (Figure 15 C). Importantly, in Loucy cells, the only one cell line responsive to IPI-145, proliferation was impaired already at 0.5  $\mu$ M after treatment with this dual inhibitor (Figure 15 B and C).

To ascertain that the observed effects of ZSTK-474 on cell growth rate were due to a proliferative impairment, we also evaluated the expression of the proliferation marker Ki-67, a nuclear antigen present throughout the cell cycle. In accordance with growth curves analyses, Ki-67 decreased broadly in all the cell lines after 72 h treatment with the pan inhibitor ZSTK-474 (Figure 15 D).

These results demonstrated that PI3K pan inhibition impaired cell proliferation more efficiently than dual p110 $\gamma/\delta$  inhibition and supported its highest anticancer activity.

### **6.3. Antiproliferative effects are independent from total PtdIns(3,4,5)P<sub>3</sub> level reduction**

To evaluate the impact of the inhibitors on PI3K activity, total PtdIns(3,4,5)P<sub>3</sub> levels were quantified by flow cytometry. Firstly, we investigated cell lines with regard to PI3K isoforms and PTEN expression. As shown in Figure 16 A, the catalytic subunits p110 $\alpha$ , - $\beta$ , - $\gamma$  and - $\delta$ , target of the PI3K inhibitors, were expressed in control as well as treated samples. As expected, PTEN protein was absent in deleted Jurkat and Loucy cells, but abundantly expressed and unaffected by treatments in non deleted ALL-SIL and DND-41 cells. Nevertheless, in both of these cell lines, PTEN resulted phosphorylated at Ser380, which is a marker of PTEN posttranslational inactivation and consequent PI3K pathway activation<sup>89</sup>. This observation could explain the absence of differences among the two cell line groups, PTEN deleted and non deleted.

Flow cytometry analysis of untreated samples showed different basal levels of PtdIns(3,4,5)P<sub>3</sub> irrespective of *PTEN* status, with an amount in deleted Jurkat and non deleted DND-41 approximately of 48% and 45%, respectively, and 77% vs 75% in deleted Loucy vs non deleted ALL-SIL (Figure 16 B). Interestingly, after 6 h treatment, in all cases the compounds induced a decrease of the second messenger, demonstrating that each PI3K catalytic isoform contribute to PtdIns(4,5)P<sub>3</sub> phosphorylation in T-ALL cells (Figure 16 C). While in Jurkat cells all the inhibitors drastically decreased PtdIns(3,4,5)P<sub>3</sub>, the other cell lines displayed significantly decreased PtdIns(3,4,5)P<sub>3</sub> only in response to some treatments (CAL-101 in DND-41; A-66, AS-605240 and combination of AS-605240 plus CAL-101 in ALL-SIL; A-66, CAL-101 and combination of AS-605240 plus CAL-101 in Loucy). Importantly, pan inhibition was able to induce a significant reduction of

PtdIns(3,4,5)P<sub>3</sub> in all cell lines. Moreover, PtdIns(3,4,5)P<sub>3</sub> decreased in a concentration-dependent fashion in Loucy cells treated with the dual p110γ/δ inhibitor IPI-145 (0.5, 1 and 5 μM; Figure 16 B). These observations suggested a peculiar addiction to PI3K isoforms of the different cell lines with regard to PtdIns(4,5)P<sub>3</sub> phosphorylation, suggesting a potential influence of cellular-specific mechanisms in PtdIns(3,4,5)P<sub>3</sub> generation. However, both PtdIns(3,4,5)P<sub>3</sub> basal level and PtdIns(3,4,5)P<sub>3</sub> reduction did not correlate with the observed antiproliferative effects. We also evaluated the individual contribution of p110α, -β, -γ and -δ to PtdIns(3,4,5)P<sub>3</sub> levels, by treating the cells with a combination of three different selective inhibitors. Nevertheless, results showed only the reduction of PtdIns(3,4,5)P<sub>3</sub>, but in no cases we observed the complete abrogation of the second messenger, supporting a role for each isoform in PtdIns(3,4,5)P<sub>3</sub> synthesis and PI3K pathway activation (data not shown).

Taken together, these data demonstrated that each isoform can sustain PtdIns(3,4,5)P<sub>3</sub> synthesis in T-ALL, but its total intracellular amount is not directly related to cellular proliferation.

#### **6.4. Pan inhibition of PI3K and PtdIns(3,4,5)P<sub>3</sub> decreases Akt-mediated signaling**

We next examined the effects of the different isoforms inhibition to understand their role in PI3K signaling. One of the major PI3K target is the serine/threonine kinase Akt, which is recruited to the plasma membrane through direct interaction with PtdIns(3,4,5)P<sub>3</sub> and subsequent phosphorylation on Thr308 by PDK1 and Ser473 by mTORC2 for fully activation. In all cell line, selective p110α, -β or -γ inhibition was unable to reduce Akt(Thr308) phosphorylation, whereas p110δ and dual p110γ/δ inhibition both induced a comparable decrease, suggesting a major role for p110δ isoform in Akt activation (Figure 17 A). Conversely, pan inhibition exerted the strongest effect on Akt activation, with a complete abrogation of phosphorylation at Thr308. Most importantly, only pan PI3K

inhibition induced a significant reduction of p-Ser473 in all the cell lines, which is essential for switching off Akt signaling, already after 6 h (Jurkat, Loucy and DND-41; Figure 17 A) or 24 h (ALL-SIL; Figure 17 B) treatment. Analysis of Akt downstream targets showed a congruent pattern of dephosphorylation, with the decrease of p-P70S6K both Thr421/Ser424 (auto-inhibitory domain) and Thr389 (mTORC1 phosphorylation site), and p-S6RP(Ser235/236), after pan or, to a lesser extent, dual p110 $\gamma/\delta$  inhibition (Figure 17 A). These results confirmed PI3K pathway inhibition. In all cases, total proteins levels were unaffected. Consistently with cell viability and proliferation analyses, only in the Loucy cell line repression of p110 $\gamma/\delta$  with the dual inhibitor IPI-145 was effective and displayed a concentration-dependent trend of pathway inhibition (Figure 17 A). To assess if other targets beyond Akt could be affected by PI3K inhibition and PtdIns(3,4,5)P<sub>3</sub> decrease, we further investigated PDK1 together with several of its downstream targets, PKC $\alpha$  and PKC $\beta$ . We observed that neither specific, dual or pan inhibitors reduced phosphorylated levels of these proteins, in agreement with their PtdIns(3,4,5)P<sub>3</sub> independent and PDK1 dependent mechanism of activation <sup>177</sup>. Therefore, block of PI3K activity mainly inhibits PtdIns(3,4,5)P<sub>3</sub> dependent Akt pathway.

### **6.5. Aniproliferative activity of pan PI3K inhibition acts through cell cycle arrest and caspase-independent cell death**

Next, we investigated the mechanisms likely involved in proliferation impairment. Because PI3K/Akt signaling mediates different cellular pathways, we examined the effects on cell cycle and induction of apoptosis. Cell cycle phase distribution strongly changed in all cell lines as a result of pan-inhibition (ZSTK-474 treatment for 48 h) (Figure 18 A). Flow cytometry analysis showed an accumulation of cells in G<sub>0</sub>/G<sub>1</sub> and consequent decrease of S or G<sub>2</sub>/M cell phase, as previously reported <sup>134</sup>, which reached a statistical significance in ALL-SIL and DND-41 cells. Moreover, in Jurkat, Loucy and ALL-SIL cells ZSTK-474

increased the subG<sub>1</sub> cell fraction, which comprises death cells. Lesser effects were observed with the other inhibitors, which affected only ALL-SIL and Loucy cells. In ALL-SIL cells, selective-isoform inhibitors and the combination of AS-605240 and CAL-101 induced an accumulation of G<sub>0</sub>/G<sub>1</sub> cells and a consequent reduction of S or G<sub>2</sub>/M cells, without affecting subG<sub>1</sub> cell phase. Combination of AS-605240 and CAL-101 inhibition altered cell cycle phase distribution in Loucy cells, inducing the expansion of G<sub>0</sub>/G<sub>1</sub> fraction. However, the dual  $\gamma/\delta$  inhibitor IPI-145 had no effects.

Annexin V-FITC/PI analysis confirmed a significant increase of apoptotic cells following treatment with ZSTK-474 for 48 h in all the cell lines, whereas dual p110 $\gamma/\delta$  inhibition had limited effects, inducing significant cell death only in the Loucy cell line (Figure 18 B). Western blot analysis revealed the absence of cleaved effector caspase 3 both at 24 and 48 h treatment (Figure 18 C and data not shown), suggesting that caspases did not contribute to cell death. To prove that, we treated these cells with ZSTK-474 in the presence or absence of the polycaspase inhibitor N-benzyloxycarbonyl-Val-Ala-Asp-fluoromethylketone, z-VAD-fmk. As shown in Figure 18 D, cell death induced by pan PI3K inhibition not only was not affected by caspases inhibition, but in some instances it was even increased.

Overall, these results demonstrated as PI3K inhibition caused cell cycle arrest in G<sub>0</sub>/G<sub>1</sub> cell phase, but only pan inhibition was able to efficiently induce cell death with a caspase independent mechanism.

## **6.6. Autophagy is a protective mechanism against pan PI3K inhibition**

Autophagy is a homeostatic cellular process which regulate protein and organelle turnover by lysosomal destruction<sup>178</sup>. This process would also execute cell demise, and autophagic cell death is one of the better recognized independent programmed cell death mechanisms<sup>179</sup>. With respect to autophagy induction, we investigated the expression of

LC3B I/II, a recognized autophagy marker <sup>180</sup>. Western blot analysis showed a strong increase in LC3B II, the lower migrating form of the protein which is bound to the autophagosome membranes, in Loucy, ALL-SIL and DND-41 cells especially following 24 h ZSTK-474 treatment, whereas almost no changes were observed in Jurkat cells (Figure 19 A). Because pan PI3K inhibition with ZTK-474 treatment induced a considerable percentage of apoptosis in Jurkat compared to the other cell lines, we supposed a protective role of autophagy in this context. To test our hypothesis, we inhibited autophagy with the early-stage autophagy inhibitor 3-methyladenine (3-MA) and subsequently evaluated cell death percentage induced by treatment with the pan inhibitor ZSTK-474. The results demonstrated that addition of 3-MA increased the cytotoxic effect of pan PI3K inhibition, since the percentage of Annexin V/PI positive cells was significantly greater in Loucy, ALL-SIL and DND-41 cells compared to samples treated with ZSTK-474 alone (Figure 19 B). On the contrary, in Jurkat cells, where PI3K inhibition did not induce LC3B lipidation, inhibition of autophagy did not increase cytotoxicity (Figure 19 B). The same results have been obtained with the autophagy inhibitors bafilomycin A1 or E64D (data not shown). To ascertain whether the dissimilar behavior between Jurkat and the other cell lines was related to a different modulation of autophagy-related genes, a screening for gene expression was performed using a quantitative real time-PCR assay which interrogates 82 genes related to the autophagy pathway (Table 2 and Figure 19 C). Expression of several genes resulted undetectable in both control and treated samples: *ULK2* and *TGM2* in all the cells lines; *CDKN2A* in ALL-SIL and Jurkat cells; *RB1* and *APP* in ALL-SIL cells; *ESR1* in Jurkat cells. Unsupervised hierarchical clustering showed similarities in autophagy gene expression in each paired cell line (untreated and treated samples) (Figure 19 C). Moreover, untreated Loucy cells showed a higher expression of these genes compared to the other samples. However, no transcripts differentially clustered in Jurkat cells, despite this cell line did not activate the autophagy process

following pan PI3K inhibition. We further investigated the modulation of autophagy, comparing untreated and treated samples and assessing for each gene the fold change, expressed as  $2^{-\Delta\Delta Ct}$ . A 24 h treatment with ZSTK-474 had limited effects on autophagy at a transcriptional level, as the majority of genes resulted expressed equally to the control ( $2^{-\Delta\Delta Ct} = 1$ ) or slightly reduced ( $2^{-\Delta\Delta Ct} < 1$ ), especially in Loucy cells (Figure 6 C). Nevertheless, in some instances we observed a  $> 2$  fold increase both in components of the autophagy machinery and in genes involved in autophagy regulation (Table 3 and Figure 19 D). In particular, in Loucy, ALL-SIL and DND-41 cells, pan PI3K inhibition increased expression of *DRAM1*, *GABARAPL1*, *GABARAPL2*, *WIPI1*, *MAP1LC3B* and *ATG16L2*, all involved in autophagic vesicle nucleation and expansion, as well as increased expression of genes involved in autophagy induction and regulation (*INS*, *PIK3C*) or pro survival genes (*BCL2*, *EIF2AK3*). On the contrary, in Jurkat cells pan PI3K inhibition had limited effects on autophagy induction, as the only upregulated gene was *ULK1*. However, we observed a  $> 2$  fold change in expression of the tumor suppressor genes *CDKN1B* and *TP53*, and *CTSS* (cathepsin S) which deficiency has been associated to alterations in autophagic flux<sup>181</sup>. These results demonstrated that pan PI3K inhibition might induce autophagy which plays a protective role in T-ALL cells, and suggested that autophagy activation in the different T-ALL cell lines might be dependent on a diversified gene expression regulation.

## 6.7. Tables

Table 2: Autophagy related genes analyzed using Real-time PCR microarrays

Autophagy Machinery Components
<i>AMBRA1, ATG10, ATG12, ATG16L1, ATG16L2, ATG3, ATG4A, ATG4B, ATG4C, ATG4D, ATG5, ATG7, ATG9A, BECN1, DRAM1, GABARAP, GABARAPL1, GABARAPL2, IRGM, LAMP1, MAP1LC3A, MAP1LC3B, NPC1, RAB24, RGS19, ULK1, ULK2, WIPI1</i>
Regulation of Autophagy
<i>AKT1, APP, BAD, BAK1, BAX, BCL2, BCL2L1, BID, BNIP3, CASP3, CASP8, CDKN1B, CDKN2A, CLN3, CTSD, CTSS, CTSS, CXCR4, DAPK1, DRAM2, EIF2AK3, EIF4G1, ESR1, FADD, FAS, GAA, HDAC1, HDAC6, HGS, HSPA8, HSP90AA1, HTT, IFNG, IGF1, INS, MAPK14, MAPK8, MTOR, NFKB1, PIK3CG, PIK3C3, PIK3R4, PTEN, RB1, RPS6KB1, SNCA, SQSTM1, TGFB1, TGM2, TMEM74, TNF, TNFSF10, TP53, UVRAG</i>

Table 3: Autophagy related genes upregulated after pan-PI3K inhibition.

Autophagy Machinery Components		
<b><i>DRAM1</i></b>	DNA-damage regulated autophagy modulator 1	Lysosomal modulator of autophagy induced by p53
<b><i>GABARAPL1</i></b>	GABA(A) receptor-associated protein like 1	essential for autophagosome maturation
<b><i>GABARAPL2</i></b>	GABA(A) receptor-associated protein-like 2	essential for autophagosome maturation
<b><i>MAP1LC3B</i></b>	Microtubule-associated protein 1 light chain 3 beta	involved in formation of autophagosomes
<b><i>ATG16L2</i></b>	Autophagy related 16-like 2	May play a role in autophagy during membrane biogenesis
<b><i>ULK1</i></b>	unc-51 like autophagy activating kinase 1	Regulate the formation of autophagophores (upstream <i>PIK3C</i> )
<b><i>WIPI1</i></b>	WD repeat domain, phosphoinositide interacting 1	Required for autophagosome formation (downstream <i>ULK1</i> and <i>PIK3C</i> )
Regulation of Autophagy		
<b><i>INS</i></b>	Insulin	Peptide hormone
<b><i>BNIP3</i></b>	BCL2/adenovirus E1B 19kDa interacting protein 3	May positively modulate autophagy displacing Bcl-2 from the Bcl-2/Beclin 1 complex
<b><i>TNF</i></b>	Tumor necrosis factor	Cytokine
<b><i>ESR1</i></b>	Estrogen receptor 1	Regulate autophagy core proteins
<b><i>BCL2</i></b>	B-cell CLL/lymphoma 2	Promote cellular survival
<b><i>EIF2AK3</i></b>	Eukaryotic translation initiation factor 2-alpha kinase 3	Repress global protein synthesis. Critical effector of unfolded protein response (UPR)
<b><i>IFNG</i></b>	Interferon gamma	Cytokine
<b><i>PIK3C3</i></b>	Phosphatidylinositol 3-kinase, catalytic subunit type 3	Involved in initiation and maturation of autophagosomes
<b><i>CDKN1B</i></b>	Cyclin-dependent kinase inhibitor 1B (p27Kip1)	Cell cycle regulator. Its degradation is required for G <sub>1</sub> cell phase progression
<b><i>TP53</i></b>	Tumor protein p53	Tumor suppressor
<b><i>CTSS</i></b>	Cathepsin S	Cysteine lysosomal protease involved in autophagic flux regulation

## 6.8. Figures

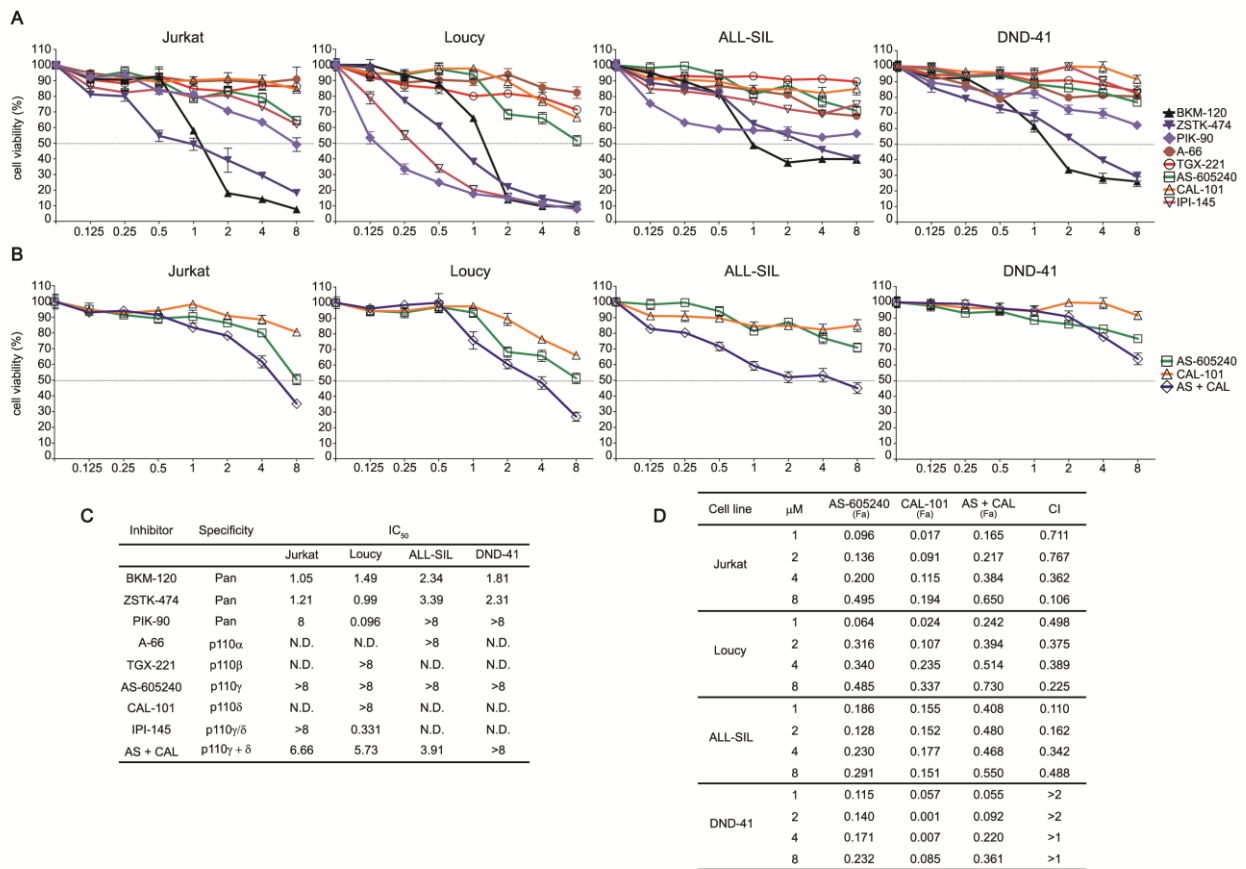


**Figure 14: Inhibition of all the PI3K catalytic isoforms exerts the strongest effect on cell viability. (A and B) MTT analysis of PTEN-deleted (Jurkat, Loucy) and non deleted (ALL-SIL, DND-41) T-ALL cell lines treated for 48 h with increasing concentration of PI3K inhibitors. (B) Effect of the combination of AS-605240 and CAL-101 on cell viability. (C) IC<sub>50</sub> values obtained through MTT assay after 48 h treatment with increasing concentration of PI3K inhibitors. (D) Analysis of the AS-605240 (p110 $\gamma$  inhibitor) and CAL-101 (p110 $\delta$  inhibitor) combination, which resulted synergistic in Jurkat, Loucy and ALL-SIL (CIs 0.1-0.9). In DND-41 CIs values > 2 indicate an antagonistic effect, whereas ICs > 1 are additive. (CI: combination index; Fa: Fraction affected).**

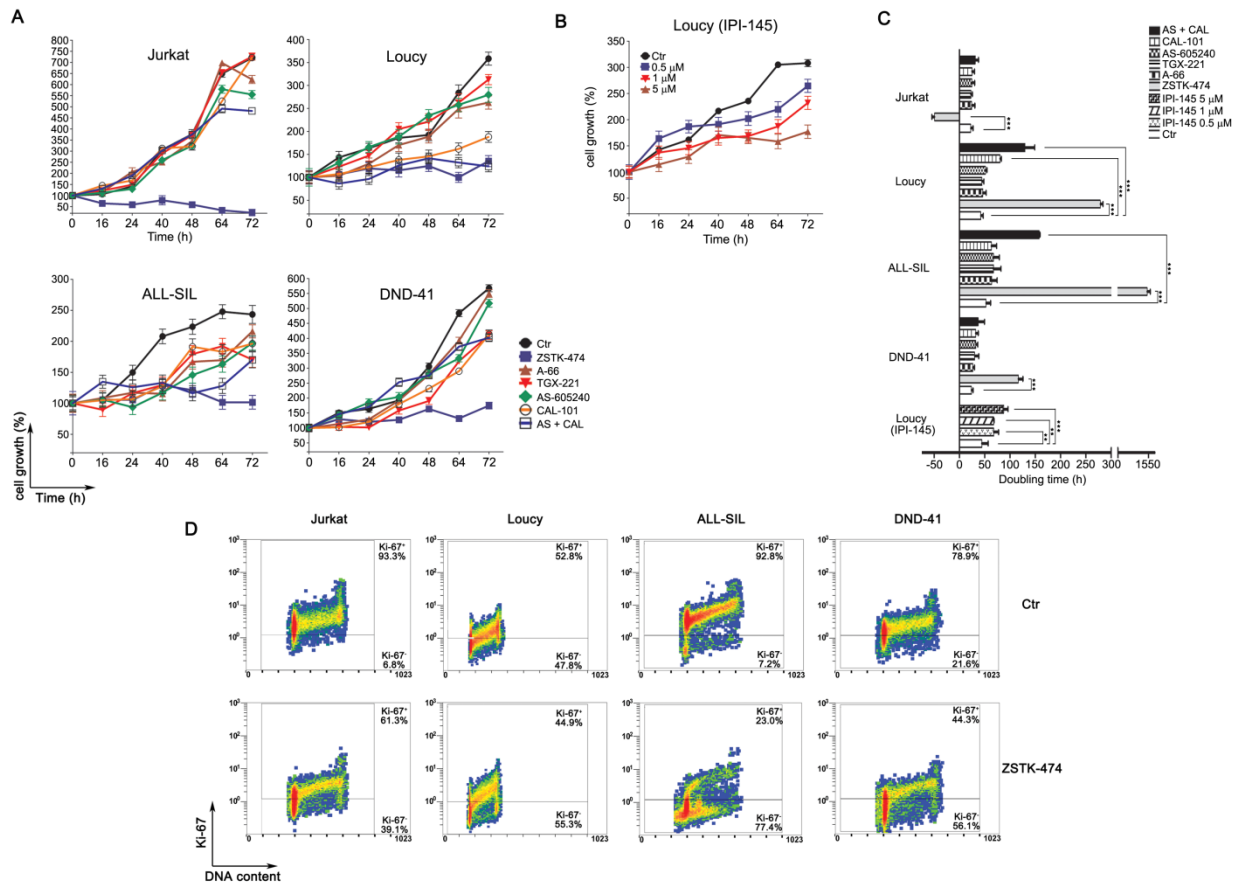


**Figure 15: Pan PI3K inhibition impairs proliferation in T-ALL cell lines.** Growth curves of T-ALL cell lines treated with 5  $\mu$ M of PI3K selective, dual and pan inhibitors (A) or with increasing concentration (0.5, 1 and 5  $\mu$ M) of the dual inhibitor IPI-145 (B). Viable cells were counted before treatment (0 h), and after 16, 24, 40, 48, 64 and 72 h from treatment. Cell growth was calculated as the percentage of viable cells compared to that at T 0 h . Four independent count for each time point and two independent experiments for each cell line were performed (bars, SD). (C) Doubling time obtained from the cell count analysis. Increase in doubling time indicate impairment of proliferation. The negative doubling time observed in Jurkat cells indicate cell death induction. Asterisks indicate statistically significant differences with respect to untreated cells (\*:  $p < 0.05$ ; \*\*:  $p < 0.01$ ; \*\*\*:  $p < 0.001$ ). (D) Flow cytometric analysis of the proliferation marker Ki-67. Cells were treated with 5  $\mu$ M of the pan inhibitor ZSTK-474 for 72 h. Upper panel: control cells (untreated). Lower panels: treated cells.

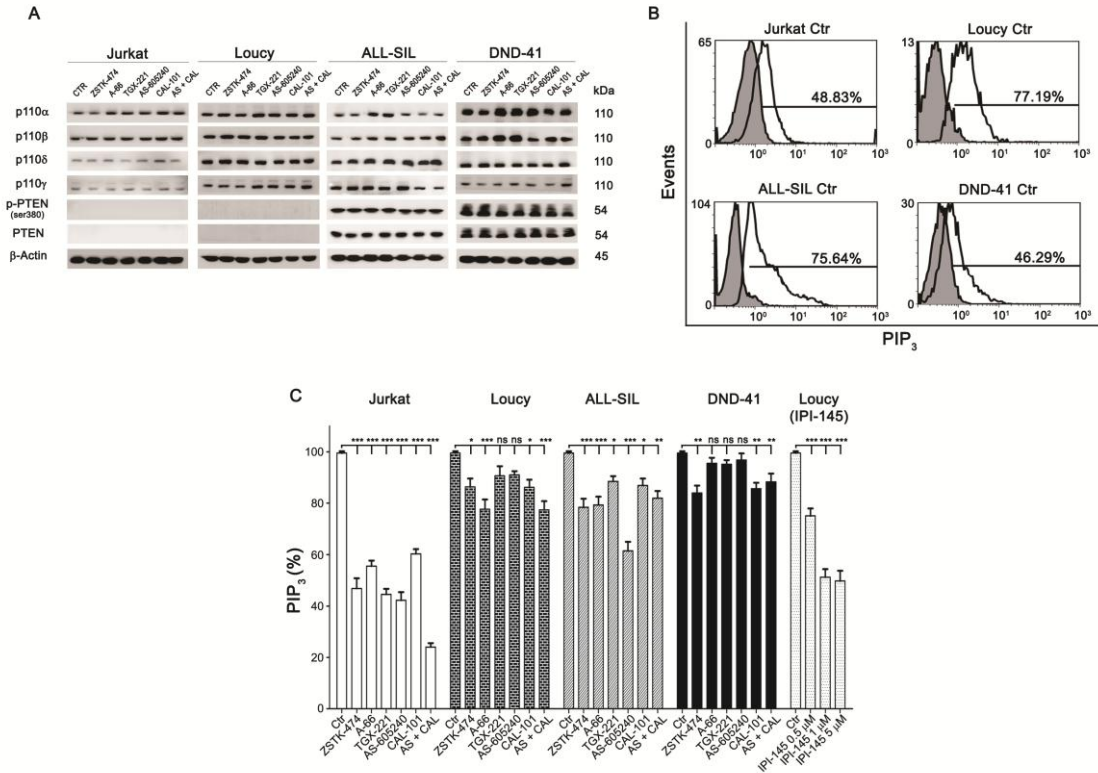


**Figure 16: Effects of PI3K inhibition on PIP<sub>3</sub> synthesis. (A)** Characterization of the T-ALL cell. Cells were cultured for 6 h with the different inhibitors, as indicated, and western blot analysis was then performed. PTEN-non deleted cell lines express abundantly PTEN protein, but it is phosphorylated at Ser380, which is an inhibitory site. Flow cytometry quantification of the second messenger PIP<sub>3</sub> in untreated cells (B) or following 5 μM of PI3K inhibitors for 6 h (C). Bars, SD. Asterisks indicate statistically significant differences with respect to untreated cells (\*: p < 0.05; \*\*: p < 0.01; \*\*\*: p < 0.001).

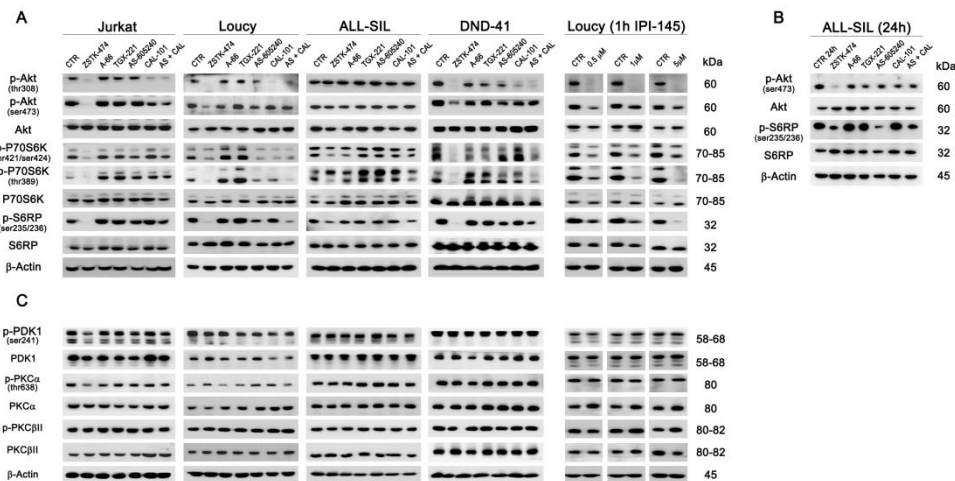


**Figure 17: Pan PI3K inhibition induces the complete block of Akt pathway** Cells were cultured for 6 h (A and C) or 24 h (B) in the presence of 5 μM of the different PI3K inhibitors, as indicated, and western blot analysis was then performed. The pan inhibitor ZSTK-474 and the combination of p110γ and p110δ inhibitors (AS-605240 and CAL-101) induced the dephosphorylation of the main PI3K downstream targets Akt, P70S6K and S6RP (A and B) but only the pan inhibitor ZSTK-474 decreased both the phosphorylated residues of Akt, Thr308 and Ser473. Only in Loucy the dual p110γ/δ IPI-145 exerted a dose-dependent activity on PI3K downstream targets. (C) PDK1, PKCα and PKCβII proteins were not modulated by inhibition of PI3K. Thirty μg of protein was blotted to each lane. Antibody to β-Actin served as a loading control. Molecular weights are indicated at right. Ctr, untreated cells.

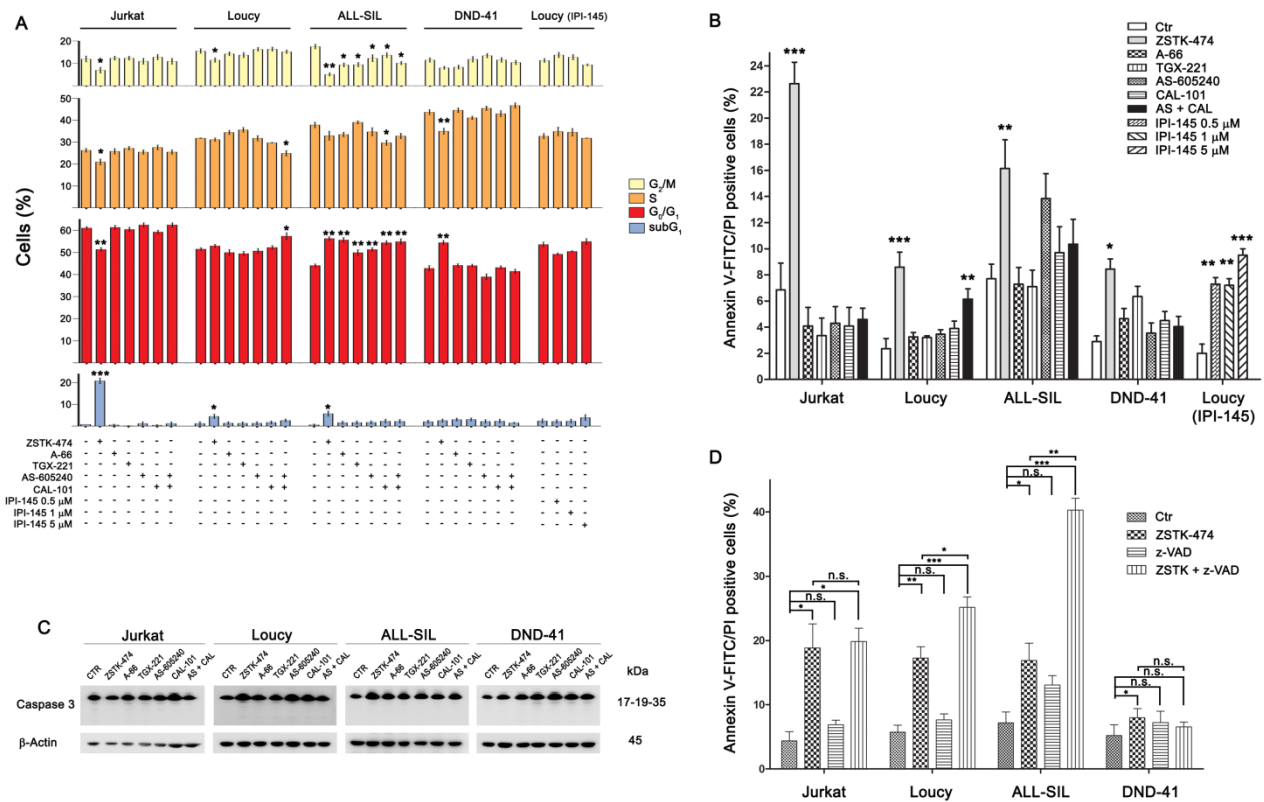


**Figure 18: Pan PI3K inhibition affect cell cycle and induce caspase independent cell death (A)** Flow cytometry analysis of PI-stained cells treated with 5  $\mu$ M of the different PI3K inhibitors (as indicated) for 48 h. The pan inhibitor ZSTK-474 increased the subG<sub>1</sub> and/or the G<sub>0</sub>/G<sub>1</sub> cell fraction, with the consequent decrease of the other cell phases, whereas the dual p110 $\gamma$ / $\delta$  exerted limited effects on cell cycle distribution. The dual inhibitor IPI-145 did not perturb cell cycle of the sensitive Loucy cell line. **(B)** Flow cytometric analysis of Annexin V-FITC/PI-stained T-ALL cells treated with 5  $\mu$ M of the different PI3K inhibitors (as indicated) for 48 h documented a significant increase in cell death fraction with respect to untreated cells only after pan PI3K inhibition. The dual inhibitor IPI-145 exerted a concentration-dependent effect on Loucy cell line. **(C)** Western blotting revealed that PI3K inhibition did not induce caspase activation. Thirty  $\mu$ g of protein was blotted to each lane. Antibody to  $\beta$ -Actin served as a loading control. Molecular weights are indicated at right. **(D)** T-ALL cells were treated with 5  $\mu$ M ZSTK-474 for 48 h with or without the pan caspase inhibitor z-VAD-fmk (50  $\mu$ M) and cell death fraction was assessed with Annexin V-FITC/PI staining. Caspase inhibition did not affect or even increase cytotoxicity. Results are the mean of three different experiments  $\pm$  SD. Asterisks indicate statistically significant differences with respect to untreated cells (\*:  $p < 0.05$ ; \*\*:  $p < 0.01$ ; \*\*\*:  $p < 0.001$ ).

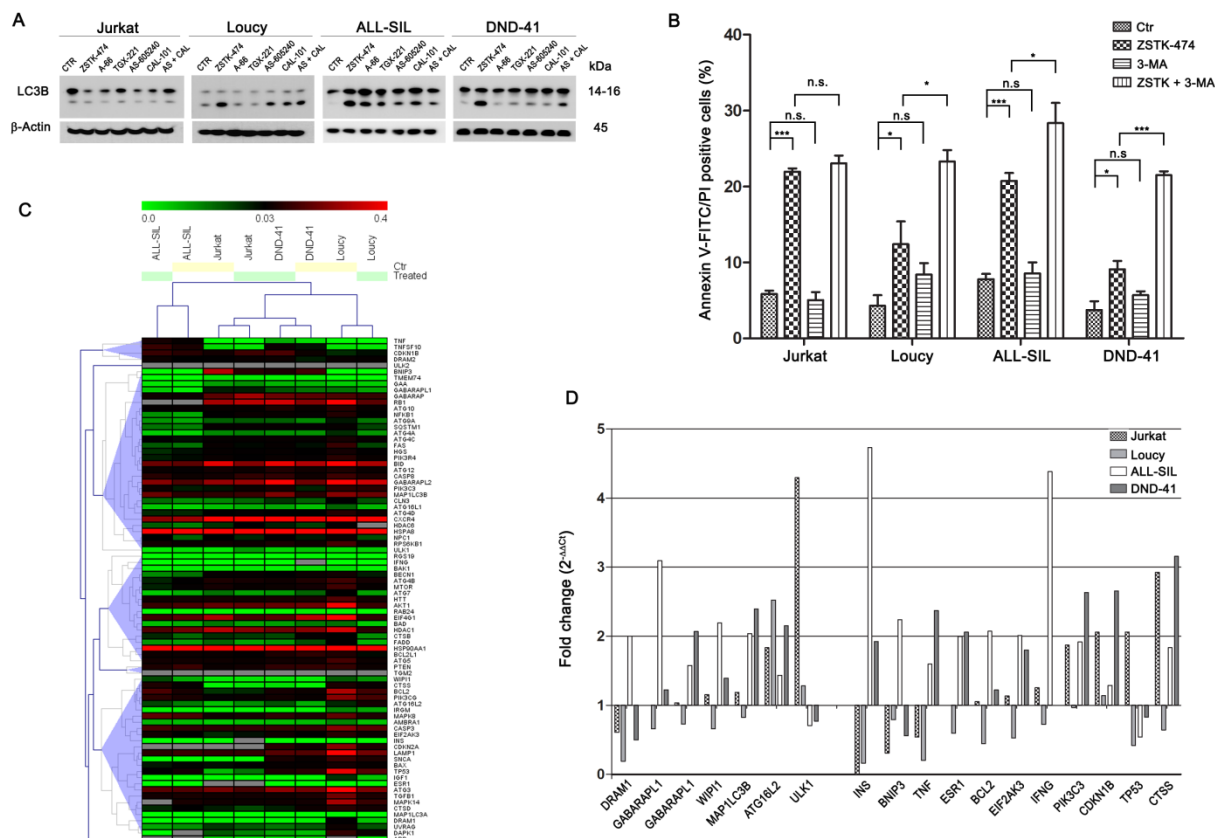


**Figure 19: Pan PI3K inhibition might induce autophagy which plays a protective role. (A)** Western blotting revealed autophagy activation in Loucy, ALL-SIL and DND-41 cell lines. Thirty  $\mu$ g of protein was blotted to each lane. Antibody to  $\beta$ -Actin served as a loading control. Molecular weights are indicated at right. **(B)** T-ALL cells were treated with 5  $\mu$ M ZSTK-474 for 48 h with or without the autophagy inhibitor 3-MA (200  $\mu$ M) and cell death fraction was assessed with Annexin V-FITC/PI staining. Autophagy inhibition significantly increased cell demise, revealing its protective role in Loucy, ALL-SIL and DND-41 cell lines, whereas did not affect Jurkat cells. Results are the mean of three different experiments  $\pm$  SD. Asterisks indicate statistically significant differences with respect to untreated cells (\* :  $p < 0.05$ ; \*\* :  $p < 0.01$ ; \*\*\* :  $p < 0.001$ ). **(C)** Real-time PCR expression profiling of 82 autophagy related genes in T-ALL cell lines untreated (Ctr) or treated for 24 h with 5  $\mu$ M ZSTK-474 were visualized using an unsupervised heatmap. Data are presented as  $2^{-\Delta\Delta Ct}$  ( $\Delta\Delta Ct = Ct \text{ target gene} - Ct \text{ RLP0}$ ). **(D)** Histograms represent the relative gene expression of several autophagy-related genes in T-ALL cells treated with ZSTK-474 and compared to untreated paired sample. Data are presented as  $2^{-\Delta\Delta Ct}$  ( $\Delta\Delta Ct = \Delta Ct \text{ treated sample} - \Delta Ct \text{ Ctr sample}$ ). When fold change values are =1, the regulation in treated samples is equal to the paired control sample. When fold change values are >1 or <1, the autophagy related genes are up- or downregulated, respectively, compared to untreated samples.

## **7.DISCUSSION**

PI3K signaling pathway is often deregulated in malignancies and contribute to the oncogenic process. The mechanisms responsible for class I PI3Ks activity upregulation diverge among the distinct tumors. For example, gain of function mutations in *PIK3CA* that encodes the catalytic subunit p110 $\alpha$ , have been detected in a wide variety of human solid cancers<sup>182</sup>, whereas p110 $\delta$  is implicated in cancers derived from B lymphoid cells<sup>183</sup>. Recently, the oncogenic potential of p110 $\beta$ <sup>184</sup> has emerged in breast<sup>185</sup> and prostate cancers<sup>186</sup>. Tumor cells addiction to the activity of specific class I PI3K isoforms has lead to the development of efficacious therapies based on the application of selective PI3K inhibitors which target selective catalytic subunit<sup>187</sup>. In T-ALL, PI3K upregulation has been found in nearly 80% of cases<sup>120</sup> and targeting PI3K is an attractive novel strategy to treat these patients. Nevertheless, at present it is still controversial the role played by the different PI3K catalytic subunits in T-ALL and therefore which might be the most useful therapeutic strategy. It is well established that both p110 $\gamma$  and p110 $\delta$ , enriched in leukocytes, are involved in thymocyte development and activity<sup>55</sup>. The catalytic subunits p110 $\alpha$  and p110 $\beta$  are ubiquitously expressed so that it is extremely difficult to dissect their roles in lymphocytes, due to the embryonic lethality induced by loss of either p110 $\alpha$  or p110 $\beta$ <sup>188</sup>. However, there is a complex interplay between the class I PI3K members, as inhibition or loss of a specific isoform might be compensated by the others<sup>189</sup>. Subramanian et al. proposed the predominant role of p110 $\gamma$  and p110 $\delta$  in *PTEN*-deleted T-ALL, suggesting the possibility to target cancer cells by inhibiting specifically these isoforms<sup>146</sup>. Conversely, a more recent paper could not confirm those findings and documented a higher effect of the pan PI3K inhibition in *PTEN*-deleted T-ALL cell lines<sup>147</sup>. However, both these studies did not take into account *PTEN* non deleted T-ALL. Indeed, *PTEN* deletions or inactivating gene mutations are rare in primary T-ALL specimens, whereas posttranslational inactivation of PTEN is a more frequent event<sup>120</sup>. In this study we have used isoform-selective, pan and dual p110 $\gamma/\delta$  inhibitors to compare their effects

in both *PTEN*-deleted and non deleted cell lines. Our results demonstrated that blockage of all the class I PI3K catalytic isoforms exert a greater cytotoxic effect compared to the dual p110 $\gamma$ / $\delta$  inhibition, as exemplified by the lower IC<sub>50</sub> reached in all the cell lines, whereas isoform-selective inhibition resulted negligible. Among the pan inhibitors, PIK-90 was effective only in Loucy cells, highlighting that the chemical structure might affect drug action. Moreover, the Loucy cell line was the only sensitive to the dual inhibitor IPI-145. The peculiar sensitivity of Loucy cells to PI3K pathway inhibition is remarkable, as this cell line displays a transcriptional signature similar to that of early T-precursor (ETP)-ALL, a T-ALL subtype associated with an extremely poor prognosis<sup>190</sup>. Moreover, only pan-inhibition strongly impair leukemic T-cell proliferation. Notably, we did not observe differences between *PTEN*-deleted and non deleted cell lines. Indeed, despite the expression of PTEN protein, we found that in *PTEN*-non deleted cells the phosphatase was phosphorylated at Ser380 and thus inactivated. This observation highlights the importance of assessing PI3K pathway activation in T-ALL rather than *PTEN* mutations, to evaluate patients prognosis or therapeutic interventions. We also observed a decrease of total PtdIns(3,4,5)P<sub>3</sub> following inhibition of each PI3K catalytic subunit, suggesting that all the PI3K isoforms contribute to its synthesis in T-ALL cells. However, effects on PtdIns(3,4,5)P<sub>3</sub> did not correlate to cytotoxicity. This apparent contradiction might be due to the presence of different PtdIns(3,4,5)P<sub>3</sub> pools which mediate specific cellular processes, so that reduction of total PtdIns(3,4,5)P<sub>3</sub> could not reflect correctly impairment of cell proliferation mechanisms<sup>191</sup>. Regardless of PI3K downstream targets, we observed a downmodulation of the Akt/mTOR pathway. Interestingly, only the pan PI3K inhibitor completely switched off Akt signaling, as demonstrated by the reduction or complete abrogation of both Thr308 and Ser473 phosphorylated Akt proteins. It has been previously reported that a limited PI3K activity is sufficient to support cell survival and proliferation and, consequently, complete PI3K inhibition is required to induce cell death<sup>189</sup>. Consistently, in spite of changes in cell cycle

progression, we observed a significant cell death induction almost exclusively after pan PI3K inhibition, with the exception of Loucy cells where the dual inhibition of p110 $\gamma/\delta$  was also effective. Importantly, we demonstrated that, at least in the case of ZSTK-474 drug, the mechanisms involved in cell death are independent of caspases activity as the pan caspase inhibitor did not reduce cell death. Different studies have clarified the existence of various types of programmed cell death besides apoptosis including autophagy, an important catabolic mechanism which can play both a pro-survival or pro-death role<sup>192</sup>. Importantly, PI3K and autophagy pathways are tightly related, as mTORC1 suppresses autophagy inhibiting ULK1, and the transcription factor FoxO3, which is inhibited by Akt, regulates the expression of a number of autophagy related genes, including *LC3*, *GABARAPL1*, *BNIP3*, *PIK3C3* and *ULK1*<sup>178,193-194</sup>. Our findings demonstrate that activation of autophagy can sustain cell survival after PI3K inhibition. In fact, inhibitors that interfere with the autophagic process increased the cytotoxic effects of PI3K inhibitors. However, autophagy activation was not seen in all T-ALL cell lines, suggesting the influence of a more complex cellular background. To address this issue we examined the expression of autophagy related genes. No specific expression profiles were observed related to autophagy activation or pan PI3K inhibition and overall gene expression of paired samples was similar. Nonetheless, inhibition of PI3K specifically modulated few genes that might trigger autophagy. While the Loucy cell line showed a higher autophagy gene expression profile already at basal level, we observed the upregulation of few analyzed genes in Jurkat, ALL-SIL and DND-41 cells. Increase of these transcripts appear to be cell type dependent, as ALL-SIL, DND-41 and partially Loucy cells, which activated autophagy after pan PI3K inhibition, upregulated numerous genes involved in the formation of autophagosomes (*DRAM1*, *GABARAPL1*, *GABARAPL2*, *MAP1LC3B*, *ATG16L2*, *WIPI1*, *PIK3C*), antiapoptotic genes (*BCL2*) and genes of the unfolded protein response signaling (*EIF2AK3*). Conversely, in Jurkat cells, which did not activate autophagy, gene modulation

was affected at a lesser extent and preferentially involved antiproliferative targets, as the cell cycle inhibitors *CDKN1B* and *TP53*. These observations suggest a role for the PI3K pathway in modulating at a transcriptional level the complex relationship between pro- and anti-survival signals and ultimately the balance between autophagy and apoptosis. Of course, more studies are needed to clarify these relationships.

In conclusion, we demonstrated the strongest effect of pan PI3K inhibition in both PTEN deleted and non deleted T-ALL cell lines. Although dual inhibition of p110 $\gamma/\delta$  PI3K isoforms could be less toxic with fewer side effects<sup>176</sup>, its efficacy could be limited only to a subset of T-ALL, i.e. ETP-ALL. Moreover, our findings shed light on the protective role of autophagy in response to pan PI3K inhibition, supporting the evaluation of a combination of autophagy inhibitors and pan PI3K inhibitors. Further investigation will be necessary to discriminate the cellular context(s) responsible for autophagy activation. Addressing this question will help to understand which T-ALL patients may best benefit from a therapeutic strategy involving class I PI3Ks inhibition.

# REFERENCES

1. Whitman M, Kaplan DR, Schaffhausen B, Cantley L, Roberts TM. Association of phosphatidylinositol kinase activity with polyoma middle-T competent for transformation. *Nature*. 1985 May 16-22;315(6016):239-42.
2. Porta C, Paglino C, Mosca A. Targeting PI3K/Akt/mTOR Signaling in Cancer. *Front Oncol*. 2014;4:64.
3. Engelman JA, Luo J, Cantley LC. The evolution of phosphatidylinositol 3-kinases as regulators of growth and metabolism. *Nat Rev Genet*. 2006 Aug;7(8):606-19.
4. Liu P, Cheng H, Roberts TM, Zhao JJ. Targeting the phosphoinositide 3-kinase pathway in cancer. *Nat Rev Drug Discov*. 2009 Aug;8(8):627-44.
5. Vanhaesebroeck B, Leever SJ, Ahmadi K, Timms J, Katso R, Driscoll PC, et al. Synthesis and function of 3-phosphorylated inositol lipids. *Annu Rev Biochem*. 2001;70:535-602.
6. Fruman DA, Meyers RE, Cantley LC. Phosphoinositide kinases. *Annu Rev Biochem*. 1998;67:481-507.
7. Voigt P, Dorner MB, Schaefer M. Characterization of p87PIKAP, a novel regulatory subunit of phosphoinositide 3-kinase gamma that is highly expressed in heart and interacts with PDE3B. *J Biol Chem*. 2006 Apr 14;281(15):9977-86.
8. Suire S, Coadwell J, Ferguson GJ, Davidson K, Hawkins P, Stephens L. p84, a new Gbetagamma-activated regulatory subunit of the type IB phosphoinositide 3-kinase p110gamma. *Curr Biol*. 2005 Mar 29;15(6):566-70.
9. Vanhaesebroeck B, Guillermet-Guibert J, Graupera M, Bilanges B. The emerging mechanisms of isoform-specific PI3K signalling. *Nat Rev Mol Cell Biol*. 2010 May;11(5):329-41.
10. Backer JM. The regulation and function of Class III PI3Ks: novel roles for Vps34. *Biochem J*. 2008 Feb 15;410(1):1-17.
11. Zhao L, Vogt PK. Class I PI3K in oncogenic cellular transformation. *Oncogene*. 2008 Sep 18;27(41):5486-96.
12. Carpenter CL, Auger KR, Chanudhuri M, Yoakim M, Schaffhausen B, Shoelson S, et al. Phosphoinositide 3-kinase is activated by phosphopeptides that bind to the SH2 domains of the 85-kDa subunit. *J Biol Chem*. 1993 May 5;268(13):9478-83.
13. Cully M, You H, Levine AJ, Mak TW. Beyond PTEN mutations: the PI3K pathway as an integrator of multiple inputs during tumorigenesis. *Nat Rev Cancer*. 2006 Mar;6(3):184-92.

14. Shaw RJ, Cantley LC. Ras, PI(3)K and mTOR signalling controls tumour cell growth. *Nature*. 2006 May 25;441(7092):424-30.
15. Fruman DA, Rommel C. PI3K and cancer: lessons, challenges and opportunities. *Nat Rev Drug Discov*. 2014 Feb;13(2):140-56.
16. Courtney KD, Corcoran RB, Engelman JA. The PI3K pathway as drug target in human cancer. *J Clin Oncol*. 2010 Feb 20;28(6):1075-83.
17. Burgering BM, Coffey PJ. Protein kinase B (c-Akt) in phosphatidylinositol-3-OH kinase signal transduction. *Nature*. 1995 Aug 17;376(6541):599-602.
18. Fyfe C, Falasca M. 3-Phosphoinositide-dependent protein kinase-1 as an emerging target in the management of breast cancer. *Cancer Manag Res*. 2013;5:271-80.
19. Wick MJ, Ramos FJ, Chen H, Quon MJ, Dong LQ, Liu F. Mouse 3-phosphoinositide-dependent protein kinase-1 undergoes dimerization and trans-phosphorylation in the activation loop. *J Biol Chem*. 2003 Oct 31;278(44):42913-9.
20. Staal SP. Molecular cloning of the akt oncogene and its human homologues AKT1 and AKT2: amplification of AKT1 in a primary human gastric adenocarcinoma. *Proc Natl Acad Sci U S A*. 1987 Jul;84(14):5034-7.
21. Hassan B, Akcakanat A, Holder AM, Meric-Bernstam F. Targeting the PI3-kinase/Akt/mTOR signaling pathway. *Surg Oncol Clin N Am*. 2013 Oct;22(4):641-64.
22. Osaki M, Oshimura M, Ito H. PI3K-Akt pathway: its functions and alterations in human cancer. *Apoptosis*. 2004 Nov;9(6):667-76.
23. Sarbassov DD, Guertin DA, Ali SM, Sabatini DM. Phosphorylation and regulation of Akt/PKB by the rictor-mTOR complex. *Science*. 2005 Feb 18;307(5712):1098-101.
24. Martelli AM, Nyakern M, Tabellini G, Bortul R, Tazzari PL, Evangelisti C, et al. Phosphoinositide 3-kinase/Akt signaling pathway and its therapeutical implications for human acute myeloid leukemia. *Leukemia*. 2006 Jun;20(6):911-28.
25. Nave BT, Ouwens M, Withers DJ, Alessi DR, Shepherd PR. Mammalian target of rapamycin is a direct target for protein kinase B: identification of a convergence point for opposing effects of insulin and amino-acid deficiency on protein translation. *Biochem J*. 1999 Dec 1;344 Pt 2:427-31.
26. Inoki K, Li Y, Zhu T, Wu J, Guan KL. TSC2 is phosphorylated and inhibited by Akt and suppresses mTOR signalling. *Nat Cell Biol*. 2002 Sep;4(9):648-57.
27. Laplante M, Sabatini DM. mTOR signaling in growth control and disease. *Cell*. 2012 Apr 13;149(2):274-93.

28. Chiarini F, Evangelisti C, McCubrey JA, Martelli AM. Current treatment strategies for inhibiting mTOR in cancer. *Trends Pharmacol Sci.* 2014 Dec 10.
29. Li J, Yen C, Liaw D, Podsypanina K, Bose S, Wang SI, et al. PTEN, a putative protein tyrosine phosphatase gene mutated in human brain, breast, and prostate cancer. *Science.* 1997 Mar 28;275(5308):1943-7.
30. Carracedo A, Pandolfi PP. The PTEN-PI3K pathway: of feedbacks and cross-talks. *Oncogene.* 2008 Sep 18;27(41):5527-41.
31. Salmena L, Carracedo A, Pandolfi PP. Tenets of PTEN tumor suppression. *Cell.* 2008 May 2;133(3):403-14.
32. Choi Y, Zhang J, Murga C, Yu H, Koller E, Monia BP, et al. PTEN, but not SHIP and SHIP2, suppresses the PI3K/Akt pathway and induces growth inhibition and apoptosis of myeloma cells. *Oncogene.* 2002 Aug 8;21(34):5289-300.
33. Markman B, Atzori F, Perez-Garcia J, Tabernero J, Baselga J. Status of PI3K inhibition and biomarker development in cancer therapeutics. *Ann Oncol.* 2010 Apr;21(4):683-91.
34. Thompson JE, Thompson CB. Putting the rap on Akt. *J Clin Oncol.* 2004 Oct 15;22(20):4217-26.
35. Basu S, Totty NF, Irwin MS, Sudol M, Downward J. Akt phosphorylates the Yes-associated protein, YAP, to induce interaction with 14-3-3 and attenuation of p73-mediated apoptosis. *Mol Cell.* 2003 Jan;11(1):11-23.
36. Brozovic A, Fritz G, Christmann M, Zisowsky J, Jaehde U, Osmak M, et al. Long-term activation of SAPK/JNK, p38 kinase and fas-L expression by cisplatin is attenuated in human carcinoma cells that acquired drug resistance. *Int J Cancer.* 2004 Dec 20;112(6):974-85.
37. Zhou BP, Hung MC. Novel targets of Akt, p21(Cip1/WAF1), and MDM2. *Semin Oncol.* 2002 Jun;29(3 Suppl 11):62-70.
38. Carroll PE, Okuda M, Horn HF, Biddinger P, Stambrook PJ, Gleich LL, et al. Centrosome hyperamplification in human cancer: chromosome instability induced by p53 mutation and/or Mdm2 overexpression. *Oncogene.* 1999 Mar 18;18(11):1935-44.
39. Arden KC, Biggs WH, 3rd. Regulation of the FoxO family of transcription factors by phosphatidylinositol-3 kinase-activated signaling. *Arch Biochem Biophys.* 2002 Jul 15;403(2):292-8.
40. Blagosklonny MV, Pardee AB. The restriction point of the cell cycle. *Cell Cycle.* 2002 Mar-Apr;1(2):103-10.

41. Diehl JA, Cheng M, Roussel MF, Sherr CJ. Glycogen synthase kinase-3beta regulates cyclin D1 proteolysis and subcellular localization. *Genes Dev.* 1998 Nov 15;12(22):3499-511.
42. Liang J, Slingerland JM. Multiple roles of the PI3K/PKB (Akt) pathway in cell cycle progression. *Cell Cycle.* 2003 Jul-Aug;2(4):339-45.
43. Sherr CJ, Roberts JM. CDK inhibitors: positive and negative regulators of G1-phase progression. *Genes Dev.* 1999 Jun 15;13(12):1501-12.
44. Hanada M, Feng J, Hemmings BA. Structure, regulation and function of PKB/AKT-- a major therapeutic target. *Biochim Biophys Acta.* 2004 Mar 11;1697(1-2):3-16.
45. Ramaswamy S, Nakamura N, Sansal I, Bergeron L, Sellers WR. A novel mechanism of gene regulation and tumor suppression by the transcription factor FKHR. *Cancer Cell.* 2002 Jul;2(1):81-91.
46. Tran H, Brunet A, Grenier JM, Datta SR, Fornace AJ, Jr., DiStefano PS, et al. DNA repair pathway stimulated by the forkhead transcription factor FOXO3a through the Gadd45 protein. *Science.* 2002 Apr 19;296(5567):530-4.
47. Potter CJ, Pedraza LG, Xu T. Akt regulates growth by directly phosphorylating Tsc2. *Nat Cell Biol.* 2002 Sep;4(9):658-65.
48. Shaw RJ, Kosmatka M, Bardeesy N, Hurley RL, Witters LA, DePinho RA, et al. The tumor suppressor LKB1 kinase directly activates AMP-activated kinase and regulates apoptosis in response to energy stress. *Proc Natl Acad Sci U S A.* 2004 Mar 9;101(10):3329-35.
49. Hardt SE, Sadoshima J. Glycogen synthase kinase-3beta: a novel regulator of cardiac hypertrophy and development. *Circ Res.* 2002 May 31;90(10):1055-63.
50. Prunier C, Hocevar BA, Howe PH. Wnt signaling: physiology and pathology. *Growth Factors.* 2004 Sep;22(3):141-50.
51. Katoh M. WNT signaling pathway and stem cell signaling network. *Clin Cancer Res.* 2007 Jul 15;13(14):4042-5.
52. Hennessy BT, Smith DL, Ram PT, Lu Y, Mills GB. Exploiting the PI3K/AKT pathway for cancer drug discovery. *Nat Rev Drug Discov.* 2005 Dec;4(12):988-1004.
53. Juntilla MM, Koretzky GA. Critical roles of the PI3K/Akt signaling pathway in T cell development. *Immunol Lett.* 2008 Mar 15;116(2):104-10.
54. Fayard E, Moncayo G, Hemmings BA, Hollander GA. Phosphatidylinositol 3-kinase signaling in thymocytes: the need for stringent control. *Sci Signal.* 2010;3(135):re5.

55. So L, Fruman DA. PI3K signalling in B- and T-lymphocytes: new developments and therapeutic advances. *Biochem J.* 2012 Mar 15;442(3):465-81.
56. Okkenhaug K, Vanhaesebroeck B. PI3K in lymphocyte development, differentiation and activation. *Nat Rev Immunol.* 2003 Apr;3(4):317-30.
57. Pui CH, Relling MV, Downing JR. Acute lymphoblastic leukemia. *N Engl J Med.* 2004 Apr 8;350(15):1535-48.
58. Van Vlierberghe P, Ferrando A. The molecular basis of T cell acute lymphoblastic leukemia. *J Clin Invest.* 2012 Oct 1;122(10):3398-406.
59. Aifantis I, Raetz E, Buonamici S. Molecular pathogenesis of T-cell leukaemia and lymphoma. *Nat Rev Immunol.* 2008 May;8(5):380-90.
60. Cauwelier B, Dastugue N, Cools J, Poppe B, Herens C, De Paepe A, et al. Molecular cytogenetic study of 126 unselected T-ALL cases reveals high incidence of TCRbeta locus rearrangements and putative new T-cell oncogenes. *Leukemia.* 2006 Jul;20(7):1238-44.
61. Carroll AJ, Crist WM, Link MP, Amylon MD, Pullen DJ, Ragab AH, et al. The t(1;14)(p34;q11) is nonrandom and restricted to T-cell acute lymphoblastic leukemia: a Pediatric Oncology Group study. *Blood.* 1990 Sep 15;76(6):1220-4.
62. Mellentin JD, Smith SD, Cleary ML. lyl-1, a novel gene altered by chromosomal translocation in T cell leukemia, codes for a protein with a helix-loop-helix DNA binding motif. *Cell.* 1989 Jul 14;58(1):77-83.
63. Xia Y, Brown L, Yang CY, Tsan JT, Siciliano MJ, Espinosa R, 3rd, et al. TAL2, a helix-loop-helix gene activated by the (7;9)(q34;q32) translocation in human T-cell leukemia. *Proc Natl Acad Sci U S A.* 1991 Dec 15;88(24):11416-20.
64. Wang J, Jani-Sait SN, Escalon EA, Carroll AJ, de Jong PJ, Kirsch IR, et al. The t(14;21)(q11.2;q22) chromosomal translocation associated with T-cell acute lymphoblastic leukemia activates the BHLHB1 gene. *Proc Natl Acad Sci U S A.* 2000 Mar 28;97(7):3497-502.
65. McGuire EA, Hockett RD, Pollock KM, Bartholdi MF, O'Brien SJ, Korsmeyer SJ. The t(11;14)(p15;q11) in a T-cell acute lymphoblastic leukemia cell line activates multiple transcripts, including Ttg-1, a gene encoding a potential zinc finger protein. *Mol Cell Biol.* 1989 May;9(5):2124-32.
66. Royer-Pokora B, Loos U, Ludwig WD. TTG-2, a new gene encoding a cysteine-rich protein with the LIM motif, is overexpressed in acute T-cell leukaemia with the t(11;14)(p13;q11). *Oncogene.* 1991 Oct;6(10):1887-93.

67. Rabbitts TH. LMO T-cell translocation oncogenes typify genes activated by chromosomal translocations that alter transcription and developmental processes. *Genes Dev.* 1998 Sep 1;12(17):2651-7.
68. Ferrando AA, Neuberg DS, Staunton J, Loh ML, Huard C, Raimondi SC, et al. Gene expression signatures define novel oncogenic pathways in T cell acute lymphoblastic leukemia. *Cancer Cell.* 2002 Feb;1(1):75-87.
69. van Oostveen J, Bijl J, Raaphorst F, Walboomers J, Meijer C. The role of homeobox genes in normal hematopoiesis and hematological malignancies. *Leukemia.* 1999 Nov;13(11):1675-90.
70. Soulier J, Clappier E, Cayuela JM, Regnault A, Garcia-Peydro M, Dombret H, et al. HOXA genes are included in genetic and biologic networks defining human acute T-cell leukemia (T-ALL). *Blood.* 2005 Jul 1;106(1):274-86.
71. Speleman F, Cauwelier B, Dastugue N, Cools J, Verhasselt B, Poppe B, et al. A new recurrent inversion, inv(7)(p15q34), leads to transcriptional activation of HOXA10 and HOXA11 in a subset of T-cell acute lymphoblastic leukemias. *Leukemia.* 2005 Mar;19(3):358-66.
72. Ferrando AA, Neuberg DS, Dodge RK, Paietta E, Larson RA, Wiernik PH, et al. Prognostic importance of TLX1 (HOX11) oncogene expression in adults with T-cell acute lymphoblastic leukaemia. *Lancet.* 2004 Feb 14;363(9408):535-6.
73. Bernard OA, Busson-LeConiat M, Ballerini P, Mauchauffe M, Della Valle V, Monni R, et al. A new recurrent and specific cryptic translocation, t(5;14)(q35;q32), is associated with expression of the Hox11L2 gene in T acute lymphoblastic leukemia. *Leukemia.* 2001 Oct;15(10):1495-504.
74. Tycko B, Smith SD, Sklar J. Chromosomal translocations joining LCK and TCRB loci in human T cell leukemia. *J Exp Med.* 1991 Oct 1;174(4):867-73.
75. Clappier E, Cuccuini W, Cayuela JM, Vecchione D, Baruchel A, Dombret H, et al. Cyclin D2 dysregulation by chromosomal translocations to TCR loci in T-cell acute lymphoblastic leukemias. *Leukemia.* 2006 Jan;20(1):82-6.
76. Karrman K, Kjeldsen E, Lassen C, Isaksson M, Davidsson J, Andersson A, et al. The t(X;7)(q22;q34) in paediatric T-cell acute lymphoblastic leukaemia results in overexpression of the insulin receptor substrate 4 gene through illegitimate recombination with the T-cell receptor beta locus. *Br J Haematol.* 2009 Feb;144(4):546-51.

77. Ferrando AA, Look AT. Clinical implications of recurring chromosomal and associated molecular abnormalities in acute lymphoblastic leukemia. *Semin Hematol.* 2000 Oct;37(4):381-95.
78. Asnafi V, Radford-Weiss I, Dastugue N, Bayle C, Leboeuf D, Charrin C, et al. CALM-AF10 is a common fusion transcript in T-ALL and is specific to the TCRgammadelta lineage. *Blood.* 2003 Aug 1;102(3):1000-6.
79. Van Vlierberghe P, van Grotel M, Tchinda J, Lee C, Beverloo HB, van der Spek PJ, et al. The recurrent SET-NUP214 fusion as a new HOXA activation mechanism in pediatric T-cell acute lymphoblastic leukemia. *Blood.* 2008 May 1;111(9):4668-80.
80. Zipfel PA, Zhang W, Quiroz M, Pendergast AM. Requirement for Abl kinases in T cell receptor signaling. *Curr Biol.* 2004 Jul 27;14(14):1222-31.
81. Hagemeyer A, Graux C. ABL1 rearrangements in T-cell acute lymphoblastic leukemia. *Genes Chromosomes Cancer.* 2010 Apr;49(4):299-308.
82. Flex E, Petrangeli V, Stella L, Chiaretti S, Hornakova T, Knoops L, et al. Somaticly acquired JAK1 mutations in adult acute lymphoblastic leukemia. *J Exp Med.* 2008 Apr 14;205(4):751-8.
83. Otsubo K, Kanegane H, Eguchi M, Eguchi-Ishimae M, Tamura K, Nomura K, et al. ETV6-ARNT fusion in a patient with childhood T lymphoblastic leukemia. *Cancer Genet Cytogenet.* 2010 Oct 1;202(1):22-6.
84. Ellisen LW, Bird J, West DC, Soreng AL, Reynolds TC, Smith SD, et al. TAN-1, the human homolog of the *Drosophila* notch gene, is broken by chromosomal translocations in T lymphoblastic neoplasms. *Cell.* 1991 Aug 23;66(4):649-61.
85. Weng AP, Ferrando AA, Lee W, Morris JPt, Silverman LB, Sanchez-Irizarry C, et al. Activating mutations of NOTCH1 in human T cell acute lymphoblastic leukemia. *Science.* 2004 Oct 8;306(5694):269-71.
86. Koch U, Radtke F. Notch in T-ALL: new players in a complex disease. *Trends Immunol.* 2011 Sep;32(9):434-42.
87. Breit S, Stanulla M, Flohr T, Schrappe M, Ludwig WD, Tolle G, et al. Activating NOTCH1 mutations predict favorable early treatment response and long-term outcome in childhood precursor T-cell lymphoblastic leukemia. *Blood.* 2006 Aug 15;108(4):1151-7.
88. Thompson BJ, Buonamici S, Sulis ML, Palomero T, Vilimas T, Basso G, et al. The SCFFBW7 ubiquitin ligase complex as a tumor suppressor in T cell leukemia. *J Exp Med.* 2007 Aug 6;204(8):1825-35.

89. Palomero T, Sulis ML, Cortina M, Real PJ, Barnes K, Ciofani M, et al. Mutational loss of PTEN induces resistance to NOTCH1 inhibition in T-cell leukemia. *Nat Med.* 2007 Oct;13(10):1203-10.
90. Bar-Eli M, Ahuja H, Foti A, Cline MJ. N-RAS mutations in T-cell acute lymphocytic leukaemia: analysis by direct sequencing detects a novel mutation. *Br J Haematol.* 1989 May;72(1):36-9.
91. Balgobind BV, Van Vlierberghe P, van den Ouweland AM, Beverloo HB, Terlouw-Kromosoeto JN, van Wering ER, et al. Leukemia-associated NF1 inactivation in patients with pediatric T-ALL and AML lacking evidence for neurofibromatosis. *Blood.* 2008 Apr 15;111(8):4322-8.
92. Van Vlierberghe P, Meijerink JP, Stam RW, van der Smissen W, van Wering ER, Beverloo HB, et al. Activating FLT3 mutations in CD4+/CD8- pediatric T-cell acute lymphoblastic leukemias. *Blood.* 2005 Dec 15;106(13):4414-5.
93. Paietta E, Ferrando AA, Neuberg D, Bennett JM, Racevskis J, Lazarus H, et al. Activating FLT3 mutations in CD117/KIT(+) T-cell acute lymphoblastic leukemias. *Blood.* 2004 Jul 15;104(2):558-60.
94. Kleppe M, Lahortiga I, El Chaar T, De Keersmaecker K, Mentens N, Graux C, et al. Deletion of the protein tyrosine phosphatase gene PTPN2 in T-cell acute lymphoblastic leukemia. *Nat Genet.* 2010 Jun;42(6):530-5.
95. Tosello V, Mansour MR, Barnes K, Paganin M, Sulis ML, Jenkinson S, et al. WT1 mutations in T-ALL. *Blood.* 2009 Jul 30;114(5):1038-45.
96. Gutierrez A, Sanda T, Ma W, Zhang J, Grebliunaite R, Dahlberg S, et al. Inactivation of LEF1 in T-cell acute lymphoblastic leukemia. *Blood.* 2010 Apr 8;115(14):2845-51.
97. Hebert J, Cayuela JM, Berkeley J, Sigaux F. Candidate tumor-suppressor genes MTS1 (p16INK4A) and MTS2 (p15INK4B) display frequent homozygous deletions in primary cells from T- but not from B-cell lineage acute lymphoblastic leukemias. *Blood.* 1994 Dec 15;84(12):4038-44.
98. Mullighan CG, Goorha S, Radtke I, Miller CB, Coustan-Smith E, Dalton JD, et al. Genome-wide analysis of genetic alterations in acute lymphoblastic leukaemia. *Nature.* 2007 Apr 12;446(7137):758-64.
99. Remke M, Pfister S, Kox C, Toedt G, Becker N, Benner A, et al. High-resolution genomic profiling of childhood T-ALL reveals frequent copy-number alterations affecting

the TGF-beta and PI3K-AKT pathways and deletions at 6q15-16.1 as a genomic marker for unfavorable early treatment response. *Blood*. 2009 Jul 30;114(5):1053-62.

100. Mullighan CG, Phillips LA, Su X, Ma J, Miller CB, Shurtleff SA, et al. Genomic analysis of the clonal origins of relapsed acute lymphoblastic leukemia. *Science*. 2008 Nov 28;322(5906):1377-80.

101. Iacobucci I, Papayannidis C, Lonetti A, Ferrari A, Baccharani M, Martinelli G. Cytogenetic and molecular predictors of outcome in acute lymphocytic leukemia: recent developments. *Curr Hematol Malig Rep*. 2012 Jun;7(2):133-43.

102. Van Vlierberghe P, Palomero T, Khiabani H, Van der Meulen J, Castillo M, Van Roy N, et al. PHF6 mutations in T-cell acute lymphoblastic leukemia. *Nat Genet*. 2010 Apr;42(4):338-42.

103. Huh HJ, Lee SH, Yoo KH, Sung KW, Koo HH, Jang JH, et al. Gene mutation profiles and prognostic implications in Korean patients with T-lymphoblastic leukemia. *Ann Hematol*. 2013 May;92(5):635-44.

104. Wang Q, Qiu H, Jiang H, Wu L, Dong S, Pan J, et al. Mutations of PHF6 are associated with mutations of NOTCH1, JAK1 and rearrangement of SET-NUP214 in T-cell acute lymphoblastic leukemia. *Haematologica*. 2011 Dec;96(12):1808-14.

105. Coustan-Smith E, Mullighan CG, Onciu M, Behm FG, Raimondi SC, Pei D, et al. Early T-cell precursor leukaemia: a subtype of very high-risk acute lymphoblastic leukaemia. *Lancet Oncol*. 2009 Feb;10(2):147-56.

106. Rothenberg EV, Moore JE, Yui MA. Launching the T-cell-lineage developmental programme. *Nat Rev Immunol*. 2008 Jan;8(1):9-21.

107. Wada H, Masuda K, Satoh R, Kakugawa K, Ikawa T, Katsura Y, et al. Adult T-cell progenitors retain myeloid potential. *Nature*. 2008 Apr 10;452(7188):768-72.

108. Zhang J, Ding L, Holmfeldt L, Wu G, Heatley SL, Payne-Turner D, et al. The genetic basis of early T-cell precursor acute lymphoblastic leukaemia. *Nature*. 2012 Jan 12;481(7380):157-63.

109. Neumann M, Heesch S, Schlee C, Schwartz S, Gokbuget N, Hoelzer D, et al. Whole-exome sequencing in adult ETP-ALL reveals a high rate of DNMT3A mutations. *Blood*. 2013 Jun 6;121(23):4749-52.

110. Ley TJ, Ding L, Walter MJ, McLellan MD, Lamprecht T, Larson DE, et al. DNMT3A mutations in acute myeloid leukemia. *N Engl J Med*. 2010 Dec 16;363(25):2424-33.

111. Grossmann V, Haferlach C, Weissmann S, Roller A, Schindela S, Poetzinger F, et al. The molecular profile of adult T-cell acute lymphoblastic leukemia: mutations in RUNX1

and DNMT3A are associated with poor prognosis in T-ALL. *Genes Chromosomes Cancer*. 2013 Apr;52(4):410-22.

112. De Keersmaecker K, Atak ZK, Li N, Vicente C, Patchett S, Girardi T, et al. Exome sequencing identifies mutation in CNOT3 and ribosomal genes RPL5 and RPL10 in T-cell acute lymphoblastic leukemia. *Nat Genet*. 2013 Feb;45(2):186-90.

113. Tzoneva G, Perez-Garcia A, Carpenter Z, Khiabani H, Tosello V, Allegretta M, et al. Activating mutations in the NT5C2 nucleotidase gene drive chemotherapy resistance in relapsed ALL. *Nat Med*. 2013 Mar;19(3):368-71.

114. Wu D, Sherwood A, Fromm JR, Winter SS, Dunsmore KP, Loh ML, et al. High-throughput sequencing detects minimal residual disease in acute T lymphoblastic leukemia. *Sci Transl Med*. 2012 May 16;4(134):134ra63.

115. Flohr T, Schrauder A, Cazzaniga G, Panzer-Grumayer R, van der Velden V, Fischer S, et al. Minimal residual disease-directed risk stratification using real-time quantitative PCR analysis of immunoglobulin and T-cell receptor gene rearrangements in the international multicenter trial AIEOP-BFM ALL 2000 for childhood acute lymphoblastic leukemia. *Leukemia*. 2008 Apr;22(4):771-82.

116. Bagley BN, Keane TM, Maklakova VI, Marshall JG, Lester RA, Cancel MM, et al. A dominantly acting murine allele of Mcm4 causes chromosomal abnormalities and promotes tumorigenesis. *PLoS Genet*. 2012;8(11):e1003034.

117. Zhang L, Xu HG, Lu C. A novel long non-coding RNA T-ALL-R-LncR1 knockdown and Par-4 cooperate to induce cellular apoptosis in T-cell acute lymphoblastic leukemia cells. *Leuk Lymphoma*. 2013 Aug 28.

118. Yan B, Wang Z. Long noncoding RNA: its physiological and pathological roles. *DNA Cell Biol*. 2012 Oct;31 Suppl 1:S34-41.

119. Pui CH, Mullighan CG, Evans WE, Relling MV. Pediatric acute lymphoblastic leukemia: where are we going and how do we get there? *Blood*. 2012 Aug 9;120(6):1165-74.

120. Silva A, Yunes JA, Cardoso BA, Martins LR, Jotta PY, Abecasis M, et al. PTEN posttranslational inactivation and hyperactivation of the PI3K/Akt pathway sustain primary T cell leukemia viability. *J Clin Invest*. 2008 Nov;118(11):3762-74.

121. Cardoso BA, Girio A, Henriques C, Martins LR, Santos C, Silva A, et al. Aberrant signaling in T-cell acute lymphoblastic leukemia: biological and therapeutic implications. *Braz J Med Biol Res*. 2008 May;41(5):344-50.

122. Bauer TM, Patel MR, Infante JR. Targeting PI3 kinase in cancer. *Pharmacol Ther.* 2014 Sep 18.
123. Maser RS, Choudhury B, Campbell PJ, Feng B, Wong KK, Protopopov A, et al. Chromosomally unstable mouse tumours have genomic alterations similar to diverse human cancers. *Nature.* 2007 Jun 21;447(7147):966-71.
124. Yilmaz OH, Valdez R, Theisen BK, Guo W, Ferguson DO, Wu H, et al. Pten dependence distinguishes haematopoietic stem cells from leukaemia-initiating cells. *Nature.* 2006 May 25;441(7092):475-82.
125. Zhang J, Grindley JC, Yin T, Jayasinghe S, He XC, Ross JT, et al. PTEN maintains haematopoietic stem cells and acts in lineage choice and leukaemia prevention. *Nature.* 2006 May 25;441(7092):518-22.
126. Silva A, Girio A, Cebola I, Santos CI, Antunes F, Barata JT. Intracellular reactive oxygen species are essential for PI3K/Akt/mTOR-dependent IL-7-mediated viability of T-cell acute lymphoblastic leukemia cells. *Leukemia.* 2011 Jun;25(6):960-7.
127. Larson Gedman A, Chen Q, Kugel Desmoulin S, Ge Y, LaFiura K, Haska CL, et al. The impact of NOTCH1, FBW7 and PTEN mutations on prognosis and downstream signaling in pediatric T-cell acute lymphoblastic leukemia: a report from the Children's Oncology Group. *Leukemia.* 2009 Aug;23(8):1417-25.
128. Jabbour E, Ottmann OG, Deininger M, Hochhaus A. Targeting the phosphoinositide 3-kinase pathway in hematologic malignancies. *Haematologica.* 2014 Jan;99(1):7-18.
129. Lonetti A, Antunes IL, Chiarini F, Orsini E, Buontempo F, Ricci F, et al. Activity of the pan-class I phosphoinositide 3-kinase inhibitor NVP-BKM120 in T-cell acute lymphoblastic leukemia. *Leukemia.* 2014 Jun;28(6):1196-206.
130. Rodon J, Brana I, Siu LL, De Jonge MJ, Homji N, Mills D, et al. Phase I dose-escalation and -expansion study of buparlisib (BKM120), an oral pan-Class I PI3K inhibitor, in patients with advanced solid tumors. *Invest New Drugs.* 2014 Mar 21.
131. Ando Y, Inada-Inoue M, Mitsuma A, Yoshino T, Ohtsu A, Suenaga N, et al. Phase I dose-escalation study of buparlisib (BKM120), an oral pan-class I PI3K inhibitor, in Japanese patients with advanced solid tumors. *Cancer Sci.* 2014 Mar;105(3):347-53.
132. Bendell JC, Rodon J, Burris HA, de Jonge M, Verweij J, Birlle D, et al. Phase I, dose-escalation study of BKM120, an oral pan-Class I PI3K inhibitor, in patients with advanced solid tumors. *J Clin Oncol.* 2012 Jan 20;30(3):282-90.

133. Yaguchi S, Fukui Y, Koshimizu I, Yoshimi H, Matsuno T, Gouda H, et al. Antitumor activity of ZSTK474, a new phosphatidylinositol 3-kinase inhibitor. *J Natl Cancer Inst.* 2006 Apr 19;98(8):545-56.
134. Dan S, Yoshimi H, Okamura M, Mukai Y, Yamori T. Inhibition of PI3K by ZSTK474 suppressed tumor growth not via apoptosis but G0/G1 arrest. *Biochem Biophys Res Commun.* 2009 Jan 30;379(1):104-9.
135. Dan S, Okamura M, Mukai Y, Yoshimi H, Inoue Y, Hanyu A, et al. ZSTK474, a specific phosphatidylinositol 3-kinase inhibitor, induces G1 arrest of the cell cycle in vivo. *Eur J Cancer.* 2012 Apr;48(6):936-43.
136. Jia S, Liu Z, Zhang S, Liu P, Zhang L, Lee SH, et al. Essential roles of PI(3)K-p110beta in cell growth, metabolism and tumorigenesis. *Nature.* 2008 Aug 7;454(7205):776-9.
137. Gilbert JA. Idelalisib: targeting PI3Kdelta in B-cell malignancies. *Lancet Oncol.* 2014 Mar;15(3):e108.
138. Weigelt B, Downward J. Genomic Determinants of PI3K Pathway Inhibitor Response in Cancer. *Front Oncol.* 2012;2:109.
139. Zenatti PP, Ribeiro D, Li WQ, Zuurbier L, Silva MC, Paganin M, et al. Oncogenic IL7R gain-of-function mutations in childhood T-cell acute lymphoblastic leukemia. *Nat Genet.* 2011 Oct;43(10):932-U31.
140. Simioni C, Neri LM, Tabellini G, Ricci F, Bressanin D, Chiarini F, et al. Cytotoxic activity of the novel Akt inhibitor, MK-2206, in T-cell acute lymphoblastic leukemia. *Leukemia.* 2012 Nov;26(11):2336-42.
141. Shepherd C, Banerjee L, Cheung CW, Mansour MR, Jenkinson S, Gale RE, et al. PI3K/mTOR inhibition upregulates NOTCH-MYC signalling leading to an impaired cytotoxic response. *Leukemia.* 2013 Mar;27(3):650-60.
142. Maira SM, Pecchi S, Huang A, Burger M, Knapp M, Sterker D, et al. Identification and characterization of NVP-BKM120, an orally available pan-class I PI3-kinase inhibitor. *Mol Cancer Ther.* 2012 Feb;11(2):317-28.
143. Zheng Y, Yang J, Qian J, Zhang L, Lu Y, Li H, et al. Novel phosphatidylinositol 3-kinase inhibitor NVP-BKM120 induces apoptosis in myeloma cells and shows synergistic anti-myeloma activity with dexamethasone. *J Mol Med (Berl).* 2012 Jun;90(6):695-706.
144. Amrein L, Shawi M, Grenier J, Aloyz R, Panasci L. The phosphatidylinositol-3 kinase I inhibitor BKM120 induces cell death in B-chronic lymphocytic leukemia cells in vitro. *Int J Cancer.* 2013 Jul;133(1):247-52.

145. Zang C, Eucker J, Liu H, Coordes A, Lenarz M, Possinger K, et al. Inhibition of pan-class I PI3 kinase by NVP-BKM120 effectively blocks proliferation and induces cell death in diffuse large B cell lymphoma. *Leuk Lymphoma*. 2013 May 31.
146. Subramaniam PS, Whye DW, Efimenko E, Chen J, Tosello V, De Keersmaecker K, et al. Targeting nonclassical oncogenes for therapy in T-ALL. *Cancer Cell*. 2012 Apr 17;21(4):459-72.
147. Stengel C, Jenner E, Meja K, Mayekar S, Khwaja A. Proliferation of PTEN-deficient haematopoietic tumour cells is not affected by isoform-selective inhibition of p110 PI3-kinase and requires blockade of all class 1 PI3K activity. *Br J Haematol*. 2013 Jul;162(2):285-9.
148. Matarrese P, Testa U, Cauda R, Vella S, Gambardella L, Malorni W. Expression of P-170 glycoprotein sensitizes lymphoblastoid CEM cells to mitochondria-mediated apoptosis. *Biochem J*. 2001 May 1;355(Pt 3):587-95.
149. Silva A, Laranjeira ABA, Martins LR, Cardoso BA, Demengeot J, Yunes JA, et al. IL-7 Contributes to the Progression of Human T-cell Acute Lymphoblastic Leukemias. *Cancer Res*. 2011 Jul 15;71(14):4780-9.
150. Chou TC, Talalay P. Quantitative analysis of dose-effect relationships: the combined effects of multiple drugs or enzyme inhibitors. *Adv Enzyme Regul*. 1984;22:27-55.
151. Papa V, Tazzari PL, Chiarini F, Cappellini A, Ricci F, Billi AM, et al. Proapoptotic activity and chemosensitizing effect of the novel Akt inhibitor perifosine in acute myelogenous leukemia cells. *Leukemia*. 2008 Jan;22(1):147-60.
152. Telford WG, Bradford J, Godfrey W, Robey RW, Bates SE. Side population analysis using a violet-excited cell-permeable DNA binding dye. *Stem Cells*. 2007 Apr;25(4):1029-36.
153. Martins LR, Lucio P, Melao A, Antunes I, Cardoso BA, Stansfield R, et al. Activity of the clinical-stage CK2-specific inhibitor CX-4945 against chronic lymphocytic leukemia. *Leukemia*. 2013 Aug 8.
154. Schmittgen TD, Livak KJ. Analyzing real-time PCR data by the comparative C(T) method. *Nat Protoc*. 2008;3(6):1101-8.
155. Saeed AI, Bhagabati NK, Braisted JC, Liang W, Sharov V, Howe EA, et al. TM4 microarray software suite. *Methods Enzymol*. 2006;411:134-93.

156. Forbes SA, Bindal N, Bamford S, Cole C, Kok CY, Beare D, et al. COSMIC: mining complete cancer genomes in the Catalogue of Somatic Mutations in Cancer. *Nucleic Acids Res.* 2011 Jan;39(Database issue):D945-50.
157. Willems L, Chapuis N, Puissant A, Maciel TT, Green AS, Jacque N, et al. The dual mTORC1 and mTORC2 inhibitor AZD8055 has anti-tumor activity in acute myeloid leukemia. *Leukemia.* 2012 Jun;26(6):1195-202.
158. Carracedo A, Ma L, Teruya-Feldstein J, Rojo F, Salmena L, Alimonti A, et al. Inhibition of mTORC1 leads to MAPK pathway activation through a PI3K-dependent feedback loop in human cancer. *J Clin Invest.* 2008 Sep;118(9):3065-74.
159. Konopleva M, Tabe Y, Zeng Z, Andreeff M. Therapeutic targeting of microenvironmental interactions in leukemia: mechanisms and approaches. *Drug Resist Updat.* 2009 Aug-Oct;12(4-5):103-13.
160. Li J, Law HK, Lau YL, Chan GC. Differential damage and recovery of human mesenchymal stem cells after exposure to chemotherapeutic agents. *Br J Haematol.* 2004 Nov;127(3):326-34.
161. Yamazaki J, Mizukami T, Takizawa K, Kuramitsu M, Momose H, Masumi A, et al. Identification of cancer stem cells in a Tax-transgenic (Tax-Tg) mouse model of adult T-cell leukemia/lymphoma. *Blood.* 2009 Sep 24;114(13):2709-20.
162. Hadnagy A, Gaboury L, Beaulieu R, Balicki D. SP analysis may be used to identify cancer stem cell populations. *Exp Cell Res.* 2006 Nov 15;312(19):3701-10.
163. Zhou S, Schuetz JD, Bunting KD, Colapietro AM, Sampath J, Morris JJ, et al. The ABC transporter Bcrp1/ABCG2 is expressed in a wide variety of stem cells and is a molecular determinant of the side-population phenotype. *Nat Med.* 2001 Sep;7(9):1028-34.
164. Casale F, D'Angelo V, Addeo R, Caraglia M, Crisci S, Rondelli R, et al. P-glycoprotein 170 expression and function as an adverse independent prognostic factor in childhood acute lymphoblastic leukemia. *Oncol Rep.* 2004 Dec;12(6):1201-7.
165. Koul D, Fu J, Shen R, LaFortune TA, Wang S, Tiao N, et al. Antitumor activity of NVP-BKM120--a selective pan class I PI3 kinase inhibitor showed differential forms of cell death based on p53 status of glioma cells. *Clin Cancer Res.* 2012 Jan 1;18(1):184-95.
166. Mueller A, Bachmann E, Linnig M, Khillimberger K, Schimanski CC, Galle PR, et al. Selective PI3K inhibition by BKM120 and BEZ235 alone or in combination with chemotherapy in wild-type and mutated human gastrointestinal cancer cell lines. *Cancer Chemother Pharmacol.* 2012 Jun;69(6):1601-15.

167. Juvekar A, Burga LN, Hu H, Lunsford EP, Ibrahim YH, Balmana J, et al. Combining a PI3K inhibitor with a PARP inhibitor provides an effective therapy for BRCA1-related breast cancer. *Cancer Discov.* 2012 Nov;2(11):1048-63.
168. Ibrahim YH, Garcia-Garcia C, Serra V, He L, Torres-Lockhart K, Prat A, et al. PI3K inhibition impairs BRCA1/2 expression and sensitizes BRCA-proficient triple-negative breast cancer to PARP inhibition. *Cancer Discov.* 2012 Nov;2(11):1036-47.
169. Brachmann SM, Kleylein-Sohn J, Gaulis S, Kauffmann A, Blommers MJ, Kazic-Legueux M, et al. Characterization of the mechanism of action of the pan class I PI3K inhibitor NVP-BKM120 across a broad range of concentrations. *Mol Cancer Ther.* 2012 Aug;11(8):1747-57.
170. Evangelisti C, Ricci F, Tazzari P, Tabellini G, Battistelli M, Falcieri E, et al. Targeted inhibition of mTORC1 and mTORC2 by active-site mTOR inhibitors has cytotoxic effects in T-cell acute lymphoblastic leukemia. *Leukemia.* 2011 May;25(5):781-91.
171. Lane SW, Scadden DT, Gilliland DG. The leukemic stem cell niche: current concepts and therapeutic opportunities. *Blood.* 2009 Aug 6;114(6):1150-7.
172. Kantarjian H, Thomas D, O'Brien S, Cortes J, Giles F, Jeha S, et al. Long-term follow-up results of hyperfractionated cyclophosphamide, vincristine, doxorubicin, and dexamethasone (Hyper-CVAD), a dose-intensive regimen, in adult acute lymphocytic leukemia. *Cancer.* 2004 Dec 15;101(12):2788-801.
173. Chiarini F, Fala F, Tazzari PL, Ricci F, Astolfi A, Pession A, et al. Dual inhibition of class IA phosphatidylinositol 3-kinase and mammalian target of rapamycin as a new therapeutic option for T-cell acute lymphoblastic leukemia. *Cancer Res.* 2009 Apr 15;69(8):3520-8.
174. Stengel C, Jenner E, Meja K, Mayekar S, Khwaja A. Proliferation of PTEN-deficient haematopoietic tumour cells is not affected by isoform-selective inhibition of p110 PI3-kinase and requires blockade of all class 1 PI3K activity. *Brit J Haematol.* 2013 Jul;162(2):285-9.
175. Fruman DA, Rommel C. PI3Kdelta inhibitors in cancer: rationale and serendipity merge in the clinic. *Cancer Discov.* 2011 Dec;1(7):562-72.
176. So L, Yea SS, Oak JS, Lu M, Manmadhan A, Ke QH, et al. Selective inhibition of phosphoinositide 3-kinase p110alpha preserves lymphocyte function. *J Biol Chem.* 2013 Feb 22;288(8):5718-31.
177. Griner EM, Kazanietz MG. Protein kinase C and other diacylglycerol effectors in cancer. *Nat Rev Cancer.* 2007 Apr;7(4):281-94.

178. Evangelisti C, Chiarini F, Lonetti A, Buontempo F, Neri LM, McCubrey JA, et al. Autophagy in acute leukemias: A double-edged sword with important therapeutic implications. *Biochim Biophys Acta*. 2014 Oct 2;1853(1):14-26.
179. Galluzzi L, Vitale I, Abrams JM, Alnemri ES, Baehrecke EH, Blagosklonny MV, et al. Molecular definitions of cell death subroutines: recommendations of the Nomenclature Committee on Cell Death 2012. *Cell Death Differ*. 2012 Jan;19(1):107-20.
180. Rambold AS, Lippincott-Schwartz J. Mechanisms of mitochondria and autophagy crosstalk. *Cell Cycle*. 2011 Dec 1;10(23):4032-8.
181. Pan L, Li Y, Jia L, Qin Y, Qi G, Cheng J, et al. Cathepsin S deficiency results in abnormal accumulation of autophagosomes in macrophages and enhances Ang II-induced cardiac inflammation. *PLoS One*. 2012;7(4):e35315.
182. Samuels Y, Wang Z, Bardelli A, Silliman N, Ptak J, Szabo S, et al. High frequency of mutations of the PIK3CA gene in human cancers. *Science*. 2004 Apr 23;304(5670):554.
183. Tzenaki N, Papakonstanti EA. p110delta PI3 kinase pathway: emerging roles in cancer. *Front Oncol*. 2013;3:40.
184. Kang S, Denley A, Vanhaesebroeck B, Vogt PK. Oncogenic transformation induced by the p110beta, -gamma, and -delta isoforms of class I phosphoinositide 3-kinase. *Proc Natl Acad Sci U S A*. 2006 Jan 31;103(5):1289-94.
185. Dbouk HA, Khalil BD, Wu H, Shymanets A, Nurnberg B, Backer JM. Characterization of a tumor-associated activating mutation of the p110beta PI 3-kinase. *PLoS One*. 2013;8(5):e63833.
186. Li B, Sun A, Jiang W, Thrasher JB, Terranova P. PI-3 kinase p110beta: a therapeutic target in advanced prostate cancers. *Am J Clin Exp Urol*. 2014;2(3):188-98.
187. Fruman DA, Cantley LC. Idelalisib--a PI3Kdelta inhibitor for B-cell cancers. *N Engl J Med*. 2014 Mar 13;370(11):1061-2.
188. Vanhaesebroeck B, Ali K, Bilancio A, Geering B, Foukas LC. Signalling by PI3K isoforms: insights from gene-targeted mice. *Trends Biochem Sci*. 2005 Apr;30(4):194-204.
189. Foukas LC, Berenjeno IM, Gray A, Khwaja A, Vanhaesebroeck B. Activity of any class IA PI3K isoform can sustain cell proliferation and survival. *Proc Natl Acad Sci U S A*. 2010 Jun 22;107(25):11381-6.
190. Anderson NM, Harrold I, Mansour MR, Sanda T, McKeown M, Nagykarly N, et al. BCL2-specific inhibitor ABT-199 synergizes strongly with cytarabine against the early immature LOUCY cell line but not more-differentiated T-ALL cell lines. *Leukemia*. 2014 May;28(5):1145-8.

191. Bohnacker T, Marone R, Collmann E, Calvez R, Hirsch E, Wymann MP. PI3Kgamma adaptor subunits define coupling to degranulation and cell motility by distinct PtdIns(3,4,5)P3 pools in mast cells. *Sci Signal*. 2009;2(74):ra27.
192. Ouyang L, Shi Z, Zhao S, Wang FT, Zhou TT, Liu B, et al. Programmed cell death pathways in cancer: a review of apoptosis, autophagy and programmed necrosis. *Cell Prolif*. 2012 Dec;45(6):487-98.
193. Mammucari C, Milan G, Romanello V, Masiero E, Rudolf R, Del Piccolo P, et al. FoxO3 controls autophagy in skeletal muscle in vivo. *Cell Metab*. 2007 Dec;6(6):458-71.
194. Zhao J, Brault JJ, Schild A, Cao P, Sandri M, Schiaffino S, et al. FoxO3 coordinately activates protein degradation by the autophagic/lysosomal and proteasomal pathways in atrophying muscle cells. *Cell Metab*. 2007 Dec;6(6):472-83.